MILITARY HANDBOOK

COMMUNICATIONS
TIMING AND SYNCHRONIZATION
SUBSYSTEMS

AMSC N/A

AREA TCTS/SLHC

DISTRIBUTION STATEMENT A. Approved for public release; distribution is unlimited.

MIL-HDBK-421

FOREWORD

1.   The Joint Tactical Command, Control and Communications Agency (JTC3A) developed this standardization handbook with assistance from military departments, federal agencies, and industry.

2.   Comments (recommendations, additions, deletions) and any pertinent data that may be of use in improving this document should be addressed to the Director, Joint Tactical Command, Control and Communications Agency, ATTN: C3A-STT, Fort Monmouth, New Jersey 07703-5513, by using the self-addressed Standardization Document Improvement Proposal (DD Form 1426) appearing at the end of this document, or by letter.

3.   Military communications system technical standards are now published as a MIL-STD-188 series, under the guidance of the Joint Telecommunications Standards Steering Group. These standards are subdivided into common long-haul and tactical standards (MIL-STD-188-100 series), tactical standards (MIL-STD-188-200 series), and long-haul standards (MIL-STD-188-300 series). Generally, military communications handbooks are published in the MIL-HDBK-400 series.

4.   In digital communications systems, the timing relationship of each pulse to other pulses in the same sequential stream is fundamental to interpreting the information contained in the pulses. If time-division multiplexing, time-division switching, or time-division multiple access systems are used, this time relationship is a determining factor as to whom the information belongs, as well as what it means. The loss of proper timing can be catastrophic and cause all received information to be meaningless. Therefore, it is imperative that effective, survivable, economical system timing be provided for military digital communications.

5.   Accurate timing is required for certain systems to establish synchronization under jamming conditions to enhance reception or to avoid detection. Without accurate timing, these systems would not be able to provide these capabilities.

6.   This military handbook is intended to provide assistance in understanding how timing and synchronization capabilities for Department of Defense digital communications systems are planned, engineered, procured, and used.

7.   This military handbook is a companion document to MIL-STD-188-115, *Interoperability and Performance Standards for Communications Timing and Synchronization Subsystems.*

8.   The references listed in Section 2, Applicable Documents, offer additional information.

MIL-HDBK-421

This page intentionally left blank.

MIL-HDBK-421

CONTENTS

MIL-HDBK-421

CONTENTS

PARAGRAPH PAGE

CONTENTS

v

MIL-HDBK-421

CONTENTS

CONTENTS

MIL-HDBK-421

CONTENTS

MIL-HDBK-421

CONTENTS

MIL-HDBK-421

This page intentionally left blank.

MIL-HDBK-421

1. SCOPE

1.1 <u>Purpose.</u> This handbook has been prepared to assist engineers and staff planners in understanding military communications timing and synchronization subsystems. It is designed to enhance the understanding of the parameters and characteristics found in the timing and synchronization needs of the military communications environment.

1.2 <u>Application.</u> This handbook is designed to be used in the planning and implementation of timing and synchronization for Department of Defense digital communications systems. It applies to federal-government-owned-and-operated digital communications systems and does not necessarily apply to leased commercial facilities.

1.3 <u>Objective.</u> The objective of this handbook is to provide general technical information pertaining to communications timing and synchronization subsystems. It is to be used with MIL-STD-188-115, *Interoperability and Performance Standards for Communications Timing and Synchronization Subsystems.*

This page intentionally left blank.

2. APPLICABLE DOCUMENTS

2.1 Government documents

2.1.1 Specifications, standards, and handbooks. The following specifications, standards, and handbooks form a part of this military handbook (MIL-HDBK) to the extent specified herein. Unless otherwise specified, the issues of these documents are those listed in the current issue of the Department of Defense (DoD) Index of Specifications and Standards (DoDISS) and supplements thereto.

SPECIFICATIONS

MILITARY

MIL-O-55310B Military Specifications, General Specification for Crystal Oscillators, 10 May 1988

STANDARDS

FEDERAL

FED-STD-1037A Glossary of Telecommunication Terms, 26 June 1986

MILITARY

MIL-STD-188-115 Interoperability and Performance Standards for Communications Timing and Synchronization Subsystems, 31 March 1986

[Copies of federal and military specifications, standards, and handbooks are available from the Naval Publications and Forms Center (ATTN: NPODS), 5801 Tabor Avenue, Philadelphia, PA 19120-5099.]

2.1.2 Other Government documents, drawings, and publications

DoD

DoDISS Department of Defense Index of Specifications and Standards

[Copies of the DoDISS are available by yearly subscription either from the Government Printing Office (for hardcopy), or from the Director, Navy Publications and Printing Service Office, 700 Robbins Avenue, Philadelphia, PA 19111-5093 (for microfiche copies).]

Defense Communications Engineering Center (DCEC)

DCEC
Technical Note 1-87 Application of the NAVSTAR Global Positioning System (GPS) to the Network Synchronization of the DCS, March 1987

3

DCEC Technical Comment 49-73	Discrete Control Correction: A Method for Timing and Synchronizing a Digital Communications System, November 1973
DCEC-EP-1-80	Attributes for Timing for a Digital DCS, July 1980
DCEC-TR-23-77	DCS II Timing Subsystem, December 1977

(Copies of DCEC publications may be obtained from the Defense Communications Engineering Center, Derey Engineering Building, 1860 Wiehle Avenue, Reston, VA 22090-5500.)

Air Force Institute of Technology (AFIT)

AFIT/CI/M12-87-17T	The Fundamentals of Timing and Synchronization for Digital Communications Networks, 25 July 1986

National Institute of Standards and Technology (NIST), U.S. Department of Commerce [formerly the National Bureau of Standards (NBS)]

NIST Special Publication 432	NIST Time and Frequency Dissemination Services, 1990
NIST Special Publication 559	Time and Frequency Users Manual, 1990.
NIST Technical Note 616	Time and Frequency Division, 1977
NIST Technical Note 1337	Characterization of Clocks and Oscillators, 1990

(Copies of NIST publications may be obtained from the Superintendent of Documents, U.S. Government Printing Office, Washington, DC 20402-0001.)

U.S. Army Laboratory Command

SLCET-TR-88-1	Quartz Crystal Resonators and Oscillators for Frequency Control and Timing Applications, Revision 4.2, March 1991; ADA231604

2.2 Non-Government publications. The following documents form a part of this MIL-HDBK to the extent specified herein. Unless otherwise specified, the issues of these documents, which are DoD adopted, are those listed in the current issue of the DoDISS.

Institute of Electrical and Electronic Engineers (IEEE)

IEEE-STD-100	IEEE Standard Dictionary of Electrical and Electronics Terms, 1988

IEEE-STD-1139   IEEE Standard Definitions of Physical
                       Quantities for Fundamental Frequency and
                       Time Metrology, 1988

(Copies may be ordered from the Institute of Electrical and Electronics Engineers, Inc., 445 Hoes Lane, P. O. Box 1331, Piscataway, NJ 08854-1331.)

International Telecommunications Union (ITU)

    Consultative Committee for International Telegraph and Telephone (CCITT)

CCITT
Recommendation 0.171   Timing Jitter Measuring Equipment for Digital
                       Systems, Volume IV, Fascicle IV.4, 1988

    International Radio Consultative Committee (CCIR)

CCIR   Characterization of Frequency and
Report 580-2   Phase Noise, 1990

CCIR   Standard-Frequency and Time-Signal
Recommendation 460-4   Emissions, 1990

CCIR   International Synchronization of UTC Time
Recommendation 685   Scales, 1990

CCIR   Glossary, 1990
Recommendation 686

[Copies of CCITT and CCIR publications may be obtained from the International Telecommunications Union (ITU), General Secretariat -:- Sales Section, Place des Nations, CH1211 Geneva 20, Switzerland.]

Gerber, E. A. and A. Ballato   *Precision Frequency Control*, Academic Press,
                                 1985*

Harris Corporation   *DCS Synchronization Subsystem Optimization
                                 Comparison Study*, November 1979 (Control
                                 Number DCA 100-77-C-0055), Government
                                 Communication Systems Division,
                                 Melbourne, FL

Kartaschoff, P.   *Frequency and Time*, Academic Press, London,
                                 1978*

* Copies may be ordered through commercial bookstores.

NOTE: Non-Government standards and other publications usually are available from the organizations that prepare or distribute them. These standards and publications also may be available in or through public libraries or other informational services.

2.3 Order of precedence. In the event of a conflict between the text of this MIL-HDBK and Federal or military standards, the text of the standard(s) shall take precedence.

This page intentionally left blank.

3. DEFINITIONS

3.1 <u>Acronyms used in this handbook.</u> The acronyms used in this handbook and not included in FED-STD-1037 are defined as follows:

a.	AFIT	Air Force Institute of Technology
b.	CNCE	communications nodal control element
c.	DCEC	Defense Communications Engineering Center
d.	DoDD	Department of Defense Directive
e.	DoDISS	Department of Defense Index of Specifications and Standards
f.	FED-STD	federal standard
g.	GPS	Global Positioning System
h.	h	hour(s)
i.	HAVE QUICK	joint tactical anti-jam communications equipment
j.	JPL	Jet Propulsion Laboratory
k.	JSC	Joint Steering Committee
l.	LPE	low probability of exploitation
m.	MCS	master control system
n.	MCXO	microcomputer-compensated crystal oscillator
o.	MIL-HDBK	military handbook
p.	MIL-STD	military standard
q.	min	minute(s)
r.	ms	millisecond(s) (10^{-3} seconds)
s.	MTCC	Modular Tactical Communications Center
t.	mW	milliwatt(s)
u.	NAVSOC	Naval Satellite Operations Center
v.	NIST	National Institute of Standards and Technology
w.	ns	nanosecond(s) (10^{-9} seconds or 10^{-3} microseconds)
x.	OCU	orderwire control unit

7

y.	OCXO	oven-controlled crystal oscillator
z.	PLL	phase-locked loop
aa.	PN	pseudonoise
ab.	PS	positioning system
ac.	PTS	precise time station
ad.	PTTI	precise time and time interval
ae.	Rb	rubidium
af.	RbXO	rubidium crystal oscillator
ag.	SATCOM	satellite communications
ah.	SINCGARS	Single Channel Ground and Airborne Radio System
ai.	SLHC	strategic long-haul communications
aj.	(S/N)	signal-to-noise ratio
ak.	SPAWAR	Space and Naval Warfare Systems Command
al.	TACAMO	Navy Airborne VLF/LF Relay Aircraft
am.	TCTS	tactical communications technical standards
an.	TCXO	temperature-compensated crystal oscillator
ao.	TOD	time of day
ap.	VLBI	very long baseline interferometry

3.2 __Accuracy__. Generally equivalent to the systematic uncertainty of a value, relative to the accepted standard for the value. In the case of time, the accepted standard for the Department of Defense is the U.S. Naval Observatory (USNO) Master Clock.

3.3 __Aging__. The relationship between oscillator frequency and time when the oscillator frequency is measured under constant environment, supply voltage, and load. This long-term frequency change is caused by secular changes in the oscillator's frequency-determining elements.

3.4 __Alternate clock__. A member of a set of redundant clocks that is not normally active in providing a time, phase, or frequency reference, but is held in reserve to take over the function of the principal clock if the principal clock should fail or some other contingency should arise. The term is used interchangeably with the term _backup clock_.

3.5   Ambiguity. The characteristics or property whereby more than one possible interpretation, management, or value satisfies the conditions stated. A clock that displays 3 hours 5 minutes could be indicating that time for either a.m., p.m., or for any day. Further information is required to remove the ambiguity if it causes any problems. In a system where the additional information is already available, it is not necessary for it to be supplied by the clock (see *time ambiguity*).

3.6   Calibration. The process of identifying and measuring errors, and either accounting for them or providing for their correction.

3.7   Closed-loop noise bandwidth. The integral, over all frequencies of the absolute value of the closed-loop transfer function of a phase-locked loop. The closed-loop noise bandwidth when multiplied by the noise spectral density gives the output noise in a phase-locked loop.

3.8   External timing reference. A timing reference obtained from a source external to the communications system, such as one of the navigation systems, many of which are referenced to Coordinated Universal Time (UTC).

3.9   False lock. A condition in which a phase-locked loop locks to a frequency other than the correct one, or to an improper phase.

3.10   Fractional frequency fluctuation. Frequency of an oscillator expressed as a fraction of the nominal or previous frequency.

3.11   Free-running capability. The capability of a normally synchronized oscillator that can operate in the absence of a synchronizing signal.

3.12   Frequency difference. The algebraic difference between two frequencies that can be of identical or different nominal values.

3.13   Hold-in frequency range. The maximum frequency range duration between the local oscillator and the reference frequency of a phase-locked loop for which the local oscillator slaves to the reference frequency.

3.14   Independence of clock-error measurement and correction. A property by which a change in the time (phase) of a clock at a particular node (whether for clock correction or any other purpose) is not permitted to affect the measurement of the error in the clock at another node.

3.15   Independent clocks. A communications network timing subsystem that uses precise free-running clocks at the nodes for synchronization purposes. Variable storage buffers installed to accommodate transmission delay variations between nodes are made large enough to accommodate small time (phase) departures among the nodal clocks that control transmission. Traffic is occasionally interrupted to reset the buffers.

3.16   Information. The meaning assigned to data.

3.17   Limit cycle. A closed curve in the stable space of a closed-loop control system to which the trajectory either approaches asymptotically (stable) or from which it recedes (unstable) for all sufficiently closed initial states.

9

3.18 Local clock. A clock located in proximity to a particular communications station, node, or other facility with which it is associated. The same clock might be a remote clock relative to some other station, node, or facility.

3.19 Long-term stability. The relationship between oscillator frequency and time when the oscillator frequency is measured under constant environment, supply voltage, and load. This long-term frequency change is caused by changes in the oscillator's frequency-determining elements.

3.20 Loop filter. A filter located between the phase detector (or time discriminator) and the voltage controlled oscillator (or phase shifter) of a phase-locked loop.

3.21 Major node. In a timing system for a communications network, a node that is connected to three or more nodes, or one that is designated a major node because of its unique location or function (see *minor node*).

3.22 Minor node. A node that is not designated a major node. Minor nodes are normally connected to no more than two other nodes (see *major node*).

3.23 Nodal clock. The principal clock or alternate clock, located at a particular node, that provides the timing reference for all major functions at that node.

3.24 Nominal value. An assigned, specified, or intended value of any quantity with uncertainty in its actual realization.

3.25 Nonlinear phase. Lack of direct proportionality of phase-shift to frequency over the frequency range required for transmission.

3.26 Offset. An intentional difference between the realized value and the nominal value.

3.27 Offset frequency. The amount by which an available frequency is intentionally offset from its nominal frequency. In the case of U.S. television networks, the offset is about 3000 parts in 10^{11}.

3.28 Overall accuracy. The total uncertainty resulting from both systematic and random contributions of all systems, operations, and equipment involved in achieving or maintaining accuracy (see *accuracy, random clock errors*).

3.29 Phase instability. Expressed by the phase change within a given time interval.

3.30 Phase microstepper. A device that generates (in response to a digital control signal) subnanosecond (or picosecond) adjustments to the phase of a reference input signal. This can be accomplished either through regular phase progression for frequency corrections or by individual phase steps. Typically, the changes are on the order of subnanoseconds/second.

3.31 Principal clock. The clock that actively provides a time, phase, or frequency reference for a node, a network, or both. Normally there is also a set of one or more alternate clocks held in reserve to take over the principal clock's function, should it fail or should some other contingency arise.

3.32 <u>Pull-in frequency range</u>. The maximum frequency that a local oscillator can deviate from the reference frequency and, upon initial receipt of the reference frequency, still achieve phase-lock.

3.33 <u>Quartz clock</u>. A clock containing a quartz oscillator that determines the clock's precision for measuring time intervals (see *quartz oscillator*).

3.34 <u>Quartz oscillator</u>. An oscillator that uses the piezoelectric property of a quartz crystal, which is caused to vibrate at a nearly constant frequency depending on its size, shape, and mode of excitation. After a crystal is placed in operation, the frequency changes slowly as a result of physical changes. Quartz oscillators are used in most frequency control applications, including atomic standards.

3.35 <u>Random clock errors</u>. Clock performance is sometimes characterized in terms of errors stemming from various noise types, one of which may predominate in a given part of the spectrum, while another may predominate in another part. However, since these cannot always be distinguished from the effects of environmental sensitivities and other systemic causes, it is not necessarily valid to presume that a specific noise type is dominant in a particular part of the spectrum, especially at the lower frequency (longer period) end of the spectrum.

3.36 <u>Rubidium clock</u>. A clock containing a rubidium standard that determines the clock's precision for measuring time intervals (see *quartz clock*).

3.37 <u>Rubidium standard</u>. A secondary frequency standard in which a rubidium gas cell is used to reduce the drift of a quartz oscillator through a frequency-locked loop. Because it depends on a cell's gas mixture and pressure, it must be calibrated. It has a drift typically 100 times less than the best quartz standard (see *quartz oscillator*).

3.38 <u>Sampling</u>. The process of obtaining a sequence of instantaneous values of a wave at regular or intermittent intervals.

3.39 <u>Secondary time standard</u>. A time standard that periodically requires calibration.

3.40 <u>Signal transit time</u>. The time required for a signal to travel from one point to another. Signal transit time delay might refer to time required for a signal to travel between specific locations within the same piece of equipment or between specific locations in widely separated pieces of equipment. The particular locations should be identified when the term is used (see *time delay*).

3.41 <u>Spectral purity</u>. The degree to which a signal is coherent, that is, a single frequency with a minimum of sideband noise power.

3.42 <u>Stability</u>. The stated amount of a clock's change over a long period of time; a digital reference clock's stability specifies its drift away from the frequency it had when locked to another source.

3.43 <u>Standard frequency</u>. A frequency with a known relationship to an accepted frequency standard.

3.44 <u>Subservient clock</u>. A clock that is synchronous to an associated master clock, but that may have a controlled-phase or time offset from its associated master. The controlled-phase offset may be a function of time, such as that required to permit a communications receiver's subservient clock to follow variations (which result from changing parameters in the circuit path) in the phase of a received signal. The controlled-phase offset allows the subservient clock to maintain a known phase (and in some cases phase-rate) relationship with the nodal clock (see *principal clock*), and to maintain proper rates during loss of signal from its master.

3.45 <u>Subservient oscillator</u>. The difference between a subservient oscillator and a subservient clock is that the subservient oscillator does not have to identify particular cycles or particular time interval markers; that is, it is only a source of frequency or of a phase modulo 1 cycle. The subservient oscillator is therefore somewhat less complex than a subservient clock. For many communications applications, either would satisfy the requirement. Some applications require a clock (see *subservient clock*).

3.46 <u>Sweep acquisition</u>. A technique whereby the frequency of the local oscillator is slowly swept past the reference to ensure that the pull-in range is reached (see *pull-in frequency range*).

3.47 <u>Synchronous system</u>. A system in which the sending and receiving instruments are operating at substantially the same rate and are maintained by means of correction, if necessary, in a fixed relationship.

3.48 <u>Time ambiguity</u>. A situation in which more than one different time or time measurement can be obtained under the stated conditions.

3.49 <u>Time delay</u>. The time interval between the manifestation of a signal at one point and the manifestation or detection of the same signal at another point (see *signal transit time*).

3.50 <u>Time-division analog switching</u>. Analog switching with common time-divided paths for simultaneous calls.

3.51 <u>Time-division digital switching</u>. Digital switching with common time-divided paths for simultaneous calls.

3.52 <u>Time interval</u>. The duration between two instants read on the same time scale.

3.53 <u>Time marker</u>. A reference signal, often repeated periodically, enabling numerical values to be assigned to specific events on a time scale. Time markers are used in some systems for establishing synchronization.

3.54 <u>Time measurement tolerance</u>. The maximum permissible error of a time measurement.

3.55 <u>Time-reference distribution correction</u>. A time-reference distribution technique that employs independence of clock-error measurement and correction. It also permits the time-reference information for each node to be derived from a near-optimum weight average of several paths between that node and the master node, while avoiding all closed loops.

3.56 <u>Timing</u>. A broad term that includes synchronizing as a special case. It implies (a) scheduling; (b) making coincident in time or causing to occur in unison; (c) setting the tempo or regulating the speed; (d) ascertaining the length of time or period during which an action, process, or condition continues; (e) causing an action or event to occur at a desired instant relative to some other action or event; (f) producing a desired relative motion between objects; (g) causing an event to occur after a particular time delay; or (h) determining the moment of an event.

3.57 <u>Timing ambiguity</u>. See *time ambiguity*.

3.58 <u>Timing reference</u>. A frequency reference for a clock to follow.

3.59 <u>Timing signal</u>. A signal used to aid the synchronization of interconnected equipment.

3.60 <u>Tracking error</u>. The deviation of a dependent variable with respect to a reference function.

3.61 <u>Transit time</u>. The time required for a signal to travel from one point to another. Sometimes it is called *propagation time delay*. Propagation time delay can refer to time required for a signal to travel between specific locations within the same piece of equipment or between specific locations in widely separated pieces of equipment. The particular locations should be identified when the term is used (see *time delay, signal transit time*).

3.62 <u>Uniform time-scale</u>. Uses equal intervals for its successive scale intervals.

3.63 <u>Variable storage buffers</u>. Digital data storage units in which a signal can be temporarily stored to correct its timing. The signal is usually written into the buffer by one clock that has incorrect timing, and read out of the buffer by a different clock that has correct (or nearly correct) timing. They are also called *elastic buffers* or, simply, *buffers*.

3.64 <u>Warm-up characteristics</u>. The behavior of a device from the time power is applied until thermally-induced transient effects have subsided. Some of the warm-up characteristics for a clock or oscillator are (a) the time required for the frequency rate, if it is to come within some accuracy or some specified steady-state value; (b) the time required for the drift rate to fall within some maximum specified value; and (c) the time required for the frequency rate to recover to within a specified tolerance of the rate that had existed just before the device was previously turned off (defined as *retrace*).

This page intentionally left blank.

4. GENERAL REQUIREMENTS

4.1   General. As electronic communications has progressed, many of its stages of advancement have required significant improvements in frequency sources. Radio communications progressed from the inaccurate frequency requirements of spark transmitters to the relatively accurate reinsertion of the carrier frequency in single sideband-suppressed carrier voice communications. Through the various stages of progress, receivers for several types of communications systems have employed automatic frequency control, but further improvements in stability and accuracy of oscillators have made such feedback control systems unnecessary for many of these applications. For the information signals required by some forms of communications, such as television and facsimile, maintaining a desired frequency tolerance is not sufficient. The relative phase also must be controlled; that is, the receiver must be synchronized to the received signal. Digital communications is one type of communications requiring phase control. As the use of digital communications increases, becomes more complex, and employs higher data rates, requirements for phase control become more demanding. In addition, the number of systems that require an accurate knowledge of time (including the time of day) to acquire synchronization is increasing.

The timing function so pervades the field of electronic communications that choices applied to other functions often depend on the quality and availability of the timing function. For this reason, whenever improved timing capabilities can be accomplished with no significant penalty, they are to be included in the planning and implementation of new digital communications systems or major modifications to existing systems. The need for timing and synchronization becomes more apparent every day as new, more sophisticated digital systems are developed and fielded.

Technology has reached the point where past compromises can be minimized. The effect that this could have on other functional disciplines could be very significant. The benefits of such new designs (cost reduction, new functional capabilities, or improved system survivability) must be extensively available in interfacing systems and equipment. Indeed, such planned availability of the timing capability is necessary to avoid discouraging the development of potential future benefits. Network timing and synchronization are critical design issues, since the system objectives established for future switched communication systems reflect a need for systems that are predominantly digital and oriented toward (a) the satisfaction of end-to-end security requirements, and (b) the unification of voice and nonvoice communication networks. Time-division multiplexing (TDM), time-division switching, and time-division multiple access all place stringent requirements on the allowable timing variations within a single bit stream and between a network's different bit streams.

The timing subsystem's function is to provide and regulate the timing signals of all subsystems to meet the bit integrity and transmission synchronization requirements of the specification. Bit integrity requires that all bits inserted into the system be ultimately delivered to the intended destination in the proper order, and that spurious bits not be added within the system. Obtaining and retaining synchronization is essential in all digital transmission systems. Both bit integrity and communications are lost when a transmission link loses synchronization.

4.2   Frequency sources. The need for greater precision and accuracy in frequency control devices continues to grow. New communications systems are being developed that have the need for very precise and accurate frequency. The general types of frequency and time standards consist of atomic, quartz, and crystal standards. Atomic resonance standards use quantum mechanical effects in the energy states of matter, particularly transitions between states separated by energies corresponding to microwave frequencies. Transitions having properties well suited to use in standards occur in cesium, rubidium, thallium, hydrogen, mercury, and other elements. Stability ranges $[\sigma_y(\tau)]$ for cesium, rubidium, and quartz oscillators, and the hydrogen maser are shown in Figure 1; nominal power spectral density $[S_\varnothing(f)]$ of phase is shown in Figure 2.

This military handbook focuses on three atomic oscillator devices: the cesium beam tube, the rubidium gas-cell resonator, and the hydrogen maser. The cesium and rubidium devices use passive atomic resonators to steer conventional quartz crystal oscillators via feedback control circuits. The hydrogen maser, as an active device, derives its signal from stimulated emission of microwave energy, which may be amplified by electronic means to a useful power level and is normally used to steer a quartz oscillator. A newer version of the hydrogen maser uses a smaller cavity than required to bring about oscillation, and hydrogen resonance is used passively to control a quartz oscillator's frequency. Passive hydrogen masers, much smaller and lighter than the active ones, are now under development for both space and ground military applications.

The following atomic clocks have been developed and are operational and practical:

a.   the cesium beam clock,
b.   the rubidium resonance cell clock, and
c.   the hydrogen maser clock.

Of the three, only the rubidium and cesium clocks are off-the-shelf items. Other frequency standard devices that have been investigated are the ammonia maser, the methane stabilized laser, the rubidium gas-cell maser, the thallium beam tube, and the stored mercury ion standard. The ammonia maser was attractive because of the high spectral purity and excellent short-term stability it offered. The rubidium maser is a more recent development, which offered the prospect of exceptional spectral purity. The thallium beam tube offered greater relative precision and reduced magnetic field dependence. The stored mercury ion standard, developed for the United States Naval Observatory (USNO) and currently being evaluated by them, appears to have very good retrace characteristics and may be usable as a primary standard. However, the cost, size, and complexity of these devices has limited their current use to the laboratory. The methane stabilized laser offers low cost, easy fabrication, and excellent short-term stability. A current disadvantage is that it operates in the infrared region and hence is difficult to use. The quartz crystal is the workhorse of the frequency control devices. Although it is a secondary standard and must be calibrated (and perhaps periodically recalibrated) from other standards, it has adequate stability for many of the less demanding frequency-reference duties. It is the basis for the short-term stability of most atomic standards, but by itself it is inferior to the atomic standards for long-term timekeeping.
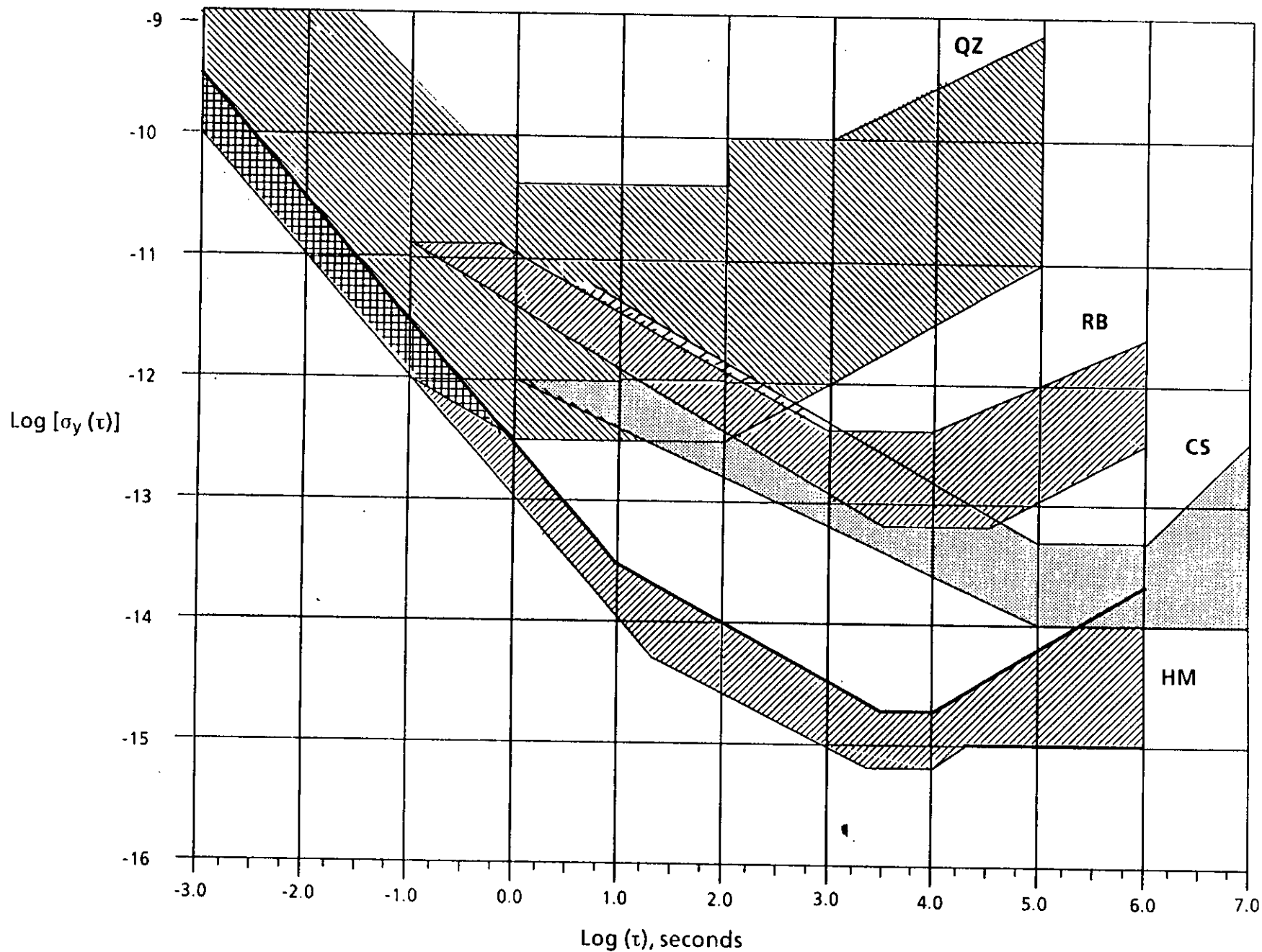
FIGURE 1. Stability ranges of various frequency standards.

MIL-HDBK-421

17
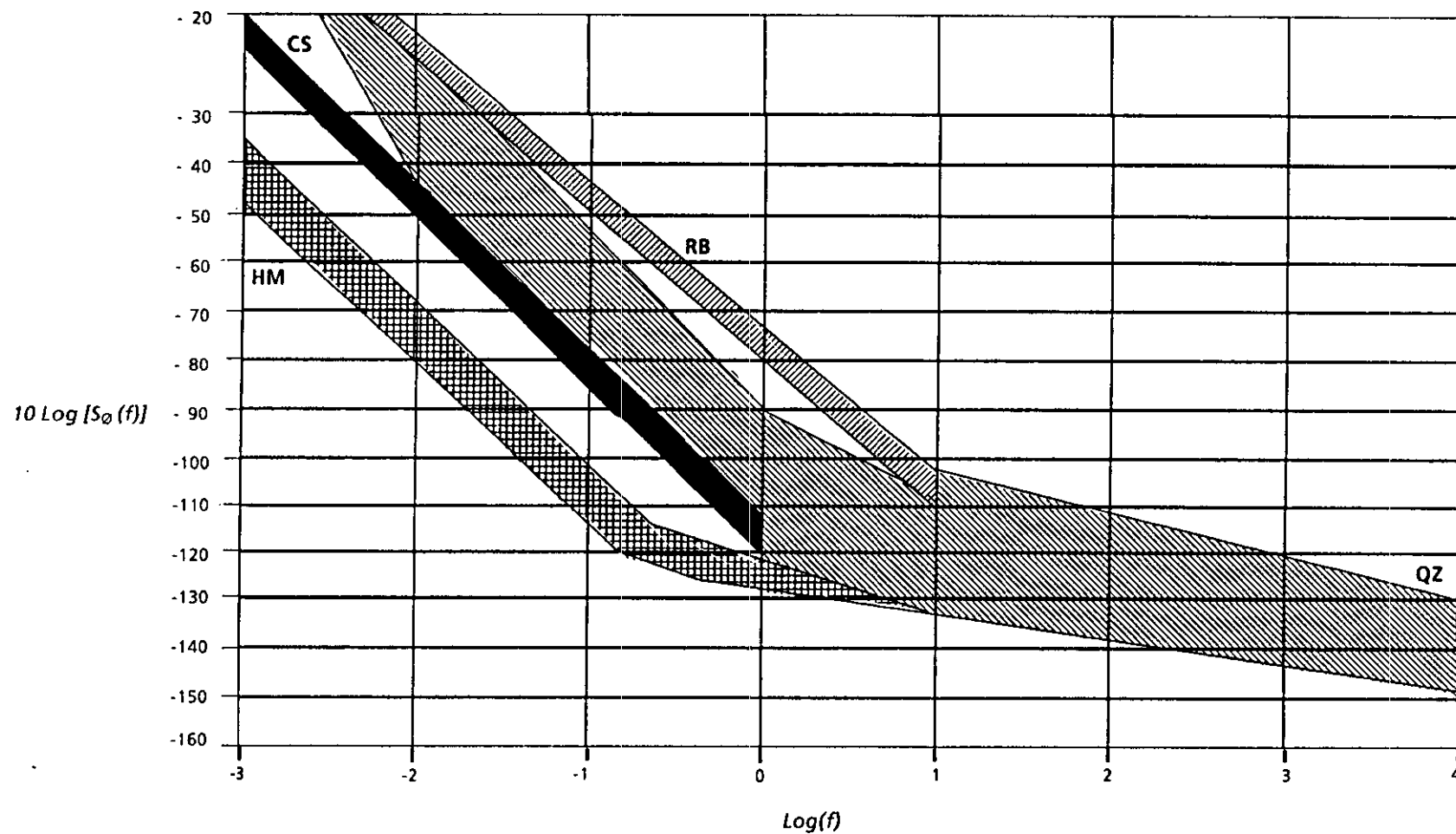
FIGURE 2. Nominal power spectral density of phase for various standards calculated at 5 MHz.

MIL-HDBK-421

18

4.3 Data buffers. In a switched synchronous digital communications network employing time-division switching, each bit must be available at TDMs or time-division switches at the correct time to fill its assigned time slot in the interleaved bit stream. There are always variations in the internodal transit time for signals because of variations in the transmission medium, variations in time delay through transmission equipment, variations in clocks, and variations in the length of the signal path. Buffers are used to accommodate these variations. These buffers act as reservoirs in which bits are temporarily stored to accommodate variations in the signal's transit time from one node to another node, and also to accommodate variations in nodal clocks. To process different TDM signals at the switching nodes, one must have the various inputs at exactly the same frequency. This requirement can be met in one of two ways: either the various inputs must be completely synchronous, or each input must be buffered prior to being combined or processed. The latter situation requires a buffer storage capacity that depends on the frequency difference between the input signal and the local clock used for sampling the buffer output. It also depends on the period of time since the buffer was reset.

4.4 Network internal timing methods. Network timing and synchronization are critical design issues, since some communications objectives reflect a need for automated digital systems specifically designed to accommodate both voice and nonvoice traffic and to provide communications security (COMSEC) on an end-to-end basis. For satisfactory system operation, stringent requirements must be satisfied with regard to the timing variations allowable both within and among the digital bit streams handled by the systems. Several different synchronous and asynchronous concepts could be employed to provide network timing. Independent stable clocks and bit stuffing represent two possible asynchronous concepts. Master-slave and frequency averaging represent two possible synchronous concepts. Basic operational requirements that concern network timing relate to the need for systems to accommodate TDM, digital switching, and encryption, and to maintain bit-count integrity. Precise timing is also required for obtaining end-to-end COMSEC, electronic counter-countermeasures with pseudonoise (PN)-coded signals, and an acceptable data transmission capability. In some systems, an accurate knowledge of time is required to acquire synchronization within an acceptable period of time.

In a digital system, all switching operations within a node are timed at a local clock rate so that processor operation is synchronous. Since the incoming bit streams from other nodes may differ slightly in actual transmission rate, it is necessary to regenerate and retime the received signals to avoid losing information. Data is read into the retiming unit at the incoming rate and transferred out at the rate determined by the local clock. If the incoming rates and the local rate are the same, then the retiming unit is needed only for the proper phasing of sampling times. Since the rates of different links are not identical, data can accumulate in the stores associated with the retiming units. From a practical viewpoint, the link rates would differ instantaneously, due to propagation variations, even if the links had the same long-term average value; consequently, buffers would be required in any case to compensate for large transient disturbances. In some applications, when buffers are employed and overflow or depletion occurs, the stores must be automatically reset.

The ultimate time or frequency reference for most communications systems is the USNO Master Clock. This means that clocks of each node should be traceable to that reference; however, the means of accomplishing traceability may be external or internal to the system, or a combination of external and internal dissemination. A "primary" frequency standard, such as a cesium standard, would give a *frequency*

reference that agrees with the USNO Master Clock within, perhaps, 1 part in 10^{11} or a few parts in 10^{12} without resorting to the USNO clock. When *time* (as, for example, time of day) must be known, some means of time dissemination traceable to USNO is needed. (Some systems have an inherent capability to disseminate time within the system, yet others require time from an external source before communications can be initiated.) Where an internal dissemination capability exists (normally in continuously or frequently connected links), it might be used to advantage to coordinate the nodal clocks. Traceability to USNO, if needed, may be introduced into the system through external dissemination links that are periodically exercised only if a sufficiently good timekeeping or frequency-maintaining capability is held by the network. A good internal timekeeping and frequency-maintaining capability minimizes the impact of loss or temporary denial of the external or internal dissemination services.

Timing at system nodes should not be made to depend on either continuous or prompt service from an external time-dissemination system. Practically, this may mean that precisely timed communications systems should maintain good, well-coordinated internal timekeeping capabilities. Mobile units that would have trouble maintaining a continuous time reference should be provided with a capability for transfering time at the beginning of each mission from a precise time reference maintained at a post, base, depot, or port. A degraded mode of operation should also be provided to some systems to serve when time accuracy is degraded. This might include such provisions as lower information rates and frequent resynchronization.

It is sometimes advantageous, especially within continuously or frequently connected networks, to provide an internal network time-coordination capability. There are many methods for using communications systems to provide the timing information throughout the system. Care must be taken to prevent the accumulation of timing errors through long chains of nodal links from exceeding the allowable tolerance. Care must also be taken to avoid having the entire system "walk off" from the proper time or frequency; some form of hierarchical approach in which the higher level clocks are given sufficient inherent time or frequency accuracy to support the system may be used to avoid this. An automatic capability can be provided for any of a number of high-quality clocks distributed throughout the network to take over as master for the entire network, or any severed portion of the network. As an emergency measure, the hierarchy might be altered, perhaps automatically, to preserve synchronism throughout the network. In any event, the timing system must not be designed so as to create attractive, vulnerable targets, and the clocks should be of adequate timekeeping capability to maintain time or frequency accuracy during protracted loss-of-connectivity within the system.

Although an arbitrary time scale might sometimes appear attractive as a system reference, there are two main reasons for making system timing traceable to the USNO. The first is that the number of suitable references is maximized. A time reference, whether obtained through the system or externally through another communications or navigation system, is valid for operation of any node or nodal complex if all use a common time scale. For example, several collocated nodes, including nodes of different systems, can share timing assets (both hardware and time references) to increase the survivability of all systems if all use the same time scale, even if they obtain their time information through different services.

The second reason for maintaining traceability to the USNO addresses two slightly different situations: links between systems that must interoperate, and links between infrequently connected components of a single system. With a common time scale, these links may be established without protracted synchronization searches and maintained without excessive buffering requirements. Some links, particularly those using anti-jam or low probability of interception techniques such as PN codes or burst transmissions, cannot be established within a desirable period of time without prior knowledge of precise time on both ends. In general, they depend on external time references that must be referenced to the same time scale; therefore, the availability of multiple sources of the time scale can be a significant advantage.

4.5   Fundamental timing and synchronization approaches

4.5.1   Master-slave. In the master-slave method, the clock at another node (or nodes) is locked to a signal received from the master node. In the simplest master-slave system, the clock at a slave node lags behind the clock at the master node due to accumulated time delays in the signal path. However, there are methods by which these time delays can be removed, and clocks at slave nodes can be kept in step (within very close tolerance) with the clock at the master node. In the simplest master-slave system without corrections for the signal transit time, large time delays can accumulate. Although variations due to environmental conditions can be significant in the simple system, the magnitude of the variations is always bounded as long as the system functions properly. A master-slave system employs directed control; that is, the clock at only one end of a communications link connecting two nodes is permitted to take corrective action in response to an indication of timing error between the clocks at the two nodes.

The basic elements of a master-slave configuration are a data modem, a data buffer, and a phase-locked loop. The modem is used to regenerate the incoming digital bit stream. The buffer is used to absorb differences between the local clock rate at the receiving node and the basic clock rate of the incoming digital bit stream. Clock error corrections are based on filtered clock-error information derived from the received signal(s). The local clock rate at each node is derived from a phase-locked loop that is slaved to the stable frequency standard located at the master node. (The transit time for the signal to propagate from the master to the slave can be removed from the timing reference when additional accuracy is desired.)

To achieve network synchronization, the master node transmits a reference timing signal that is tracked by each of the slaved nodes. Signal tracking consists of measuring the time difference between the received version of the reference signal, as transmitted by the master node, and a replica of the reference signal, reproduced at the receiver. When the receiver signal and the replica are synchronous, the time difference is zero and the master timing signal will have been reproduced at the slaved node. There are many different master-slave approaches. Nearly all digital communications systems employ some form of the basic master-slave approach. In some simple master-slave systems, clocks at nodes directly connected to the master clock are phase-locked to the digital signal received from the master. Other nodes not connected to the master are slaved to those supported by another master-slave system capability. This technique is generally unsuitable for providing network synchronization for major nodes of a military communications system because of survivability problems (that is, the loss of a node in a tandem group prevents synchronous operation of the system). Advanced master-slave systems exist that overcome this survivability disadvantage.

21

4.5.1.1 <u>Advantages and disadvantages of the master-slave method.</u> The primary advantage of the master-slave method in large, static networks is the long-term accuracy that can be imparted to lower hierarchical levels when properly implemented. Even with the simplest master-slave approaches, the long-term average rates of the individual clocks are very nearly identical to that of the network master. If the master is referenced to the USNO Master Clock, every node in the network has a long-term average rate very nearly identical to that of the USNO. Therefore, when clocks are operating properly, it may be unnecessary to interrupt traffic to reset buffers anywhere in the network. In a worldwide network, without proper system design, disruptions not due to a clock error at a particular node can cause some disruptions in other parts of the network even if their clocks or buffers are undisturbed. It is inconvenient to reset buffers in such a network, and it is unnecessary in normal operation, but such a capability could be provided to restore operation in the event of degraded operation.

There are several subtypes of master-slave systems. These are the simple master-slave, hierarchical master-slave, preselected alternative master-slave, and loosely coupled master-slave. Each subtype has its own advantages and disadvantages. However, they all have the same basic idea as the simple master-slave.

The simple master-slave technique is economical and convenient to implement with a simple phase-locked loop, but if it is unsupported by a capability to reorganize itself to employ alternative masters and other enhancements, it possesses some survivability problems. Such survivability problems might be lessened by providing automatic master-slave reorganization, such as selection of a new master whenever required. By providing the ability to measure and remove errors during normal operation, and to predict and remove errors during a free-running period following a period of calibration, it can provide greater accuracy and uninterrupted operation for a longer period of time in the free-running mode.

A good method for improving a master-slave system's survivability in multichannel switched systems is to employ very *loose* coupling between the error-measurement and clock-correction processes (in normal operation it might require more than a day to make a 10-microsecond correction). With adequate clocks, this maintains many of the qualities of independent clocks while providing the long-term stability of phase-locked systems. In fact, this system could be considered an independent clock system with essentially continuous calibration against a stable (master) reference.

4.5.1.2 <u>Applications of master-slave for timing.</u> The master-slave approach is one of the most commonly applied methods of synchronizing communications. It is nearly always used for single transmission link communications. It is also commonly used for large networks in which, by selecting a suitable hierarchy, all nodes of the network are slaved (most of them indirectly) to a single master with provisions for selecting an alternate master when required.

4.5.1.3 <u>Referencing master-slave timing to Coordinated Universal Time.</u> If the master of a master-slave network is referenced to Coordinated Universal Time (UTC), all of the nodes of this master-slave network are referenced to UTC. To provide for survivability, every major node of a master-slave network should be capable of automatically being selected as master for the entire network, or as master for any severed portion of the network. Although UTC is usually not essential for satisfactory operation of a network, it enhances interfacing capabilities. A UTC reference should be provided to the master and to those other nodes selected as

most likely to ascend to master. This reference can be provided by a variety of dissemination means, any of which could be used to provide a reference to the UTC USNO. A sizeable number of satellite communications stations, for example, are designated as precise time stations (PTS). A PTS participates with the USNO to maintain time directly traceable to the USNO Master Clock through portable clock trips, satellite time transfers, or other means. These stations can provide time to many other parts of the Defense Communications System and to collocated or interconnected tactical nodes.

With such a system providing an accurate reference to the master of a master-slave system that is accurately disseminated internally to the communications network, nodal clocks can be maintained accurately until they are required to maintain time accuracy in a free-running mode. The free-running mode is necessary for survivability in all systems, but it is particularly important for some time-dependent systems. Survivability in a master-slave system can be maximized with an extended free-running capability, with multiple means for updating to the Department of Defense (DoD) reference, and with the ability to function autonomously without the DoD reference.

4.5.2 Independent stable clocks. With the independent clock approach, network timing is established by employing a frequency standard at each node to provide a stable local timing reference. This method is generally considered asynchronous since the frequency standards vary slightly from node to node. It could, however, be viewed as a synchronous system, since, fundamentally, each input at the node is synchronized to a single local stable reference at the node. The differences between the basic bit rates of the incoming trunk groups and that of the local timing source are accommodated through employment of buffers used to retime the incoming trunk traffic. To minimize the differences among timing sources, atomic clocks are generally used to implement the independent clock approach.

The basic elements of the independent clock network timing approach include a modem, an m-bit buffer, and a primary (stable) frequency standard. The modem is used to regenerate the incoming digital bit stream. The stable clock is used to provide a local clock rate. The buffer is used to absorb phase differences caused by differences between the frequency of the local clock at the receiving node and the frequency associated with the incoming digital bit stream. Since buffer output is controlled by the nodal clock, the incoming digital bit stream is retimed in accordance with the local clock.

The buffer is an asynchronous first-in, first-out shift register. This enables the data to be entered and withdrawn at different rates. Since the output rate of the buffer is controlled by the nodal clock, the incoming digital bit stream is retimed in accordance with the frequency of the local clock or, in essence, each input is synchronized to the frequency of the local clock.

The apparent basic clock frequency of the incoming digital bit stream can differ from that of the local nodal clock, due to inherent differences in the clocks at the two nodes and the propagation delay variations of the internodal transmission links. These factors, as well as the link transmission rate and the allowable buffer reset period, dictate the buffer's capacity requirements.

The independent stable clock method provides frequency stability that is not affected by system operation or by any external signal source; it is therefore immune to jamming signals and lost links (destroyed nodes). The approach is also not suscep-

tible to transient disturbances in the network frequency. Buffers must be employed on each internodal link to accommodate timing differences between the sending and receiving nodes, and to accommodate frequency variations caused by the transmission media. Because of long-term accumulated phase or time differences, the buffers must be periodically reset. A major advantage of the approach is that the effects of malfunctions in links and nodes are not propagated throughout the network. Cesium clocks have an inherent frequency accuracy, although they may need occasional routine operational checks. Rubidium standards change frequency with time and must be recalibrated using a known frequency standard.

4.5.3 **Frequency averaging**. Frequency averaging is a network synchronization technique in which an oscillator at each node adjusts its frequency to the average frequency of the digital bit streams received from the nodes to which that node is connected. Using this scheme, all oscillators in the network are assigned equal weight in determining the ultimate network frequency, since there is no reference oscillator. The frequency averaging technique involves the determination of a reference phase at each node by taking the average of all the incoming clock phases, plus that of the node's local clock. Frequency averaging is a synchronous technique, and ideally all the nodal frequencies should have the same average value. Buffer storage is required on each link to compensate for dynamic variations in propagation delay and to accommodate the differences between the local clock rate and that of the distant node.

To implement frequency averaging, each internodal link terminated at the node is equipped with its own phase-locked loop, which is able to track the incoming bit stream to within a small fraction of a bit phase error. This clock is used for regeneration of an incoming bit stream, frame synchronization, and readout of bits to the retiming buffer store. Buffer storage is necessary to accommodate the accumulation of input bits when the input rate is slightly above the local clock rate, or to supply bits when the input rate is below the local clock rate.

The regenerated input bit stream is shifted through the buffer at the input clock rate for that link. The rate of extracting the data is the local clock rate, and the position for readout of the bit stream from the shift register is controlled by continuously monitoring the phase changes between the individual input clock rate and the local clock rate. When the transmission link is initially established, the point at which bits are read out from the retiming buffer is set at the center of the register. This allows the buffer to compensate for positive or negative phase changes between the clocks, equal to half the total buffer length with no loss of bits.

The advantage of the frequency averaging technique is its small size. Although the frequency averaging technique is considered to represent a plausible method for network synchronization, the technique does possess certain major disadvantages. Loss of a link, or jamming of a link, in the network introduces a transient disturbance that is propagated throughout the system. Further, there are design limitations that require parameters (such as gain, propagation delay, and bandwidth) to be maintained within certain bounds. Excessive gain delay product and improper choice of loop bandwidth can produce system instability. Parameter bounds are a function of network size, and their establishment represents a difficult problem for large networks.

4.5.4 **Pulse stuffing**. Pulse stuffing is a synchronization technique that has been found to be effective in point-to-point communications but that has distinct disadvantages in a network configuration.

24

MIL-HDBK-421

With pulse stuffing, all asynchronous inputs received at a node, at rates slightly lower than the outgoing rate of the node, have dummy bits added to make their rate equal to the local clock rate. The additional pulses are inserted at prearranged locations so that eventually they can be removed. The location of a stuff pulse is signaled by a separate channel. Since correct removal of all stuff pulses is essential, an effective error control must be provided for the signaling channel.

To provide synchronization on a network basis, pulse deletion is also required to accommodate the inputs received at rates slightly higher than the local clock rate. The deleted bits, along with information to identify the exact locations at which the bits should be inserted, must be transmitted to the distant node in an error-protected manner by the separate signaling channel.

A distinct disadvantage of pulse stuffing is the amount of processing required. The processing at the transmitter end consists of determining where each stuff pulse should occur, and signaling the locations of the stuff pulses to the receiving end. Processing at the receiving end consists of reading the location of the stuffed pulses. The technique is inherently complex for a nodal network configuration, it is expensive to implement, and its cost is sensitive to traffic growth.

4.5.5 <u>Time-dependent networks.</u> The use of a common time reference by all networks permits one to aid another and all to take advantage of the timing services offered by other systems whose timing is traceable to the USNO. It also makes possible the use of a common clock facility by collocated nodes.

Passive time-dissemination does not require the user to radiate signals in order to acquire accurate time information. The use of external time-dissemination services traceable to the USNO may be necessary in certain links or networks that, for operational or security reasons, are established or entered only at certain times.

A number of systems require precise time and must therefore continuously maintain accurate clocks. Some of these systems have a built-in capability to maintain traceability to the DoD Master Clock (USNO Master Clock), yet others use external means or a combination of internal and external means for redundancy and survivability. Some systems employ redundant local atomic clocks (generally cesium) to provide an in-house capability that would survive prolonged inability to check time against the DoD Master Clock. They may also have alternative dissemination means available for access to other traceable UTC references both to increase their own survivability, and to provide alternate links between the references and the DoD Master Clock. Some of these systems make their accurate time signals available to other collocated systems or nodes.

The issue of survivability is most important in a time-dependent system and requires that the timing and synchronization aspects of the system be identified and addressed as an integral part of the system architecture. Of particular importance are the free-running capability of each clock system and the availability of UTC reference sources. Redundancy is commonly employed in clock systems to ensure that the local time reference is not lost during free-running. Major systems frequently contain clock ensembles with comparison means to identify a substandard or malfunctioning clock. The clocks of the ensemble normally run relatively independently of each other so that no clock or control system failure seriously affects all of the clocks.

25

In time-dependent systems, loss of the accurate nodal time reference is generally of greater consequence than a temporary discontinuity in providing timing signals. Also, in time-dependent systems, the clock's free-running performance requirements are generally more difficult to meet than the requirements for an accurate frequency alone. For these reasons, clock-system design objectives for a time-dependent system may be different from those of a system whose only timing requirement is an accurate frequency or accurate timing. Compatible clock-system designs should be used wherever the clock might at some time be required to serve the dual-purpose of supplying an accurate frequency and acting as a time reference.

Intermittent or late entry into some networks can be greatly facilitated by a prior knowledge of network time, whether time is obtained by time-dissemination or by other means. Navigation systems that disseminate time are frequently employed for time dissemination. They, along with other systems, make it possible (sometimes automatically) to correct for propagation time delays.

4.5.6 Timing for networks requiring accurate time. The bit-stream timing and synchronization of a system using a UTC-traceable time reference requires an accurate frequency standard, but not necessarily accurate time. However, for some networks, accurate time (used in the sense of epoch or occasion of a nonrecurring or rarely recurring event) is required. These networks are designed to resist jamming; reduce chances of intercept or spoofing; enhance signal reception in noise; reduce or eliminate synchronization overhead; deny use of assets (such as satellites) to others; provide synergy with position-location, navigation, or intelligence systems; identify or authenticate; permit immediate or quick entry and reduce guard bands in TDMA systems; or provide combinations of these features. Although some systems that require precise time may normally operate continuously, a need for precise time is often necessary to establish or reestablish a link or network or to bring new systems on-line within the network. Therefore, nodal clocks are often required to maintain accurate time whether the node is participating in network operations or not.

Although accurate frequency can be established and maintained at any location by using "primary" atomic standards, such as cesium-beam devices, accurate time must be obtained initially from a reference outside the node and maintained locally with reference to an accurate local frequency (or rate) standard until subsequently updated. Some means of time dissemination, either internal or external to the communications network, is required to coordinate the clocks in a time-synchronized link or network. The initial setting, which may also include a frequency (or rate) calibration, is accomplished through a time-dissemination or local distribution system. The reference for clock setting might be timing disseminated through a network, a portable clock, a clock of a collocated node or a common clock of collocated nodes, a navigation system, a special timing link, a time broadcast, or certain communications links (including special synchronizing modes of the network) that can provide the required accuracy.

5. TIMING AND SYNCHRONIZATION FUNDAMENTALS, CONCEPTS, AND RELATED THEORY

5.1 Jitter. Digital telecommunications networks are expanding. They are replacing many analog systems and are filling most new communications requirements. As digital installations increase and as more of these systems are interconnected into larger networks, the interest in signal jitter increases.

5.1.1 Sources of jitter. Jitter on a digital signal can be defined as a dynamic displacement in time (from the ideal) of the signal's logic-level transitions. Jitter is characterized by the amplitude of these displacements, usually expressed in bit or unit interval variations from the ideal, and by the frequency content of these displacements.

A typical digital transmission system consists of the following components: (a) a digital multiplexer that combines several input channels into a time-division multiplexed (TDM) bit stream; (b) a transmission medium, such as radio paths; (c) a wire or optical cable; (d) a regenerative repeater; and (e) a terminating equipment, such as a demultiplexer, a digital switch, or an input to another digital system. These system components can generate, attenuate, or even amplify jitter in the digital signal.

Transients, crosstalk, and thermal noise can cause noise-like variations, or jitter, on the output signal transitions. The amplitude and frequency response of system timing recovery circuits can also affect jitter. Although one would expect these circuits to remove input jitter, they actually pass or even amplify jitter within their bands by producing frequency components outside their bandwidths.

Pattern-dependent jitter can result from intersymbol interference caused by system response misalignments or when timing recovery circuits are required to process digital signals that contain periods of minimal or nonrandom signal transitions. Digital line codes that ensure a more random-like pattern activity are often used, in part, to minimize these effects.

Another prevalent source of jitter, termed *waiting-time jitter,* arises when using certain types of multiplexing-demultiplexing processes that employ pulse stuffing. Input channels that are not synchronized to the same timing source can be multiplexed together. One common method uses positive justification, or pulse stuffing, of the input channels to a common frequency. A typical multiplexed digital signal consists of a number of channels that are TDMed together into a single data stream. Groups of these bits, separated by overhead bits inserted periodically at the multiplexer, contain (1) synchronization information, (2) an indication of whether a pulse stuff occurred in individual channels, and (3) other functions such as error detection and auxiliary signaling channels. Pulse stuffing is accomplished using elastic stores in which the continuous channel input is written into a buffer, or data store, at the channel rate and read out of the store at the multiplexer channel rate into the TDM bit stream. Phase comparisons between the input and output timing indicate if a stuff bit is required. Pulse stuffing and its subsequent removal at the demultiplexer can occur only in certain time slots, which gives rise to this term *waiting-time jitter* to describe the jitter caused by this process. In most systems, the ratio of the actual stuff rate dictated by the channel timing and multiplexer timing, and the stuff opportunity rate dictated by the overhead structure, are not rational. Frequency components of waiting-time jitter can extend down to very low

27

frequencies. This jitter is usually within the bandwidth of system components and can accumulate as systems are interconnected.

Other sources of jitter, such as the intrinsic phase noise of oscillators used as timing sources and in timing recovery phase-locked loops, also add to the overall signal jitter. At very high bit rates, a low-phase-noise oscillator may be required. Digital (or analog) phase shifters also introduce an amount of jitter that must be made small enough for the bit rate in use. A timing system designed for a certain maximum bit rate may be unsuitable at higher rates.

5.1.2   Jitter tolerance. Most sources of jitter can be defined and usually controlled by proper system design; however, system components must be able to tolerate these jitter levels for proper system performance.

Most system components, such as repeaters and demultiplexers, have input timing recovery circuits that permit them to perform their functions. The tolerance to jitter of these circuits takes the form of Figure 3, which shows tolerance levels at which errors occur in bits, or unit intervals, of jitter versus the frequency of the jitter. Frequency components of input jitter greater than the bandwidth of the timing recovery system are not tracked, and acceptable input jitter variations are usually restricted to one bit or less, as shown in the figure.
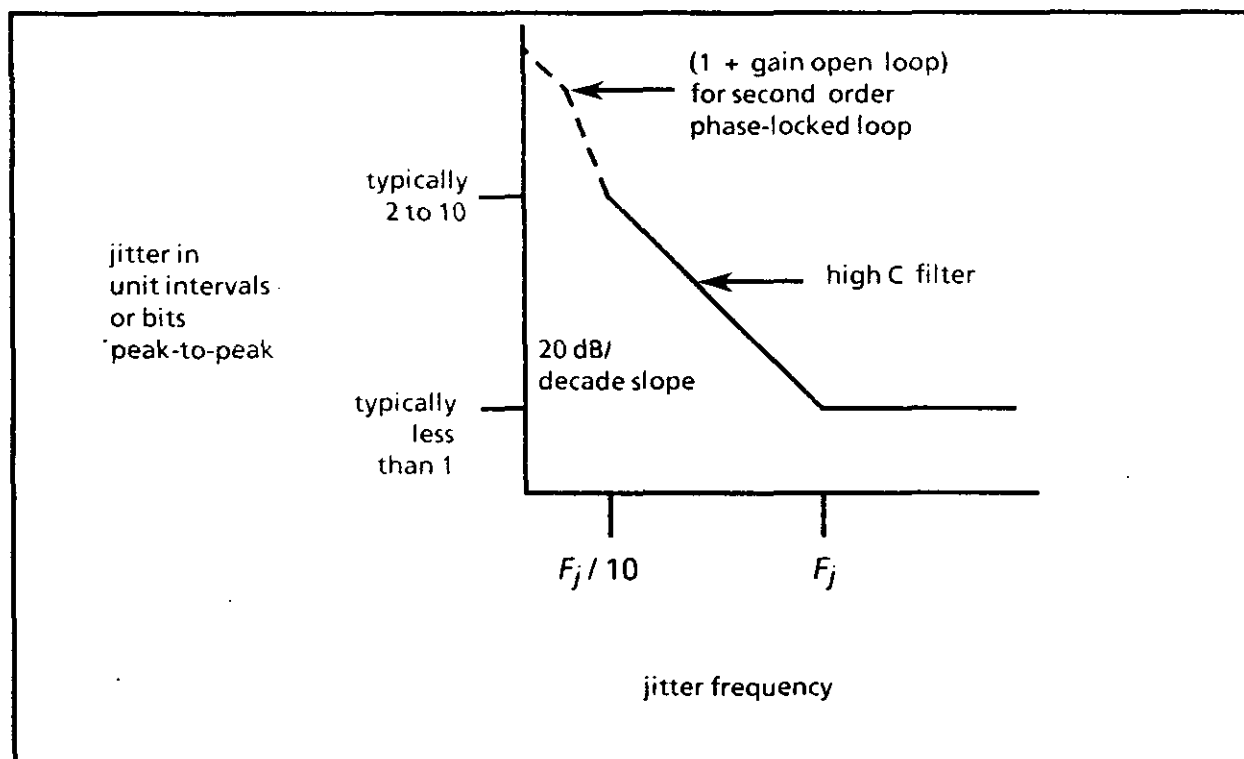
FIGURE 3.   Jitter tolerance for equipment with input timing recovery circuitry.

The recovered timing begins to follow jitter frequencies that are within the timing recovery bandwidth, and the tolerance to jitter increases for lower jitter frequencies. The jitter tolerance of components that have filters or phase-locked loop timing recovery circuits at their input are shown in Figure 3.

For equipment that incorporates an elastic store for jitter reduction or clock smoothing, such as the demultiplexer channel output previously discussed, the jitter tolerance takes a form similar to Figure 4. For this case the tolerance to input jitter is the lower of the tolerance of the input signal timing recovery circuits, or the tolerance of the very narrow phase-locked loop of the elastic store. The tolerance of the elastic store's loop is increased from 1 bit peak-to-peak at high jitter frequencies by the addition of dividers, which permit the loop-phase detector in the elastic store to tolerate greater input phase excursions without losing lock.
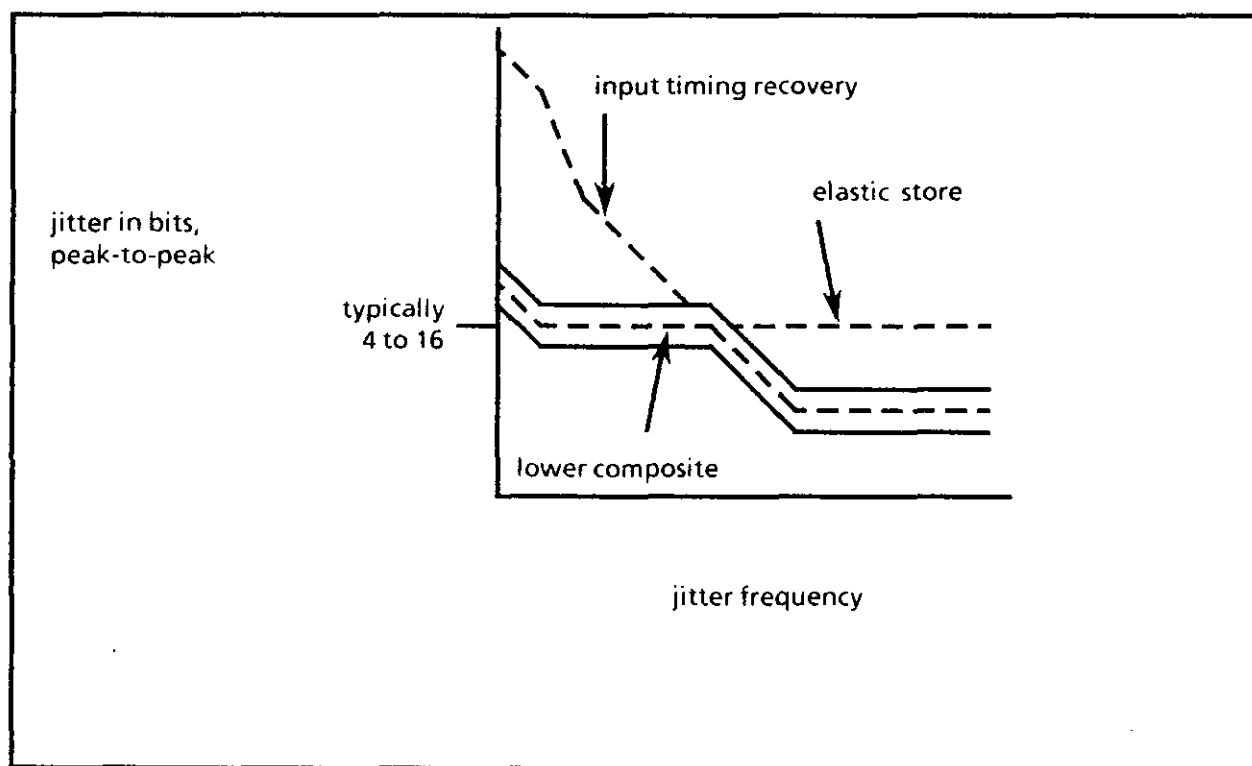
FIGURE 4. Jitter tolerance for equipment that incorporates an elastic store.

The exact characterization of jitter and its effect on performance in digital communications systems is often difficult, at best, particularly when different digital links made of equipment from different manufacturers are interconnected. In this situation it is desirable to correlate pertinent jitter measurements with specific performance parameters. The following measurements are useful in characterizing jitter and assessing its effects on performance.

5.1.3 Jitter measurements. Both the magnitude and frequency content of jitter are usually important when determining jitter tolerance because of the frequency-dependent characteristics of digital equipment. International Telegraph and Telephone Consultative Committee (CCITT) Recommendation 0.171 defines the level

and frequency ranges for jitter-generating equipment that are applicable to most systems. Jitter tolerance measurements using selected bit pattern sequences or system-generated signals are also useful to assess pattern dependency effects.

5.1.4 <u>Jitter magnitude</u>. A measurement of peak-to-peak and root-mean-square (rms) jitter is useful at the input to equipment, such as demultiplexers and digital switches, which have a jitter tolerance that is flat over a broad frequency range, as shown in Figure 4.

5.1.5 <u>Maximum jitter</u>. A stored measurement of the maximum peak-to-peak jitter that occurs during a particular measurement period serves to verify the extremes of jitter excursions on digital signals. The limits of these measurements, to assure application to most systems, are also specified in CCITT Recommendation 0.171.

5.1.6 <u>Jitter threshold seconds</u>. The number of seconds during which the peak-to-peak jitter exceeds a user-selected threshold is recorded. This measurement is useful in characterizing the jitter of a system with the threshold set relative to a particular system tolerance level.

5.2 <u>Phase-locked loop</u>. When the loop is in "lock," the frequencies of the input signal and the voltage-controlled oscillator (VCO) are identical ($f_s = f_o$) and their relative phase difference $\theta_s - \theta_o$ is determined by the phase detector characteristic and by the deviation of f_s from the free-running frequency f_f (defined with control voltage $V_d = 0$) of the VCO. If the input signal has $f_s = f_f$, a control voltage to the VCO is not needed; hence, the requirement phase detector output is 0 (see Figure 5).
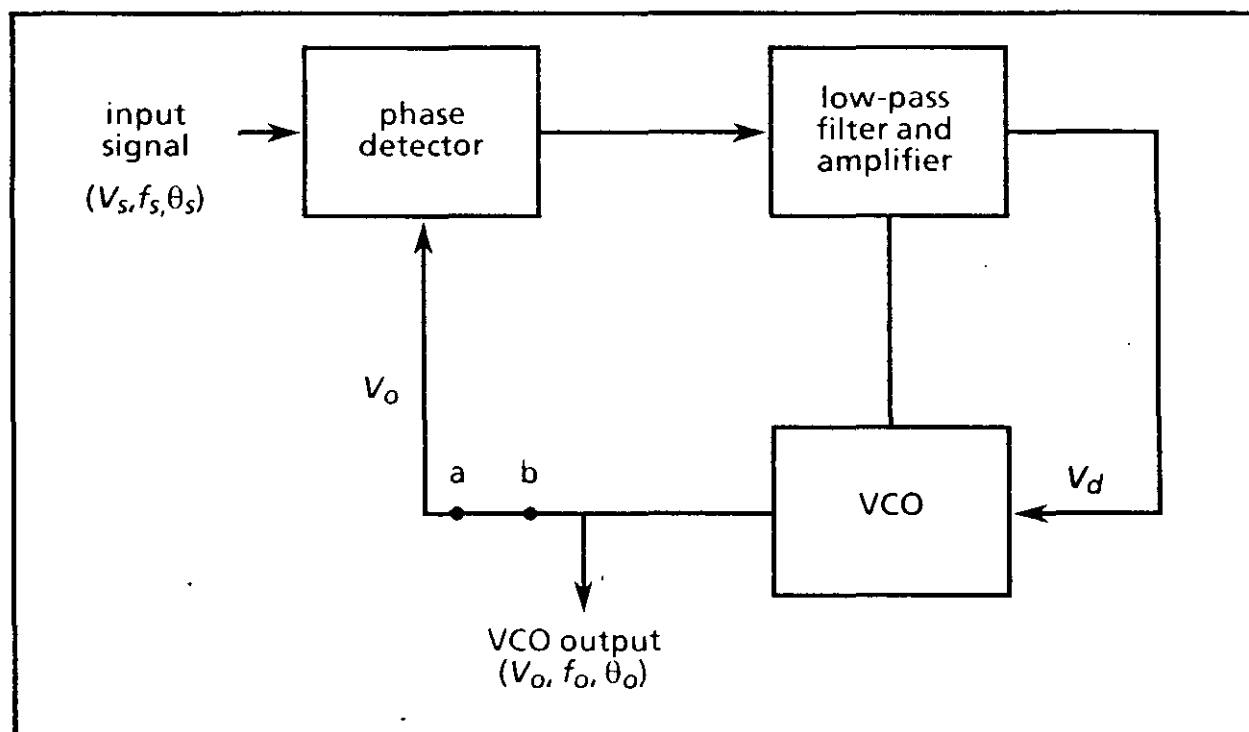
FIGURE 5. <u>Basic components of a phase-locked loop.</u>

The phase θ_o of the VCO adjusts itself to yield the phase difference $\theta_d = \theta_s - \theta_o$ that will produce 0 output from the phase detector. Angle θ_d may be either 90° or 180°, depending on the type of phase detector circuit.

If the input frequency changes so that $f_s \neq f_f$, the phase difference θ_d must change enough to produce a control voltage V_d that shifts the VCO frequency to $f_o = f_s$. The frequency range over which such control is possible is a function of the loop components, as will be discussed later. An optional input frequency divider may be inserted in the loop between points a and b in Figure 5. If the divider ratio is n, the VCO frequency $f_o = nf_s$, but the voltage feedback to the phase detector has frequency f_s. By this means, the VCO can generate a multiple of the input frequency with a precise phase relationship between the two voltages.

5.2.1 <u>Linear analysis of the phase-locked loop</u>. The following mathematical description of the phase-locked loop applies only when the loop is in lock, but it will serve to identify the characteristics of each loop component and show how they combine to yield the loop transfer function. The symbols to be used are identified in Figure 6.
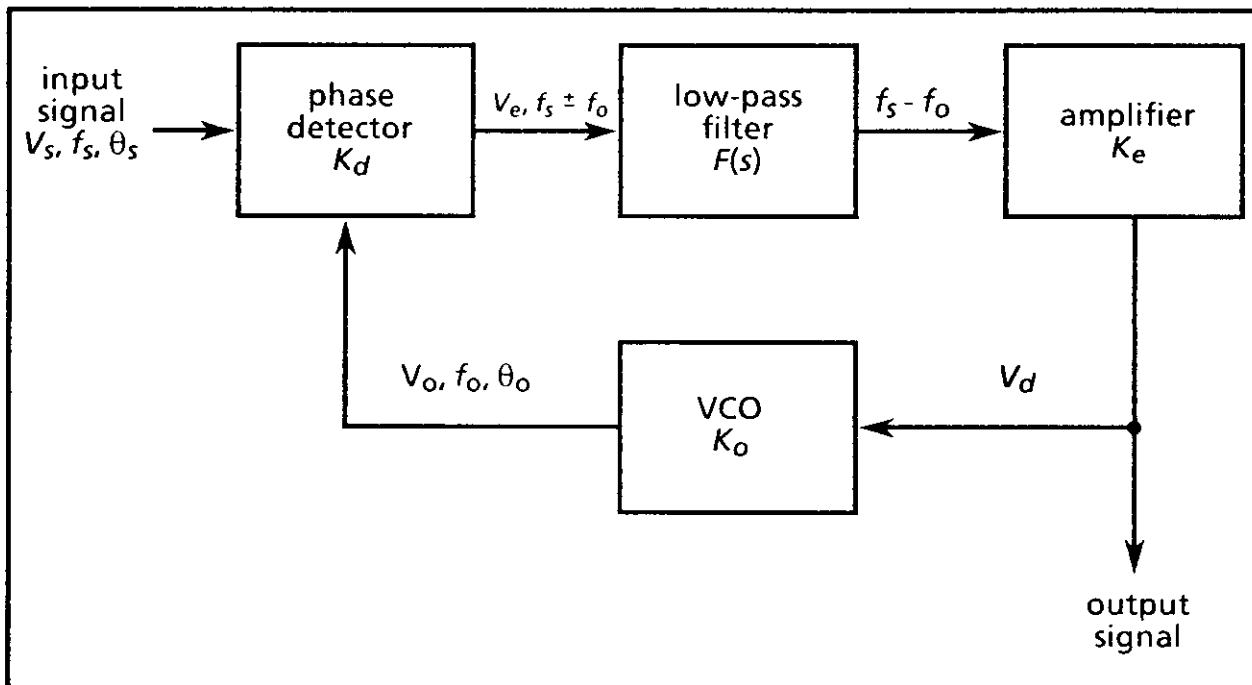
FIGURE 6. <u>Phase-locked loop diagram used to identify symbols used in the analysis.</u>

5.2.2 <u>Phase detector</u>. With the loop in lock, the difference-frequency output of the phase detector is a direct voltage V, which is a function of the phase difference $\theta_d = \theta_s - \theta_o$. If the input frequency f_s is equal to the VCO's free-running frequency f_f, the control voltage V_d into the VCO must be 0; hence, V_e must be 0. In the commonly used phase detectors, V_e is a sinusoidal, triangular, or sawtoothed function of θ_d with V_e equal to 0 when θ_d is equal to $\pi/2$ for sinusoidal and triangular and π for sawtoothed functions. Therefore, to make a direct comparison of the three types of detectors, it is convenient to plot V_e versus a "shifted" angle θ_e so that V_e will be 0 for $\theta_e = 0$, as shown in Figure 7. In this figure, $\theta_e = \theta_d - \pi/2$ in (a) and (b), and $\theta_e = \theta_d - \pi$ in (c). With the loop in lock, the angle θ_e stays within the

limits ±π/2 for curves (a) and (b), and ±π for curve (c). If the angular excursion is greater than this, the loop skips cycles or goes out of lock. Consequently, the loop should be designed to operate with the phase excursions that are small compared with the limiting values.
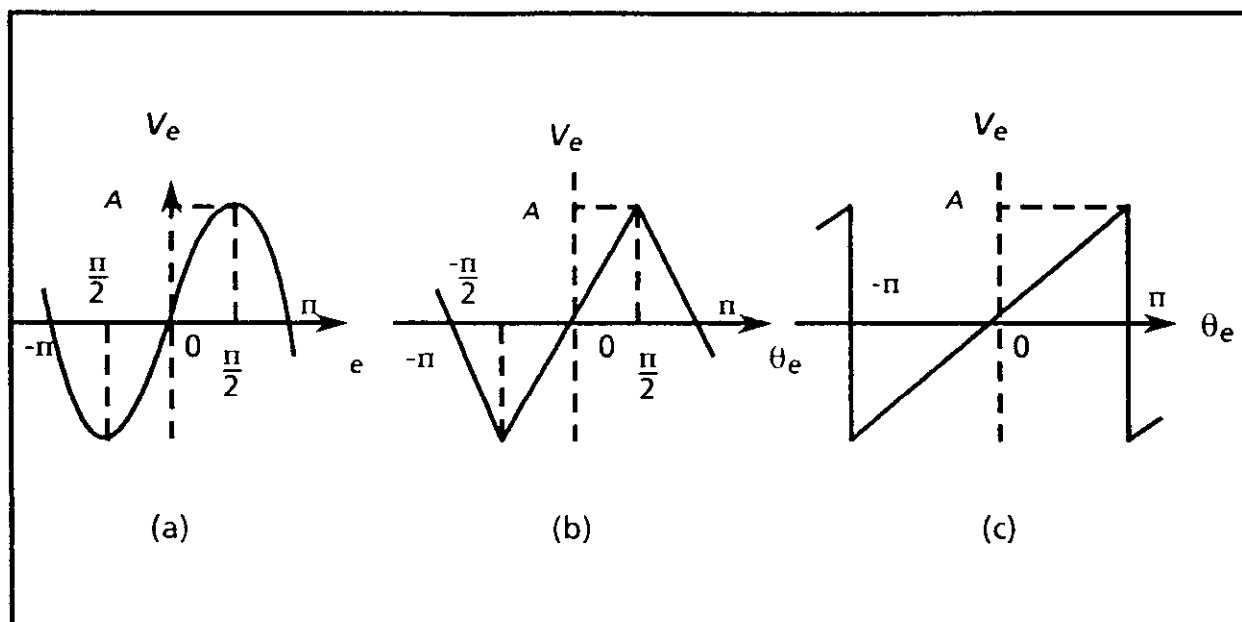
FIGURE 7. Three types of phase detector characteristics: (a) sinusoidal, (b) triangular, and (c) sawtooth.

In terms of maximum output voltage A for each type of detector, the transfer characteristics in the useful region can be expressed as

$$V_e = A \sin \theta_e \ (sinusoidal) \tag{1}$$

$$V_e = \frac{2}{\pi} A \theta_e \ (triangular) \tag{2}$$

$$V_e = \frac{1}{\pi} A \theta_e \ (sawtooth) \tag{3}$$

For loop performance calculations, the gain of each component of the loop must be known. The gain factor of the phase detector (with the loop in lock) is generally specified by the ratio of direct current (dc) output voltage to phase error, that is,

$$K_d = \frac{V_e}{\theta_e} \ V/rad \tag{4}$$

32

Equation (1), which exhibits a nonlinear relationship between V_e and θ_e, does not seem to fit the preceding definition of gain factor very well. However, phase-locked loops are usually designed to operate with small values of θ_e to minimize the likelihood that a noise pulse will throw the loop out of lock. For the sinusoidal phase detector, therefore, $\sin \theta_e \approx \theta_e$ is a reasonable approximation for performance calculations with the loop in lock, and equation (4) applies as long as $\theta_e \leq 0.2 \; rad$.

5.2.3 Loop filter. The low-pass filter in the loop generally takes one of the forms shown in Figure 8. With the passive filters of Figures 8a and b, an amplifier with gain K_a is usually required. The active filter of Figure 8c includes the gain element. For the simple filter of Figure 8, the time constant ι, and transfer function $F(s) = Vo(s)/V_i(s)$ are given by

$$\iota_1 = R_1 C \tag{5}$$

$$F(s) = \frac{1}{1 + \iota_1 s} \tag{6}$$

For the lag-lead filter of Figure 8, the relations are

$$\iota_1 = R_1 C \tag{7}$$

$$\iota_2 = R_2 C \tag{8}$$

$$F(s) = \frac{1 + \iota_2 s}{1 + (\iota_1 + \iota_2)s} \tag{9}$$

For the active filter, noting that the gain factor represents an inverting amplifier,

$$\iota_1 = R_1 C \tag{10}$$

$$\iota_2 = R_2 C \tag{11}$$

$$F(s) = \frac{K_a(1 + \iota_2 s)}{1 + [\iota_1(1 - K_a) + \iota_2]s} \tag{12}$$
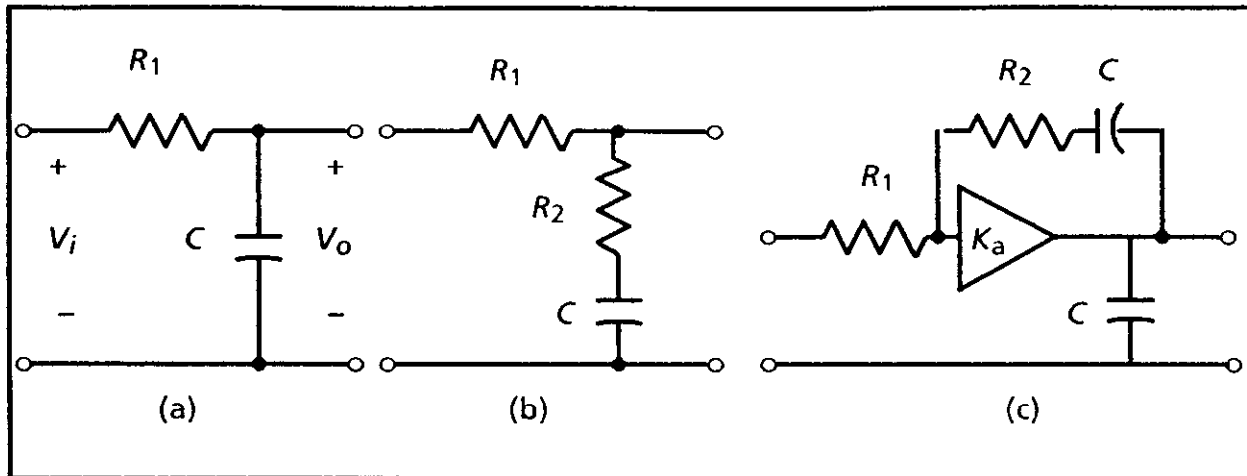
FIGURE 8. Three types of low-pass loop filters.

5.2.4 Voltage-controlled oscillator. The VCO is assumed to have a free-running frequency f_f and a frequency shift Δ_f that is proportional to the input control voltage V_d, as shown in Figure 9. The output frequency can be expressed by

$$f_o = f_f + k_o V_d \; Hz \tag{13}$$
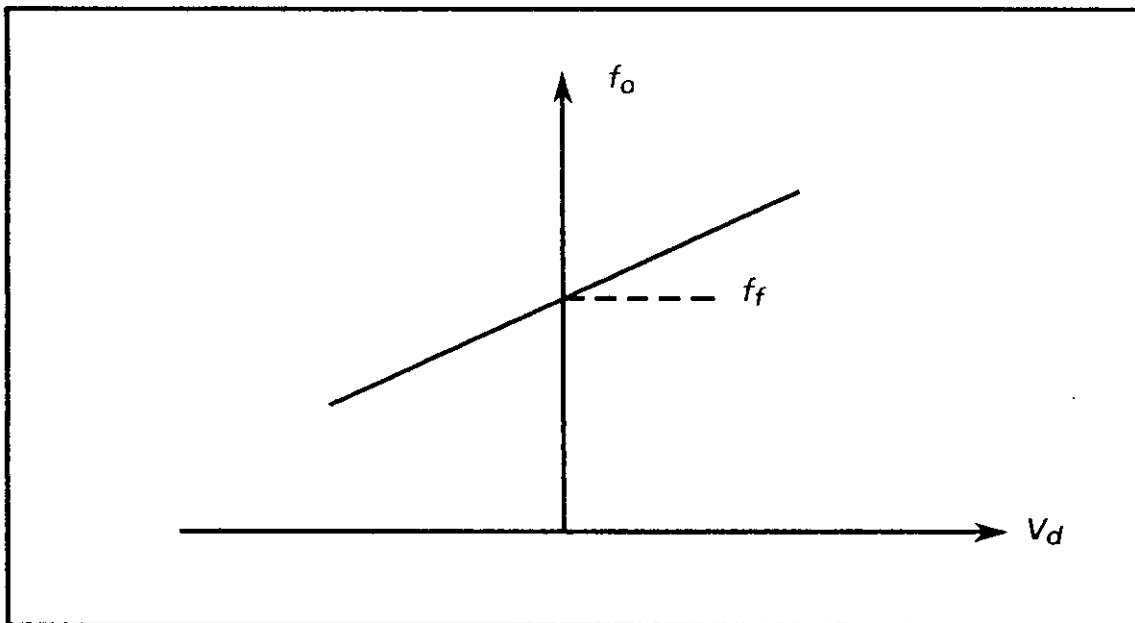
FIGURE 9. Frequency versus control voltage of a VCO.

or

$$W_o = W_f + k_o V_d \; rad/s \tag{14}$$

in which the units of k_o and V_d are hertz per volt (Hz/V) and radians per second per volt (rad/s/V), respectively. To relate the radian-frequency shift to phase angle, note that the total angle of the VCO output can be described by

$$\theta(t) = \int_o^t (\omega_f + \Delta_\omega)\, dt = \omega_f t + \theta_o(t) \tag{15}$$

in which $\omega\Delta$ is the deviation from ω_f. Thus

$$\theta_o(t) = \int_o^t \Delta \omega dt \tag{16}$$

or

$$\frac{d\theta_o(t)}{dt} = \Delta\omega = k_o\, V_d \tag{17}$$

When the loop is in lock, V_d is a dc voltage; when the loop is not in lock, V_d is a difference-frequency ($f_s - f_o$) voltage that tries to pull the VCO into synchronism with the input signal.

When equation (16) is transferred into the s domain, it becomes

$$\theta_o(s) = k_o\, \frac{V_d}{s} \tag{18}$$

with the s in the denominator indicating that the VCO acts as an integrator for phase errors. This helps to maintain the loop in lock through momentary disturbances.

5.3 <u>Phase-locked loop synchronization performance.</u> Within a multichannel switched system, the external system interface modules (fixed, static, and mobile access facilities) and the subscriber access switches all derive timing (in one instance or another) from an atomic-clock-controlled source, trunk, or access switch. Several parameters common to those facilities must be identified so that adequate synchronization performance is realized in the timing loops. The major parameters that impact timing and synchronization are as follows:

   a.   setting accuracy,
   b.   oscillator frequency stability,
   c.   frequency hold-in range,
   d.   frequency pull-in range,
   e.   acquisition time,
   f.   anti-jam (A/J) protection,
   g.   fly-wheeling capability, and
   h.   threshold carrier-to-noise $(C/N)_t$ ratio.

To identify required values for the above parameters, it is necessary to determine the transient and noise performance of synchronizing loops. A second-order (frequency-correcting) loop will be assumed in order to establish typical parameter values. Figure 10 shows a functional block diagram of a general second-order phase-locked loop synchronization system. The closed-loop transfer function is

$$\frac{\theta_o}{\theta_i}(s) = \frac{\omega_o}{\omega_i}(s) = \frac{through\ transfer\ function}{1 + loop\ transfer\ function} \tag{19}$$

$$= \frac{1 + mT_o s}{1 + mT_o s + (T_o/K)s^2} \tag{20}$$

where

T_o = time constant
K = total loop gain

substituting

$$\omega_n = \sqrt{K/T_o}\ yields$$

$$\frac{\theta_o}{\theta_i}(s) = Y(s) = \frac{1 + mT_o s}{1 + mT_o s + (1/\omega_n)^2 s^2} \tag{21}$$

The damping coefficient ξ is (from equation 21) equal to

$$\xi = \sqrt{\frac{(m\ T_o)^2}{4/w_n^2}} = \frac{m\ T_o}{2/\omega_n} \tag{22}$$

and putting ξ in equation (21) yields

$$Y(s) = \frac{1 + (2\xi/\omega_n)\ s}{1 + (2\xi/\omega_n)\ s + s^2/\omega_n^2} \tag{23}$$

Since the tracking error is given by the phase difference between the input and output phase, that is,

$$\varepsilon(s) = \theta_i(s) - \theta_o(s) \tag{24}$$

or

$$\frac{\varepsilon(s)}{\theta_i(s)} = 1 - Y(s) \tag{25}$$

36
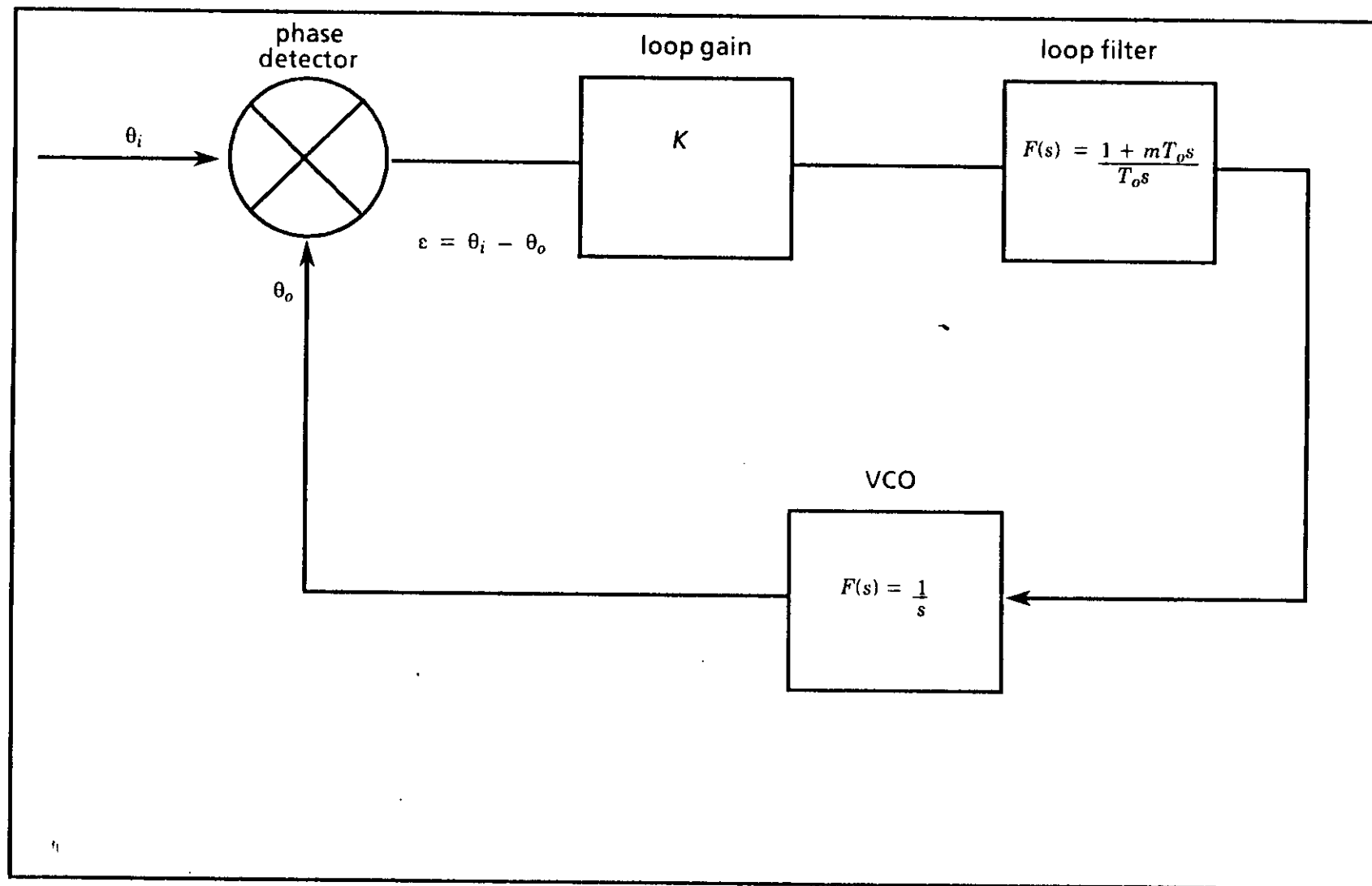
FIGURE 10. Second-order phase-locked loop synchronization system.

37

Then combining equations (23) and (25) gives

$$\varepsilon(s) = \frac{(1/\omega_n)^2 s^2}{1 + (2\xi/\omega_n)s + (1/\omega_n)^2 s^2} \theta_i(s)$$ (26)

A damping ratio of 0.5 results in a minimum noise error, and, when equal to $1/\sqrt{2}$ or .707, it yields a minimum noise plus the transient error. However, when $\xi = 1$, this minimizes the transient error and simplifies the analysis with only a small difference in the overall loop performance.

By letting $\xi = 1$

$$\varepsilon(s) = \frac{(1/\omega_n)^2 s^2}{1 + (2/\omega_n)s + (1/\omega_n)^2 s^2} \theta_i(s)$$ (27)

which reduces to

$$\varepsilon(s) = \frac{s^2}{(s + \omega_n)^2} \theta_i(s)$$ (28)

Equation (28) completely establishes the transient performance of the loop for any input function $\theta_i(s)$.

Identification of the closed-loop bandwidth parameter ω_n establishes all the principal characteristics associated with a second-order synchronizing system.

5.3.1 <u>Frequency hold-in range</u>. There is no theoretical limit for the maximum hold-in range since the steady state tracking error for a constant frequency difference is zero in a second-order loop. A continuously changing ramp frequency change, however, would result in a tracking error. The hold-in range assures that the phase tracking is maintained for any frequency changes that could occur due to oscillator instability and propagation anomalies.

For an input ramp frequency change, as shown in Figure 11, the input frequency is given by

$$\omega_i = \frac{\Omega_o}{T} t$$ (29)

MIL-HDBK-421
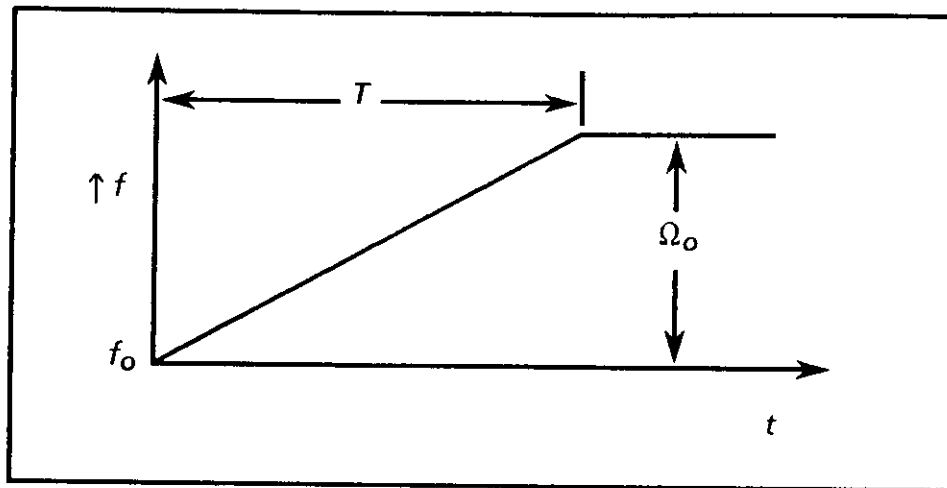
FIGURE 11. <u>An input ramp frequency</u>.

From the Laplace transform theory

$$\omega_i(s) = \frac{\Omega_o}{Ts^2} \tag{30}$$

hence

$$\theta_i(s) = \frac{\Omega_o}{Ts^3} \tag{31}$$

Setting $\xi = 1$ and combining equations (26) and (31)

$$\varepsilon(s) = \frac{\Omega_o/T}{(s + \omega_n)^2 s} \tag{32}$$

From a table of Laplace transforms

$$\varepsilon(t) = \frac{\Omega_o}{T\omega_n^2} \left| 1 - (1 + \omega_n t) e^{-\omega_n t} \right| \tag{33}$$

$\varepsilon(t)$ identifies the transient error output associated with a ramp frequency input from which the maximum transient error can be seen to occur at $t = \infty$ and is given by

$$\varepsilon_{max} = \frac{\Omega_o}{T\omega_n^2} \tag{34}$$

39

The hold-in range must be sufficient to ensure that the phase tracking error is less than $\pm \pi/2$ radians (or $\pm \tau/2$ for a pulse repetition frequency (PRF)-locked loop system) for all frequency rate changes that could occur due to oscillator instability and propagation anomalies. The maximum frequency rate that would be accommodated occurs when the tracking error is $\pi/2$ radians. The maximum allowable rate-of-change of frequency is therefore given by

$$\left(\frac{\Omega_o}{T} \right)_{max} = \pi/2 \; \omega_n^{\;2} \; rad/s^2 \tag{35}$$

5.3.2 <u>Frequency pull-in range.</u> To identify the frequency pull-in range, it is necessary to establish the transient response for a step frequency difference input, as indicated in Figure 12.
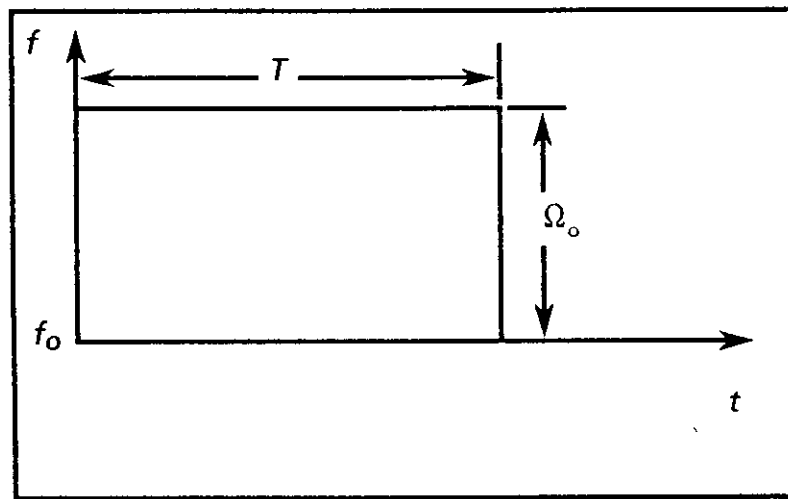
FIGURE 12. <u>A step frequency</u>.

For an input equal to

$$\omega_i = \Omega_o = constant \tag{36}$$

$$\omega_i(s) = \frac{\Omega_o}{s} \tag{37}$$

and

$$\theta_i(s) = \frac{\Omega_o}{s^2} \tag{38}$$

Recalling that for a second-order loop which is critically damped

$$\varepsilon(s) = \frac{s^2}{(s+\omega_n)^2} \theta_i(s) \tag{28}$$

40

Combining equations (38) and (28)

$$\varepsilon(s) = \frac{\Omega_o}{(s+\omega_n)^2}$$

(39)

and from a table of Laplace transforms

$$\varepsilon(t) = \Omega_o t e^{-\omega_n t}$$

(40)

Equating the derivative of equation (40) to 0 and solving for t identifies the time corresponding to the peak transient error as

$$t = \frac{1}{\omega_n}$$

(41)

which when substituted into equation (40) determines the peak transient error as

(42)

$$\varepsilon_{max} = 0.368 \frac{\Omega_o}{\omega_n}$$

The frequency pull-in range must be sufficient to ensure that the phase tracking error is less than $\pm \pi/2$ radians (or $\pm \tau/2$ for a PRF-locked loop) for all step frequency differences that could occur due to oscillator instabilities and propagation anomalies. Since the maximum pull-in frequency is identified when $\varepsilon_{max} = \pi/2$ radians, then

$$\Omega_{o_{max}} = 4.27 \ \omega_n \ rad/s$$

(43)

5.3.3 Acquisition time. In an uncoded synchronization loop, the acquisition time comprises the sweep time (if employed) plus several closed-loop time constants. A coded system requires an acquisition time given by the code length multiplied by the number of code bits in the code sequence. This assumes that all n bits are integrated. Initial integration can be over fewer than n bits to reduce the acquisition time. Another method for reducing acquisition time is to examine several sequences of the code in parallel. In all cases, the closed-loop time constant $1/f_n$ is the principal constraint. A number of alternatives exist for speeding up acquisition.

5.3.4 <u>Fly-wheeling performance of synchronizing systems.</u> The various methods for implementing a synchronization system involve a multiplier or its equivalent (such as a phase detector or time discriminator), a frequency- or phase-controlled oscillator or clock, and a filter. The important system transient characteristics (such as locking time, holding time, and frequency locking range) depend on system loop parameters such as the effective loop filter transfer function, the loop gain, and the order of control (first, second, and so on) that is employed for the closed-loop system. In general, a perfect second-order velocity correcting system provides good performance and results in a 0 error control voltage for a constant frequency difference. Consider the general second-order loop synchronizing system, shown in Figure 13.
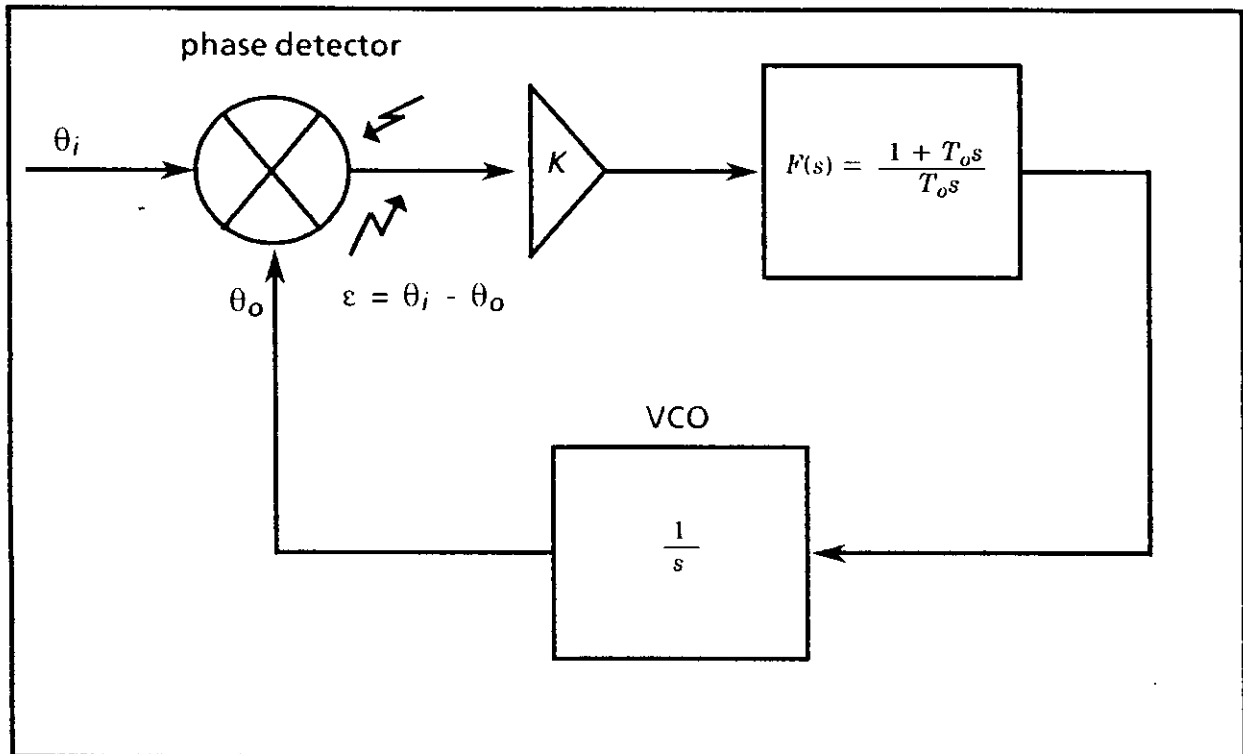
FIGURE 13. <u>A general second-order loop synchronizing system.</u>

The error control voltage is related to the input forcing function θ_i by

$$\frac{\varepsilon(s)}{\theta_i(s)} = 1 - \frac{\theta_o(s)}{\theta_i(s)} \qquad (44)$$

and we have from feedback analysis that employs Laplace transform methods

$$\frac{\varepsilon(s)}{\theta_i(s)} = \frac{1}{1 + (K/s)F(s)} \qquad (45)$$

or substituting for $F(s)$ ·

$$\varepsilon(s) = \frac{(T_o/K) \, s^2 \theta_i(s)}{1 + T_o s + (T_o/K)s^2} \tag{46}$$

For a constant frequency difference input Ω_o

$$\omega_i(s) = \frac{\Omega_o}{s} \tag{37}$$

and

$$\theta_i(s) = \frac{\Omega_o}{s^2} \tag{38}$$

hence·

$$\varepsilon(s) = \frac{\Omega_o T_o/K}{1 + T_o s + (T_o/K)s^2} \tag{47}$$

and by invoking the final limit theorem we see that

$$\varepsilon(\infty) = s\varepsilon(s) \Big|_{s=o} = 0 \tag{48}$$

The error control voltage is removed for a constant frequency difference between the synchronizing system and the input frequency. This condition automatically holds the loop clock at that frequency difference during signal fades of any duration, provided the free-running frequency of the clock remains constant during the fade. This condition emphasizes the importance of short-term stability. If the frequency difference between the oscillators remained constant during the fade, the loop would never lose synchronism in a fade situation no matter how many fades occurred. A perfect second-order loop, however, is not easily implemented. One approach is to employ an electro-mechanical system that uses a servo-motor driven capacitor to change the frequency of a VCO. An alternate approach is to use a *passive* filter with a large loop gain K to achieve an approximation to a second-order loop. Figure 14 illustrates a functional block diagram of this concept.
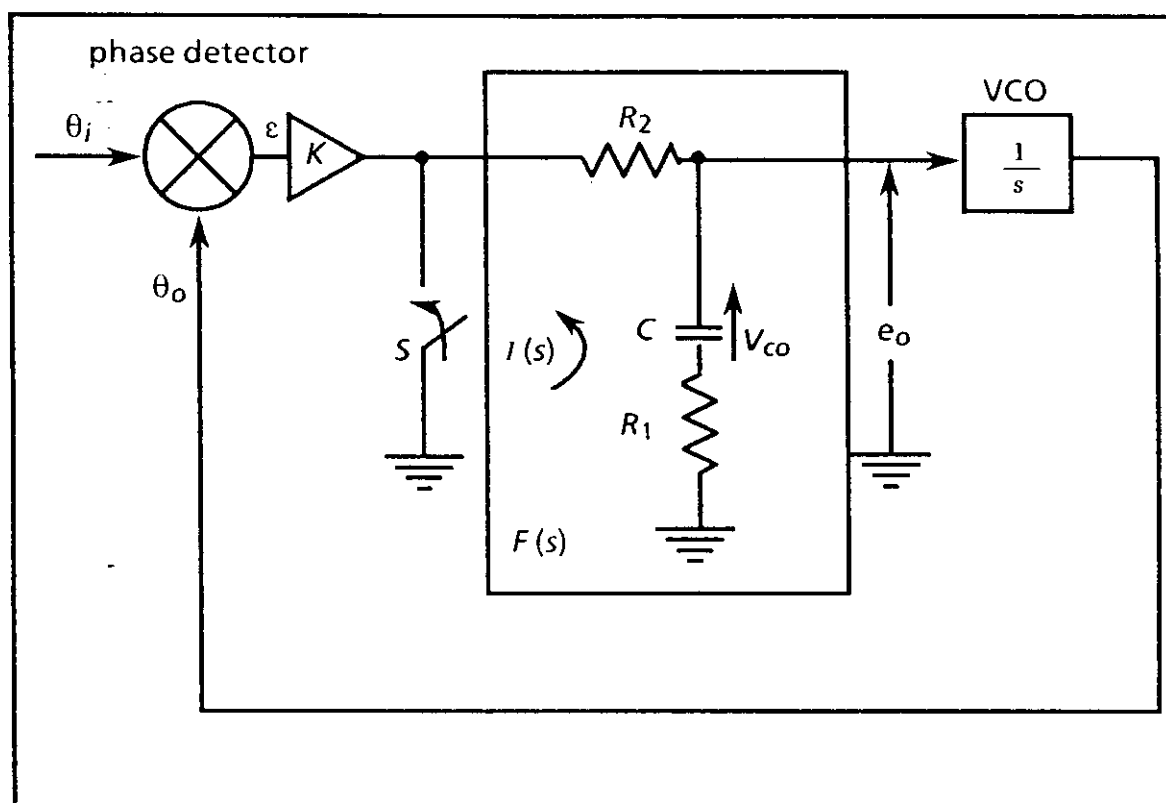
FIGURE 14. Approximate second-order phase-locked loop.

For the filter

$$F(s) = \frac{1 + mT_2 s}{1 + T_2 s} \qquad (49)$$

where

$$T_2 = (R_1 + R_2)C \qquad (50)$$

and

$$m = R_1/(R_1 + R_2) \qquad (51)$$

and since

$$\frac{\varepsilon(s)}{\theta_i(s)} = 1 - \frac{\theta_o(s)}{\theta_i(s)} \qquad (44)$$

therefore

$$\frac{\varepsilon(s)}{\theta_i(s)} = 1 - \frac{(1 + mT_2 s)}{1 + (mT_2 + 1/K)s + (T_2/K)s^2} \tag{52}$$

$$\frac{\varepsilon(s)}{\theta_i(s)} = \frac{s(1/K + T_2/K \, s)}{1 + (mT_2 + 1/K)s + (T_2/K)s^2} \tag{53}$$

For a step frequency input, Ω_o

$$\omega_i(s) = \frac{\Omega_o}{s} \tag{37}$$

and

$$\theta_i(s) = \frac{\Omega_o}{s^2} \tag{38}$$

therefore

$$\varepsilon(s) = \frac{\Omega_o(1/K + T_2/Ks)}{s[1 + (mT_2 + 1/K)s + (T_2/K)s^2]} \tag{54}$$

which results in

$$\varepsilon(\infty) = s\varepsilon(s)\Big|_{s=0} = \frac{\Omega_o}{K} \tag{55}$$

where K = total loop gain in Hz/radian. Note that a small tracking error ε is synonymous with a large open loop gain K.

When the input signal disappears during fades, the result is equivalent to shorting the input to the loop filter $F(s)$. The oscillator control voltage then reduces to 0, which returns the VCO frequency to its quiescent value.

The specific transients involved are readily identified.

Since

$$\frac{e_o(s)}{\theta_i(s)} = \frac{K \, F(s)}{1 + (K/s) \, F(s)} \tag{56}$$

45

then

$$e_o(s) = \frac{s(1 + mT_2 s)\ \theta_i(s)}{1 + (mT_2 + 1/K)s + (T_2/K)s^2} \tag{57}$$

and for a step frequency input, Ω_o

$$\theta_i(s) = \frac{\Omega_o}{s^2} \tag{38}$$

which yields

$$e_o(\infty) = \Omega_o = V_{co} \tag{58}$$

When the input signal is removed, the switch S is closed with the capacitor, C, charged to Ω_o. Applying the Laplace transform theory, we have

$$I(s) = \left(R_1 + R_2 + \frac{1}{sC} \right) = \frac{\Omega_o}{s} \tag{59}$$

and

$$e_o(s) = I(s)R_2 \tag{60}$$

Combining equations (59) and (60) produces

$$e_o(s) = \Omega_o \left(\frac{R_2}{R_1 + R_2} \right) \frac{1}{s + \dfrac{1}{C(R_1 + R_2)}} \tag{61}$$

and from a table of Laplace transforms

$$e_o(t) = \Omega_o \left(\frac{R_2}{R_1 + R_2} \right) e^{-\frac{t}{C(R_1 + R_2)}} \tag{62}$$

which for $R_2 >> R_1$ results in

$$e_o(t) = \Omega_o e^{-\frac{t}{C(R_1 + R_2)}} \tag{63}$$

Equation (63) indicates that during a fade the oscillator frequency would initially retain the frequency difference between the input and the oscillator and then decay exponentially with an open-loop time constant equal to $C(R_1 + R_2)$. The design of the synchronizing loop now becomes a compromise among the use of a sufficiently

large loop gain K, a relatively narrowband effective closed-loop bandwidth $\sqrt{K/T_2}$, and the retention of a large open-loop time constant $C(R_1 + R_2)$ for holding the VCO frequency during signal fades.

If e_o is essentially held constant during fades that use proper design constraints, then frequency changes are constrained to oscillator instability and propagation effects.

As an example for line-of-sight (LOS) and tropospheric scatter (TROPO) transmission links, the mean duration of those fades that depress the power carrier-to-noise ratios (C/N) to 5 decibels (dB) or lower is generally less than 10 second(s) with the exception of ultra high frequency (UHF)/LOS. In the case of UHF/LOS, the mean duration is less than 10 s for $C/N \leqq$ -2 dB. In essence, 10 s represents a reasonable expected fade duration for identifying the memory requirements for synchronization systems employed in fixed terrestrial transmission links. The allowable relative frequency change Ω_o/f_o is from equation (187)

$$\frac{\Omega_o}{f_o} = \frac{\varepsilon_T}{T} \tag{64}$$

Assuming a maximum allowable timing error requirement of 10 percent of the pulsewidth of the maximum trunk bit rate, which is 4.608 megabits per second (Mbps),

$$\varepsilon_T = 0.1 \times \frac{1}{4.608(10^6)} \tag{65}$$

and from equation (64)

$$\frac{\Omega_o}{f_o} = \frac{2.17(10^{-8})}{T} \tag{66}$$

therefore for T = 10 seconds

$$\frac{\Omega_o}{f_o} = 2.17 \times 10^{-9} \tag{67}$$

Hence, the short-term stability of the oscillators in conjunction with the frequency variations associated with propagation conditions must be less than 2 parts in 10^9 to retain the timing error to less than 10 percent of the pulsewidth.

5.3.5 Threshold performance of synchronizing loops. The threshold obtained in a synchronizing loop depends on the type of loop implemented. The C/N threshold is determined for the various alternative synchronization approaches to establish the threshold performance of the available synchronization concepts. These include spectral line filtering, PRF-locked loop synchronization (coherent video), and optimum coherent gated-carrier loop synchronization. Any specific implementation approach corresponds to one of these functional concepts.

5.3.5.1 Spectral line-filtering system. A functional block diagram of a spectral line-filtering system is illustrated in Figure 15. This system synchronizes to a single spectral line of a digital input pulse-train.
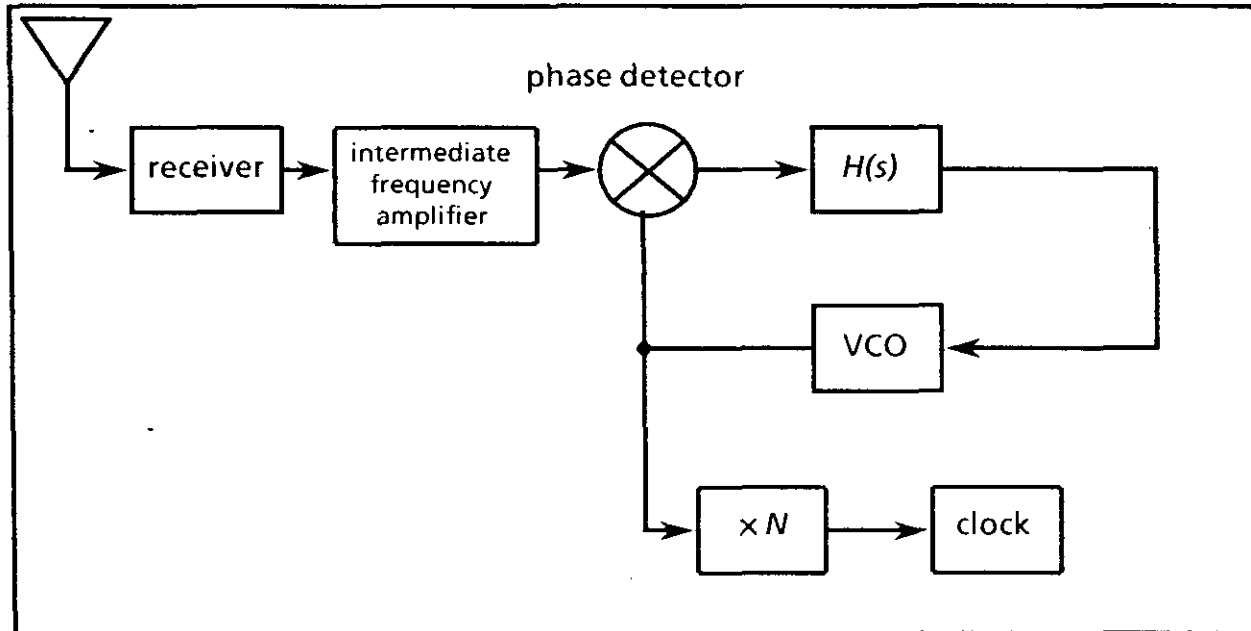
FIGURE 15. A spectral line-filtering system.

A Fourier series analysis of the input pulse-train results in the input spectrum depicted in Figure 16.
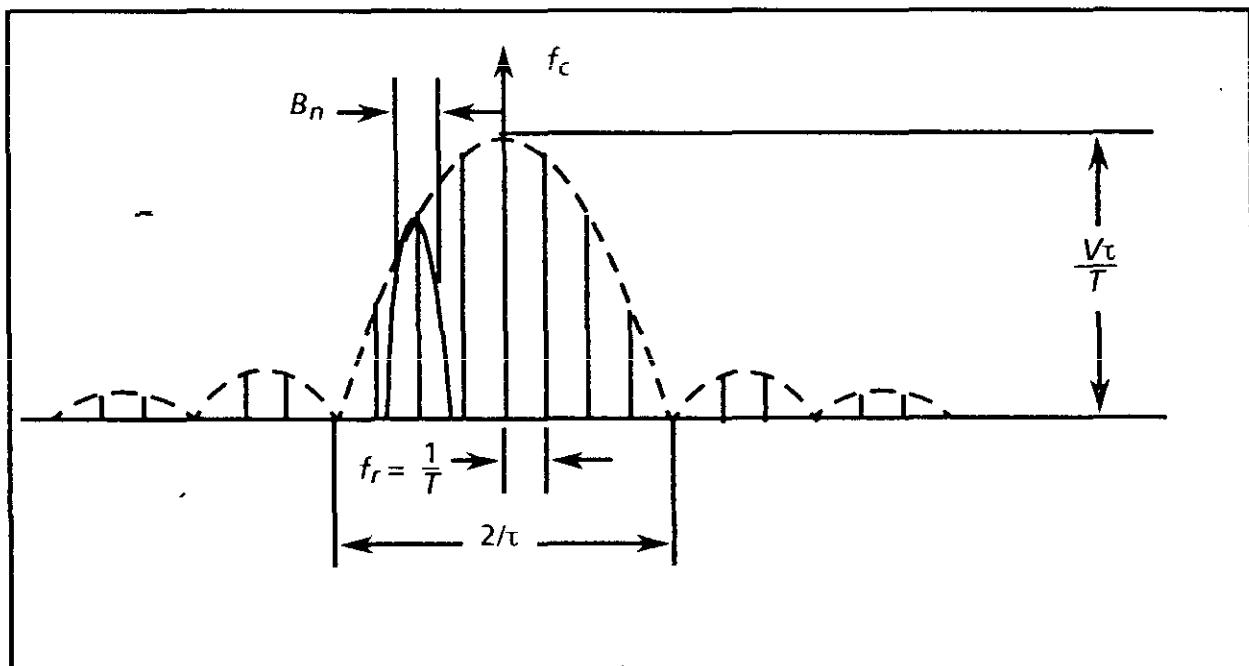
FIGURE 16. A Fourier series analysis of a pulse train.

48

Reference to this figure establishes that the voltage for spectral lines close to the carrier is

$$V_r = \frac{V_1}{T} = V \frac{f_r}{B_i} \tag{68}$$

and the received power P per spectral line is then

$$P'_r = V_r^2 = (V \frac{f_r}{B_i})^2 \tag{69}$$

$$P'_r = \frac{V^2}{M^2} = \frac{P_r}{M^2} \tag{70}$$

where M = the number of spectral lines in bandwidth B_i

$$M = \frac{B_i}{f_r} \tag{71}$$

The output noise power N_o in the closed-loop filter bandwidth B_n is given by

$$N_o = FKTB_n \tag{72}$$

where

FKT = noise power density.

Therefore, the received output signal-to-noise $(S/N)_o$ power ratio is

$$(\frac{S}{N})_0 = \frac{P'_r}{N_o} = \frac{P_r}{M^2 FKTB_n} \tag{73}$$

and the input carrier-to-noise ratio $(C/N)_i$ is

$$(\frac{C}{N})_i = \frac{P_r}{FKTB_n} \tag{74}$$

Combining equations (73) and (74) yields

$$(\frac{S}{N})_o = \frac{B_i}{M^2 B_n} (\frac{C}{N})_i \tag{75}$$

49

Threshold occurs when the phase-locked loop output rms noise-phase jitter exceeds approximately 60° or $\pi/3$ radians. This corresponds to 90° or $\pi/2$ radians being exceeded too often for recovery of loop synchronization. The relationship between the output $(S/N)_o$ ratio and the output phase jitter ϕ_{No} is given by

$$\phi_{No} = \frac{\sqrt{N_o}}{\sqrt{2S_o}} \tag{76}$$

where

$\sqrt{N_o} = $ rms noise voltage

$\sqrt{S_o} = $ rms signal voltage

Combining equations (75) and (76) in conjunction with the fact that

$$B_n = \frac{1}{Nt_r} = \frac{f_r}{N} \ and \ B_i = Mf_r$$

results in

$$\left(\frac{C}{N_i} \right) = \frac{M}{2N\phi^2_{N_o}} \tag{77}$$

which at threshold

$$\phi_{No} = \pi/3$$

becomes

$$\left(\frac{C}{N} \right)_{it} = \frac{9M}{2\pi^2 N} \tag{78}$$

where

$N = $ the number of pulses in the loop integration time.

5.3.5.2 PRF-locked loop synchronization system. A video synchronization system is equivalent to coherently multiplying the input video pulses through the process of gating and then integrating them over N pulses to enhance the output $(S/N)_o$ ratio. This coherent process is preceded by a nonlinear envelope detector such as a square law detector. The nonlinear operation degrades the $(S/N)_o$ ratio, which negates to some degree the improvement associated with the integration process occurring in the loop. In general, the overall performance is superior to filtering out a single spectral line of the input signal. A functional block diagram of a PRF-locked loop is shown in Figure 17.

50
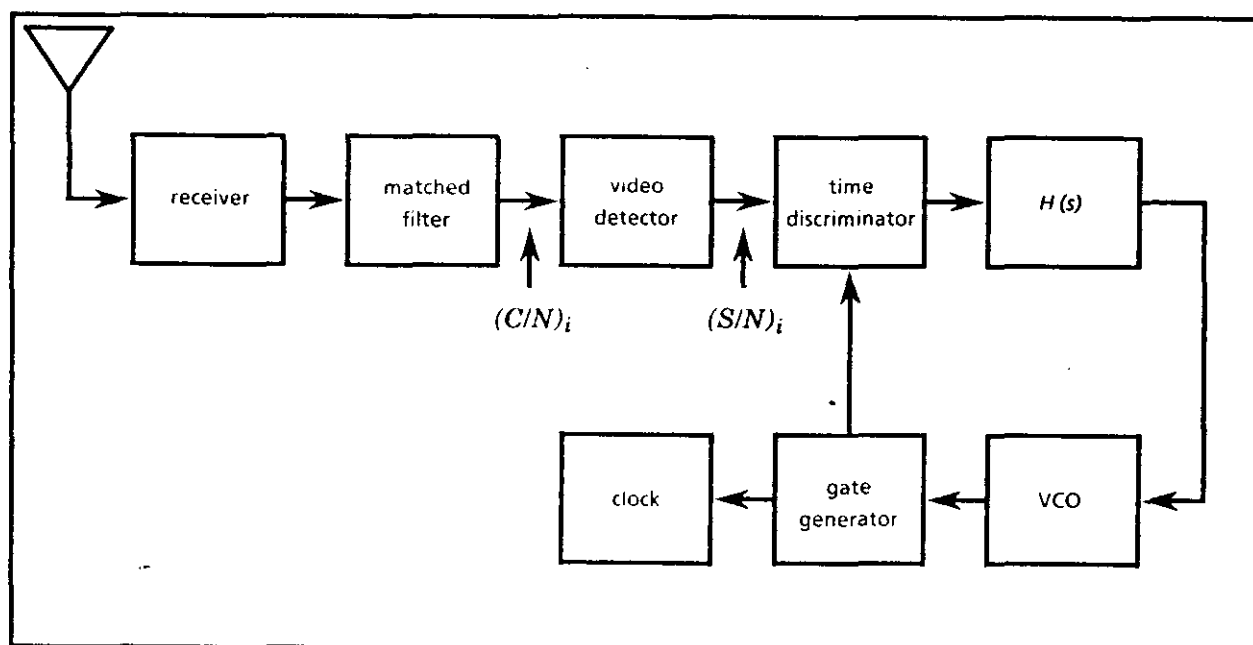
FIGURE 17. A PRF-locked loop.

The loop input signal-to-noise *(S/N)*ᵢ ratio is readily related to the receiver output carrier-to-noise *(C/N)*ᵢ ratio if a square law video detector is assumed to be used. In this case

$$(\frac{S}{N})_i = \frac{\left(\frac{C}{N}\right)_i^2}{2[1+2(\frac{C}{N})_i]} \tag{79}$$

The noise components at the input to the loop are spread over $2B_i$ due to the mixing of noise terms. Therefore, additional filtering associated with the closed loop reduces the noise by approximately

$$\frac{2 B_i}{B_n M} \tag{80}$$

where

B_i = input receiver bandwidth
B_n = closed-loop noise bandwidth
M = number of spectral lines contained in the input bandwidth B_i
$B_n M$ = total effective closed-loop noise bandwidth.

51

Since

$$M = \frac{B_i}{f_r} \tag{81}$$

and

$$B_n = \frac{1}{Nt_r} = \frac{f_r}{N} \tag{82}$$

where

N = the number of pulses integrated by the loop.

Combining equations (80), (81), and (82) results in

$$\frac{2B_i}{B_n M} = 2N \tag{83}$$

This equation is an approximate relationship since the noise is no longer exactly following the square law detector. It is, however, considered sufficiently accurate for the purpose of establishing the degree of noise reduction by the loop. The output $(S/N)_o$ ratio is then given by

$$(\frac{S}{N})_o = N \frac{(\frac{C}{N})_i^2}{[1 + 2(C/N)_i]} \tag{84}$$

To establish the threshold, it is necessary to relate the output noise-time jitter to the output signal and noise. This is accomplished by identifying the time discriminator curve and the effect of noise on the loop output for a PRF synchronizing loop. A time discriminator that provides the necessary bipolar control for synchronizing is illustrated in the Figure 18.
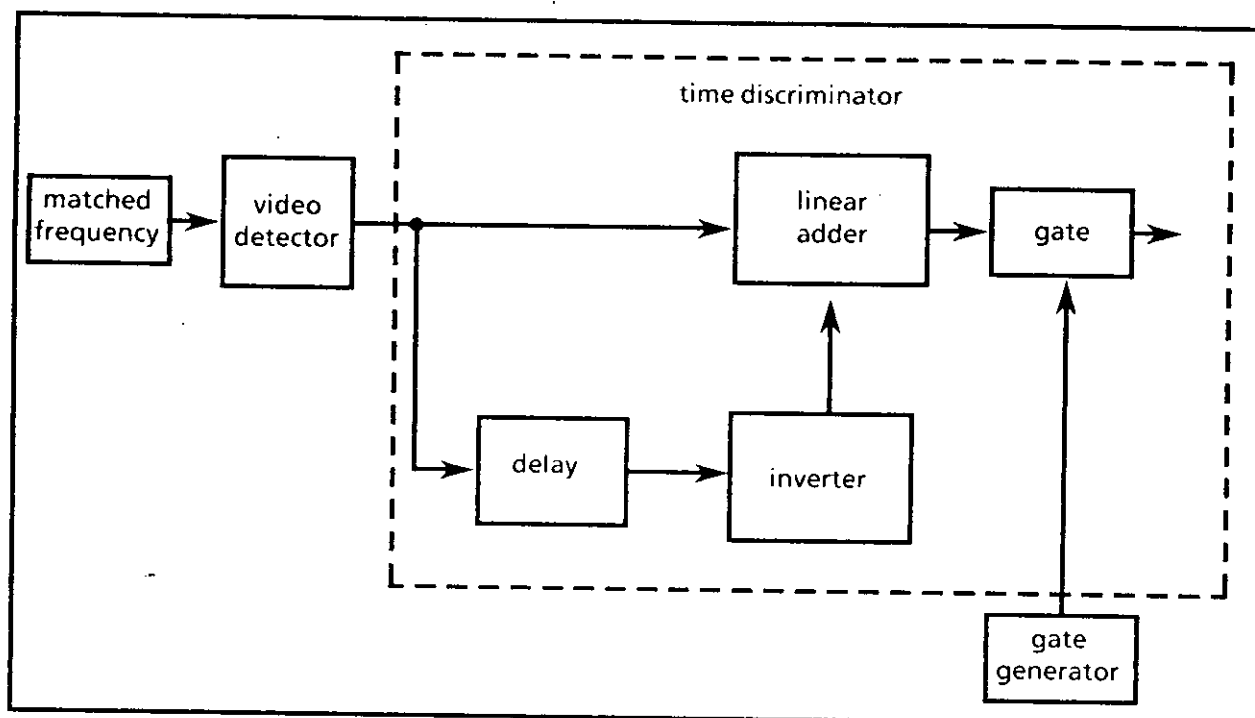
FIGURE 18. A time discriminator.

The resulting discriminator curve is shown in Figure 19, along with the timing error δT_R introduced by noise.
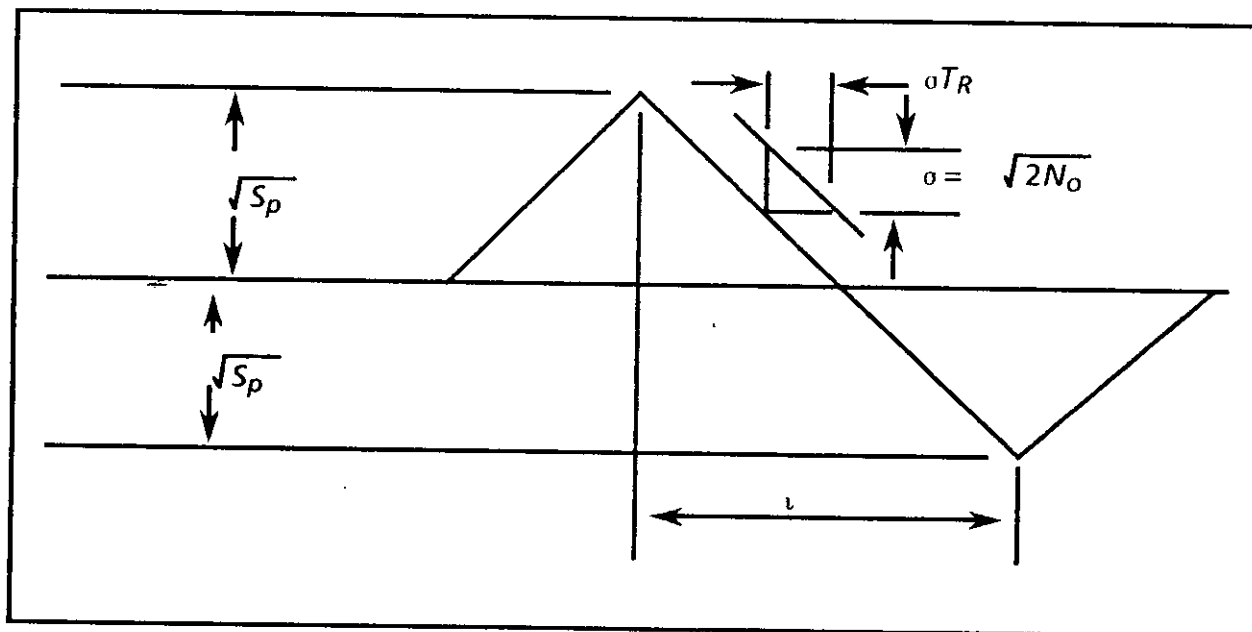
FIGURE 19. A time discriminator curve.

Referring to Figure 19

τ = input pulsewidth

σ = output rms noise amplitude, $\sqrt{2 N_o}$

where

$\sqrt{2}$ results from the summation of two uncorrelated noise sources in the error detector and

N_o = output noise power

σT_R = output rms noise-time jitter

$\sqrt{S_p}$ = output signal peak voltage

The output rms noise-time jitter may be related to the output rms noise amplitude, the pulsewidth, and the output signal from the geometry of the detector (time discrimination) output characteristic.

$$\frac{2\sqrt{S_p}}{\tau} = \frac{\sigma}{\delta T_R} \tag{85}$$

Since

$$\sqrt{S_p} = \sqrt{2 S_o} \tag{86}$$

where

$\sqrt{S_o}$ = the output rms signal voltage

then

$$\left(\frac{S}{N}\right)_o = \frac{\tau^2}{4\delta T_R^{\,2}} \tag{87}$$

Combining equations (84) and (87) yields

$$\left(\frac{C}{N}\right)_i^2 - 2\beta\left(\frac{C}{N}\right)_i - \beta = 0 \tag{88}$$

where

$$\beta = \frac{\tau^2}{4N\delta T_R^{\,2}} \tag{89}$$

54

Solving equations (88) and (89) for $(C/N)_i$ identifies the relationship between the output jitter and the input $(C/N)_i$ ratio.

$$\left(\frac{C}{N}\right)_i = \frac{\tau^2}{4N\delta T_R^{\;2}}\left[1 + \sqrt{1 + \frac{(4N\delta T_R^{\;2})}{\tau^2}}\;\right]$$ (90)

The PRF-locked loop reaches threshold when the output rms time jitter δT_R is equal to one-third the pulsewidth or $\tau/3$, yielding

$$\left(\frac{C}{N}\right)_{it} = \frac{9}{4N}\left[1 + \sqrt{1 + \frac{4N}{9}}\;\right]$$ (91)

5.3.5.3 <u>Optimum coherent gated-carrier loop synchronization system.</u> A functional block diagram for this concept is shown in Figure 20.
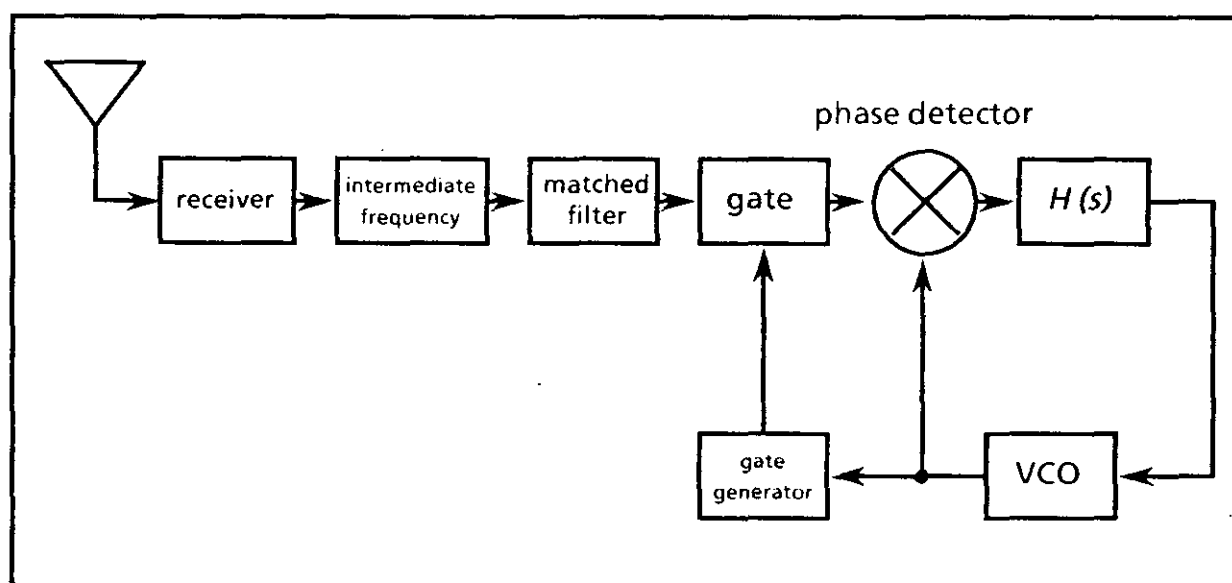
FIGURE 20. <u>An optimum coherent gated-carrier loop synchronization system.</u>

This system cross-correlation detects the input carrier pulse-train with an identical carrier pulse-train to optimally synchronize to the framing channel. All of the signal energy is used for locking-in this coherent detection system. Its implementation requires that the PRF be synchronous with the input carrier to keep the gate centered over the pulsed carrier input. Initial synchronization may be achieved with a separate PRF-locked loop to center the gate over the carrier cycles. Upon synchronizing the gated carrier loop, the PRF-locked loop then disengages. The output rms $(S/N)_o$ ratio for an optimum coherent detector is given by

$$\left(\frac{S}{N}\right)_o = \frac{E}{\eta}$$ (92)

55

where

E = received signal energy in joules
η = FKT = noise power density in watts/Hz.

Since

$$E = P_r \tau N \tag{93}$$

where

P_r = received power
τ = pulsewidth
N = the number of pulses integrated by the closed loop

and

$$B_i = \frac{1}{\tau} \tag{94}$$

then

$$\left(\frac{S}{N}\right)_o = \frac{NP_r}{FKTB_i} \tag{95}$$

or

$$\left(\frac{S}{N}\right)_o = N\left(\frac{C}{N}\right)_i \tag{96}$$

The output rms $(S/N)_o$ is also related to the output noise-phase jitter by

$$\Phi_{N_o} = \sqrt{\frac{N_o}{2S_o}} \tag{97}$$

Combining equations (96) and (97) yields

$$\left(\frac{C}{N}\right)_i = \frac{1}{2N\Phi_{N_o}^2} \tag{98}$$

which at threshold becomes

$$\left(\frac{C}{N}\right)_{it} = \frac{9}{2\eta^2 N} \tag{99}$$

5.3.5.4 <u>Summary</u>. The above equations have been derived that identify the threshold signal-to-noise ratio $(C/N)_{it}$ for three basic synchronization concepts. The results are tabulated below.

For a spectral line synchronization system

$$\left(\frac{C}{N}\right)_{it} = \frac{9M}{2\pi^2 N} \tag{100}$$

For a PRF-locked loop synchronization system

$$\left(\frac{C}{N}\right)_{it} = \frac{9}{4N}\left|1 + \sqrt{1 + \frac{4n}{9}}\right| \tag{101}$$

For a gated-carrier loop synchronization system

$$\left(\frac{C}{N}\right)_{it} = \frac{9}{2\pi^2 N} \tag{102}$$

An examination of these equations reveals that an optimum coherent system is better than one that filters out a single spectral line by the factor M, where M represents the number of spectral lines contained in the input bandwidth or, equivalently, the number of channels in a multichannel system. An optimum coherent gated-carrier loop has a threshold much lower than one for a system that filters out a single spectral line. The performance of a PRF-locked loop system is essentially between what is obtained for the other two approaches.

5.3.6 <u>Optimum synchronization loop design.</u> The following analysis establishes that an optimum design exists for a synchronized carrier loop that minimizes the transient-plus-noise errors to provide a minimum threshold $(C/N)_{it}$. As the closed-loop noise bandwidth is reduced, the output noise is reduced, which improves the threshold until the transient error approaches the maximum allowable total phase error. At some value prior to this, the threshold signal-to-noise ratio $(S/N)_{it}$ obtains its lowest possible value.

Equation (28) can be used to determine the transient performance of a critically damped second-order synchronization phase-locked loop for any input function $\theta_i(s)$.

$$\varepsilon(s) = \frac{s^2}{(s+\omega_n)^2}\,\theta_i(s) \tag{103}$$

where

s	=	the Laplace transform
ω_n	=	the loop design parameter that establishes the transient and noise performance
$\theta_i(s)$	=	the input phase as a function of s
$\varepsilon(s)$	=	the output loop-tracking error as a function of s.

57

The input rms noise jitter (ϕ_{Ni}) is related to the input signal and rms noise amplitude levels by the following equation

$$\phi_{Ni} = \frac{N_i}{\sqrt{2}\,S_i} \quad radians \tag{104}$$

where

N_i = the rms noise voltage in the input bandwidth B_c
S_i = the rms signal voltage at the input.

The phase-locked loop output noise jitter or phase noise is related to the input noise jitter or phase noise by

$$\phi_{N_o} = \phi_{N_i} \sqrt{\frac{\omega_{nt}}{B_c}} \tag{105}$$

where

ω_{nt} = the total effective closed-loop noise bandwidth
B_c = the carrier bandwidth at the input to the phase-locked loop in radians/s.

By definition

$$\omega_{nt} = \int_{-\infty}^{\infty} |Y(\omega)|^2 \, d\omega \tag{106}$$

which, for a second-order critically damped loop, is readily determined as

$$\omega_{nt} = 2.5\, n\omega_n \tag{107}$$

Combining equations (104), (105), and (106) results in

$$\left(\frac{S}{N}\right)_i = \sqrt{\frac{2.5 n\omega_n}{2B_c}} \left(\frac{I}{\phi_{No}}\right) \tag{108}$$

where

$$\left(\frac{S}{N}\right)_i = input\ signal-to-noise\ ratio\ in\ bandwidth\ B_c$$

The loop would lose synchronization when $\phi_{N_o} = \lambda(\pi/2)$ radians in the absence of transient errors, which establishes the threshold $(S/N)_{it}$ for the loop. When the transient tracking error is accounted for, the loop loses synchronization for

$$\phi_{N_o} = \lambda(\pi/2) - \varepsilon_m \tag{109}$$

58

where

$\pi/2 \geqq \lambda \geqq \pi/3$, depending on the statistics of the noise perturbations

ε_m = maximum transient tracking error.

Substituting equation (109) for (108) yields

$$\left(\frac{S}{N}\right)_i = \sqrt{\frac{1.25\pi\omega_n}{B_c}\left(\frac{1}{\lambda\,(\pi/2)\,-\,\varepsilon_m}\right)} \tag{110}$$

If stable clocks are employed, then the frequency accuracy expressed as a maximum frequency difference can be considered as a constant step-frequency difference during the loop's acquisition time. In establishing a quantitative value, care should be taken in relating the calibration and long-term frequency stability to frequency accuracy.

For a step-frequency difference Ω_o

$$\omega_i = \Omega_o = constant \tag{111}$$

hence

$$\theta_i(s) = \frac{\omega_i(s)}{s} = \frac{\Omega_o}{s^2} \tag{112}$$

therefore from equation (103)

$$\varepsilon(s) = \frac{\Omega_o}{(s+\omega_n)^2} \tag{113}$$

and from a table of Laplace transforms

$$\varepsilon(t) = \Omega_o t\, e^{-\omega_n t} \tag{114}$$

Equating the derivation of equation (114) to 0 and solving for t identifies the time corresponding to the peak transient error as

$$t = \frac{1}{\omega_n} \tag{115}$$

which when substituted into equation (114) determines the peak transient error ε_m as

$$\varepsilon_m = 0.368\,\frac{\Omega_o}{\omega_n} \tag{116}$$

59

Combining equations (110) and (116) then results in obtaining the threshold $(S/N)_{it}$ as a function of the loop design parameter ω_n

$$\left(\frac{S}{N}\right)_{it} = \sqrt{\frac{1.25\,n\omega_n}{B_c}\left(\frac{1}{\lambda n/2 - 0.368\Omega_o/\omega_n}\right)} \tag{117}$$

Let

$$\delta = \frac{\sqrt{1.25\,n}}{B_c} \tag{118}$$

then

$$\left(\frac{S}{N}\right)_{it} = \frac{\delta\,\omega_n^{3/2}}{(\lambda n/2)\omega_n - 0.368\Omega_o} \tag{119}$$

Equation (119) demonstrates that the threshold $(S/N)_{it}$ approaches infinity as $(\lambda n/)\omega_n$ approaches 0.368Ω and also as $\omega_n \to \infty$. Therefore, at least one minimum (optimum) value must exist between these extremes, which is readily determined by equating its derivative to 0.

$$\frac{1}{\delta}\frac{d\left(\frac{S}{N}\right)_{it}}{d\omega_n} =$$

$$\frac{[(\lambda n/2)\omega_n - 0.368\Omega_o]\frac{3}{2}\omega_n^{1/2} - (\lambda n/2)\omega_n^{3/2}}{[(\lambda n/2)\omega_n - 0.368\Omega_o]^2} = 0 \tag{120}$$

from which

$$\omega_n(opt) = \frac{2.2}{n\lambda}\Omega_o \tag{121}$$

Equation (121) is the desired result, which indicates that the closed-loop bandwidth parameter ω_n should be essentially equal to the frequency difference to obtain an optimum design that minimizes the transient-plus-noise error and results in a minimum threshold $(S/N)_{it}$. The corresponding threshold $(S/N)_{it}$ is readily determined by substituting equation (121) into equation (119).

$$\left(\frac{S}{N}\right)_{it(opt)} = 1.59\lambda^{-3/2}\left(\frac{\Omega_o}{B_c}\right)^{1/2} \tag{122}$$

If the phase noise or jitter is Gaussian, then phase lock is lost at 60° or $n/3$ radians, for which $\lambda = 2/3$. In this case equations (121) and (122) become

$$\omega_n(opt) = 1.05\,\Omega_o \tag{123}$$

and

$$\left(\frac{S}{N}\right)_{it\,(opt)} = 2.92\left(\frac{\Omega_o}{B_c}\right)^{1/2} \tag{124}$$

Equation (122) is the desired result, and using it as a design equation yields an extremely low threshold $(S/N)_{it}$ as indicated by equation (122) or (124). The derivation does not take into account frequency variations, due to propagation conditions involving Doppler frequencies, such as is experienced in a transceiver on a moving vehicle. It applies to fixed installations such as the trunk links of a multichannel switched system (exclusive of satellite links).

As an illustration of what threshold values might be obtained, consider a stable quartz oscillator whose long-term stability is 1×10^{-9} per day, which was calibrated precisely against an atomic cesium primary standard. After 100 days, the frequency accuracy is 1×10^{-7}. Assuming a carrier frequency of 10 megahertz (MHz) then results in $\Omega_o = 1$ Hz. For a radio frequency (rf) bandwidth of 1 MHz, the threshold $(S/N)_{it}$ is 2.92 (10^{-3}) = -25.4 dB. Care must be taken in using the derived optimum design equation, since the threshold $(S/N)_{it}$ increases very rapidly as ω_n is made smaller than the design value. A practical design must account for the maximum anticipated change expected and should then allow a reasonable margin of safety to the expected value for Ω_o.

5.4 <u>Phase-locked loop performance in a multipath environment</u>. The tracking capability of a phase-locked loop is explored when the input consists of a desired signal plus a delayed and frequency-translated replica of this signal. The purpose of the investigation is to establish how the International Telephone and Telegraph Federal Laboratories (ITTFL) Model 4004 monopulse tracking receiver is capable of performing when self-interference (due to multipath reception) is experienced. Since any loop-transient tracking error is reflected as an error in the antenna positioning outputs, a transient analysis of the loop identifies what errors in antenna tracking can be anticipated.

Figure 21 is a block diagram of the tracking receiver. In the phase-locked loop tracking mode, the sum channel consists of two stages of frequency mixing prior to phase detecting. This operation does not reflect any performance change over a basic phase-locked loop as long as the stability of the various frequency sources involved is good (that is, the phase variations of the oscillators must be slow compared to the closed-loop time constant). The phase-locked portion of the receiver is redrawn in Figure 22 to clarify that the above comments are valid. Referring to Figure 22, it is apparent that variations in either the phase or frequency of the second local oscillator or the reference oscillator are equivalent to separate interferring inputs into the loop. The effect on the resultant output error due to θ_1 and θ_2 may be maintained negligible so long as the frequency rate-of-change of the second local oscillator and the reference oscillator is kept small. This is equivalent to providing good short-term frequency stability for the oscillators in question. If this condition is satisfied, then the loop may be simplified to what is shown in Figure 23.
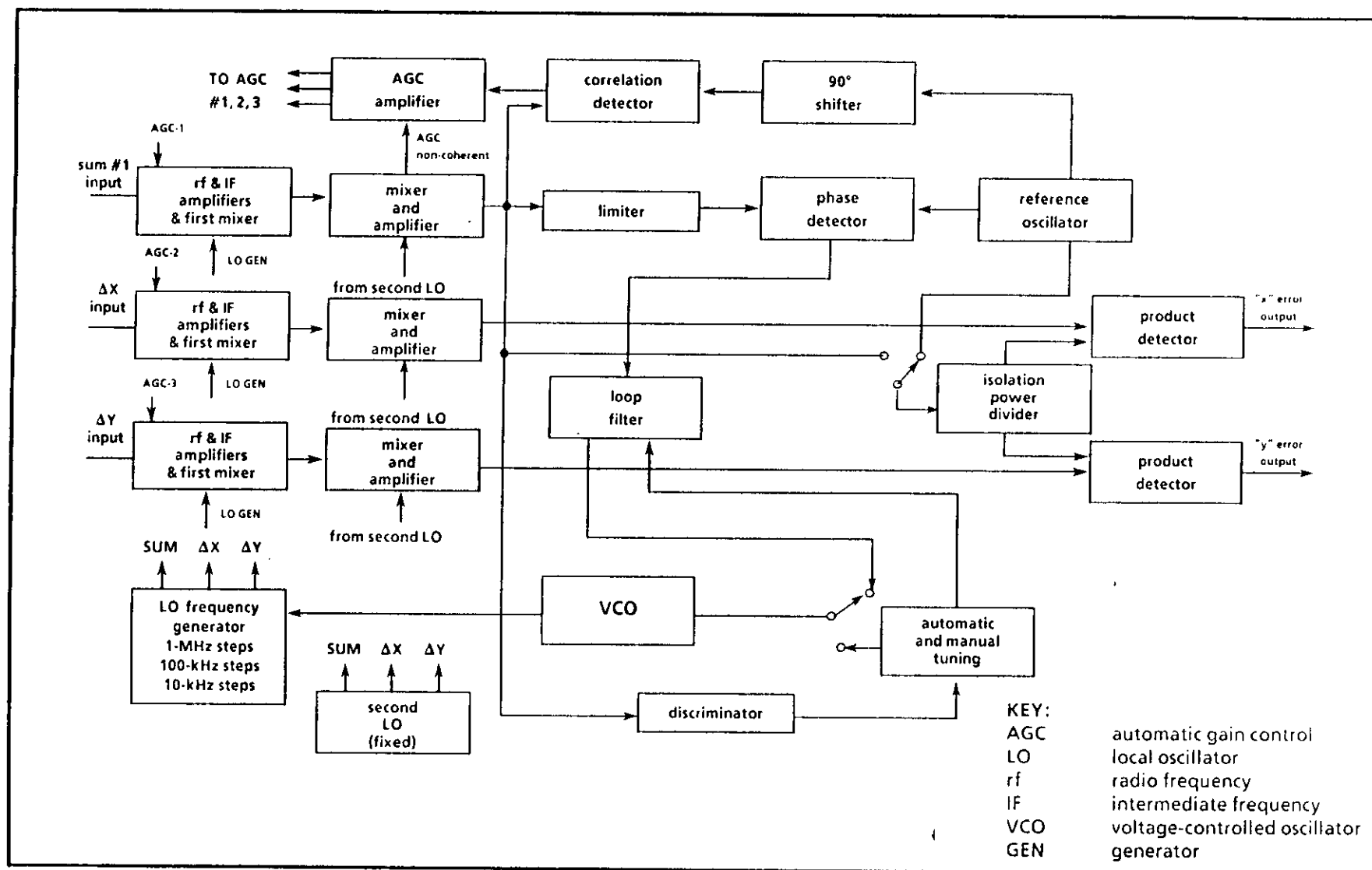
FIGURE 21.   ITTFL Model 4004 monopulse tracking receiver simplified block diagram.

MIL-HDBK-421

62
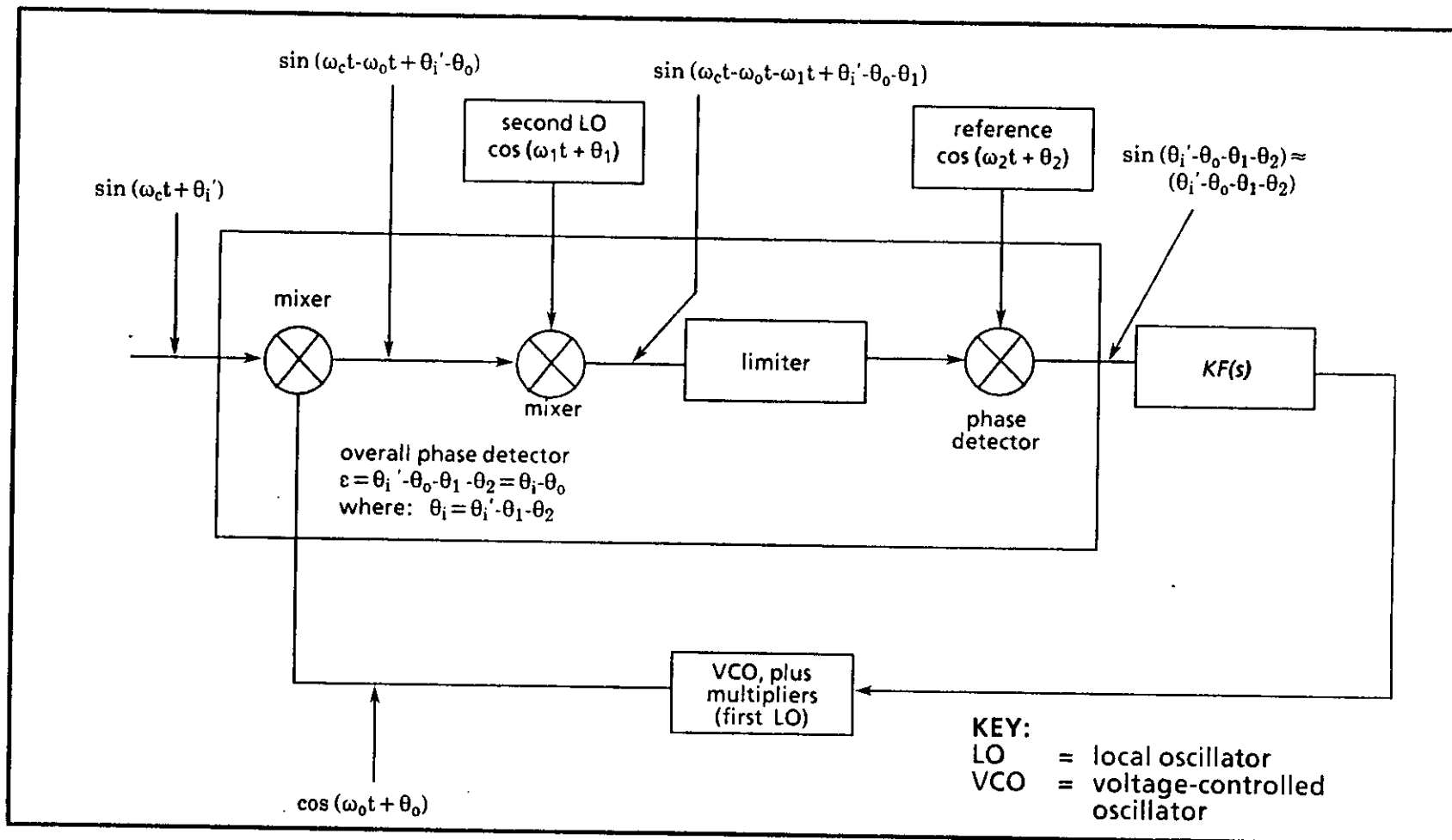
FIGURE 22. Portion of receiver functional block diagram of sum channel and phase-locked loop.

MIL-HDBK-421

63

MIL-HDBK-421
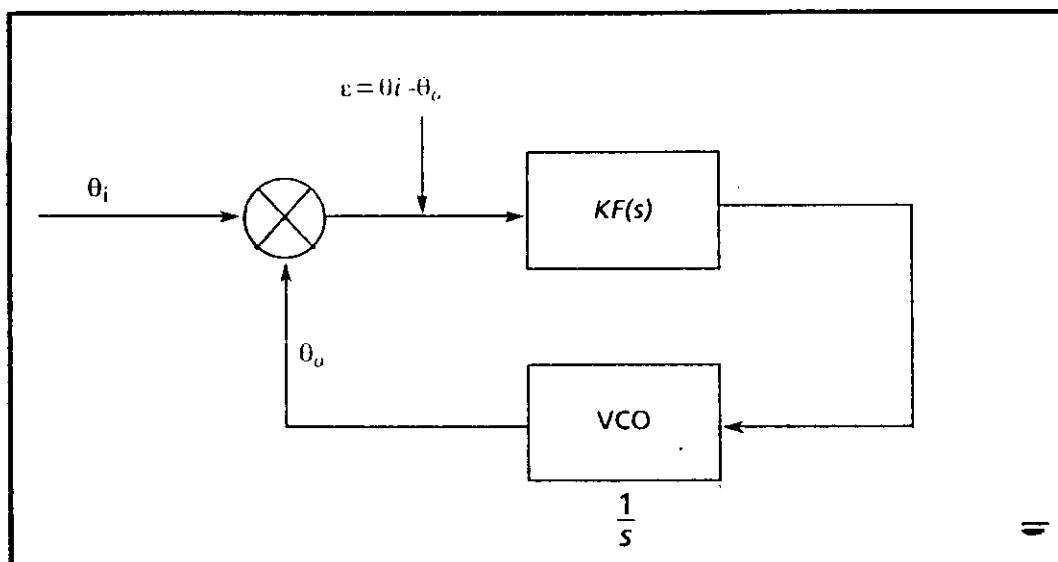
FIGURE 23. Linearized equivalent functional block diagram of a phase-locked loop.

In accomplishing the details of the analysis, a second-order critically damped loop (ξ = 1) is assumed. There is only a small difference in operational performance of phase-locked loops for the various damping ratios identified and used in the literature. For different reasons, values of ξ between 0.5 and 1 have been used. ξ = 0.5 yields a minimum noise bandwidth, and ξ = 0.1 provides good transient performance. Values of ξ between 0.5 and 1 compromise the effects of the two important fundamental considerations.

For the conditions imposed, the output error ε is readily established as

$$\varepsilon(s) = \frac{s^2}{(s+\omega_n)^2} \theta_i(s) \tag{125}$$

To determine the transient output as a function of time now requires identifying the input θ_1 in the presence of limiting. When a delayed frequency translated replica of a carrier is added to the carrier, the resultant signal becomes

$$e_t = E_1 \sqrt{(1 + m\cos\omega_r t)^2 + m^2 \sin^2\omega_r t} \times \sin\left[\omega_c t + \psi(t)\right] \tag{126}$$

where

$$\psi(t) = \tan^{-1}\left(\frac{m\sin\omega_r t}{1 + m\cos\omega_r t}\right) \tag{127}$$

64

m =   the ratio of the amplitude of the delayed signal to the desired signal $(m < 1)$.

ω_r =   the frequency difference between the two signals due to the Doppler effect.

Now the amplitude variations are eliminated, due to the limiter, which leaves a constant amplitude frequency-modulated (FM) signal. The instantaneous modulating frequency is readily obtained as

$$\omega_i = \frac{d\psi(t)}{dt} = \frac{m^2 + m \cos \omega_r t}{1 + m^2 + 2m \cos \omega_r t} \times \omega_r \tag{128}$$

Equation (128) identifies the frequency excursions that the tracking loop must follow with low transient errors in order for the multipath environment to be tolerated. In its present form, the input instantaneous frequency is not readily handled with Laplace transformations. This is overcome with the following assumptions and simplification. For values of m close to unity, ω_i appears as shown in Figure 24, with the peak negative value given by

$$\omega_i = \frac{m}{m-1} \times \omega_r$$
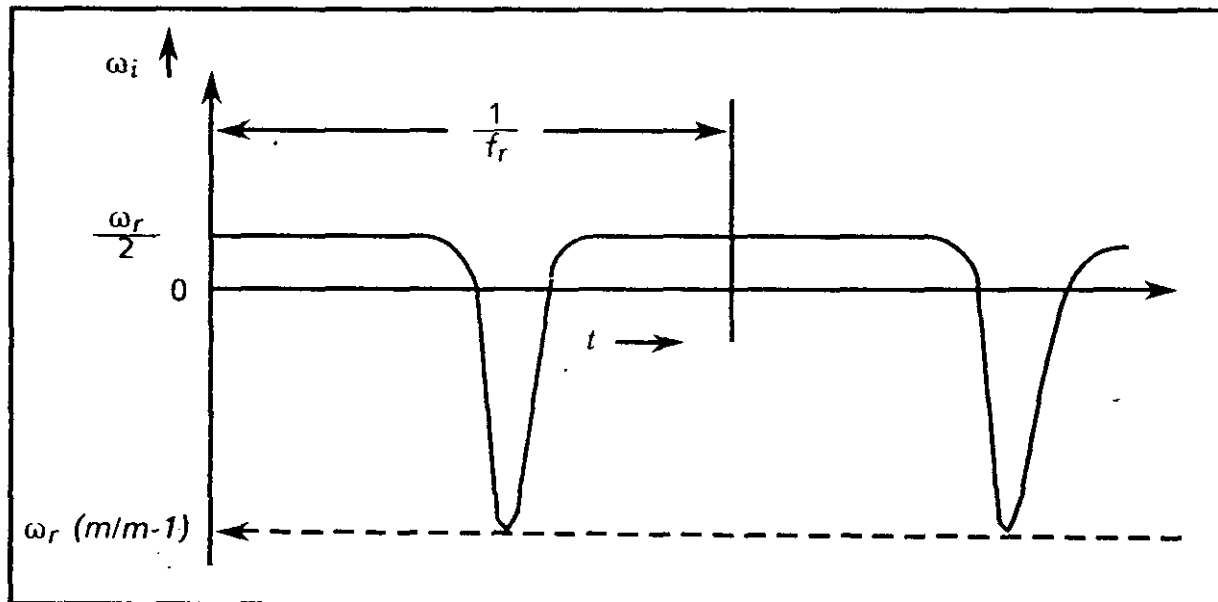
FIGURE 24. Input forcing function.

A good simple approximation to this curve is a triangular wave. The base of the triangle is determined readily since the average value of ω_1 over 1 cycle is 0. The largest multipath signal anticipated for the purposes of this study is for $m = 0.9$. This yields a total excursion of 9.5 f_r, which results in the base of the triangular wave being 2/19 f_r. A plot of this function is shown in Figure 25, in which the axis has been shifted merely to simplify the expression for the input. Using this input now makes deriving the transient output of the loops easy.
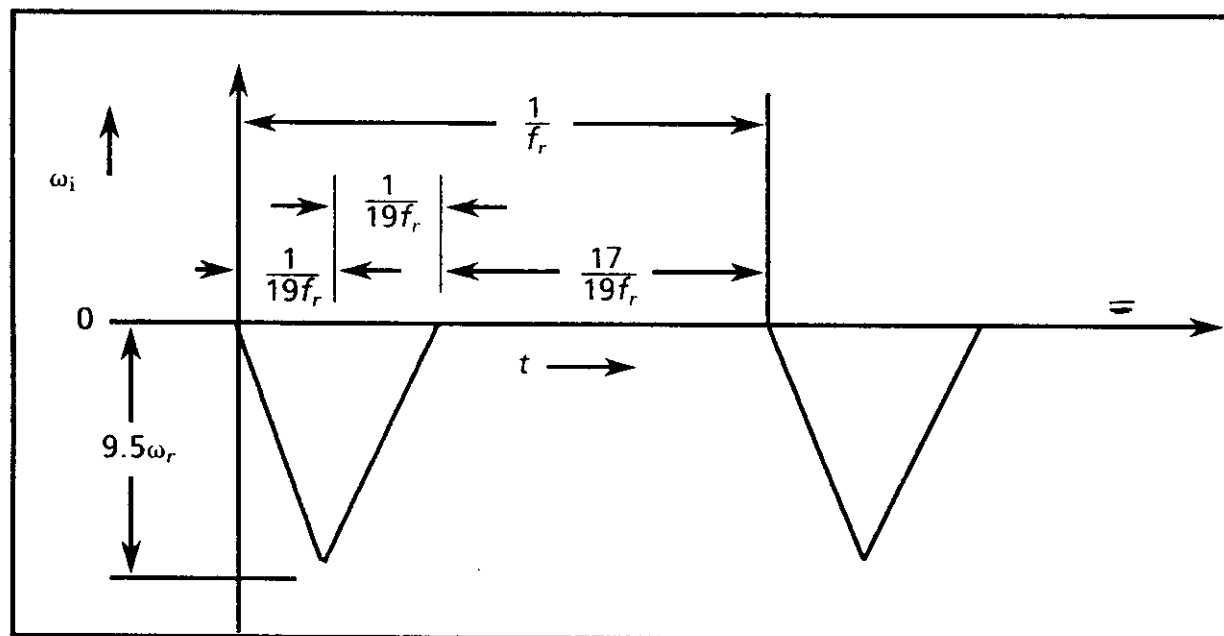
FIGURE 25. Approximate input forcing function ($m = 0.9$)

From Figure 25, the input forcing function becomes

$$\omega_i(t) = -19\,(1.51)\, \omega_r^2 t\, U\,(t-0)$$

$$+ 2\,(19)\, 1.51\, \omega_r^2 t\, U\,(t- \frac{1}{19f_r})$$

$$- 19\,(1.51)\, \omega_r^2 t\, U\,(t- \frac{2}{19f_r})$$

$$- 19\,(1.51)\, \omega_r^2 t\, U\,(t- \frac{1}{f_r})$$

$$+ \;-\;-\;-\;-\;-\;-\;-\;-\;-\;-\;-\;-\;- \tag{129}$$

Taking the Laplace transformation of this function and using the relation

$$\theta(s) = \frac{\omega(s)}{s}$$

results in

$$\theta_i(s) = -19\,(1.51)\,\omega_r^2\,\frac{1}{s^3}$$

$$+ 2\,(19)\,1.51\,\omega_r^2\,\frac{1}{s^3}\,e^{-s}\,(\frac{1}{19f_r})$$

$$- 19\,(1.51)\,\omega_r^2\,\frac{1}{s^3}\,e^{-s}\,(\frac{2}{19f_r})$$

$$- 19\,(1.51)\,\omega_r^2\,\frac{1}{s^3}\,e^{-s}\,(\frac{1}{f_r})$$

$$+ \;-\;-\;-\;-\;-\;-\;-\;-\;-\;-\;-\;-\;-\; \tag{130}$$

Combining equations (125) and (130) and obtaining the inverse Laplace transformation results in

$$\varepsilon(t) = 19\,(1.51)(\frac{\omega_r}{\omega_n})^2\,\left\{\left|-1 + \{1 + \omega_n t\}\,e^{-\omega_n t}\right|\,U(t-o)\right.$$

$$+ \left|2 - 2\{1 + \omega_n(t - \frac{1}{19f_r})\}\,e^{-\omega_n(t - \frac{1}{19f_r})}\right|\,U(t - \frac{1}{19f_r})$$

$$+ \left|-1 + \{1 + \omega_n(t - \frac{2}{19f_r})\}\,e^{-\omega_n(t - \frac{2}{19f_r})}\right|\,U(t - \frac{2}{19f_r})$$

$$+ \left|-1 + \{1 + \omega_n(t - \frac{1}{f_r})\}\,e^{-\omega_n(t - \frac{1}{f_r})}\right|\,U(t - \frac{1}{f_r})$$

$$+ \;-\;\} \tag{131}$$

Equation (131) may be written more compactly, as shown below

$$\varepsilon(t) = 19\,(1.51)\,(\frac{\omega_r}{\omega_n})^2 \sum_{n=0}^{\infty} \left\{ \left| -1 + \{1 + \omega_n(t - \frac{n}{f_r})\}\,e^{-\omega_n(t - \frac{n}{f_r})} \right| U(t - \frac{n}{f_r}) \right.$$

$$+ \left| \{2 - 2\{1 + \omega_n\,(t - \frac{1 + 19n}{19 f_r})\}\,e^{-\omega_n(t - \frac{1 + 19n}{19 f_r})} \right| U(t - \frac{1 + 19n}{19 f_r})$$

$$+ \left| -1 + \{1 + \omega_n(t - \frac{2 + 19n}{19 f_r})\}e^{-\omega_n(t - \frac{2 + 19n}{19 f_r})} \right| \left. U(t - \frac{2 + 19n}{19 f_r}) \right\} \qquad (132)$$

Equation (132) is the desired result, and it completely specifies the transient output that results from the forcing function postulated. Let us now normalize this equation by making the following substitutions

$$K_1 = \frac{\omega_n}{\omega_r} \qquad (133)$$

$$K = f_r\,t \qquad (134)$$

which yields

$$\varepsilon(t) = 19\,(1.51)\,(\frac{1}{K_1})^2 \sum_{n=0}^{\infty} \left\{ \left| -1 + \{1 + 2\pi K_1\,(K - n)\}e^{-2\pi K_1(K - n)} \right| U\,(K - n) \right.$$

$$+ \left| 2 - 2\{1 + 2\pi K_1(K - \frac{1 + 19n}{19})\}\,e^{-2\pi K_1\,(K - \frac{1 + 19n}{19})} \right| U\,(K - (\frac{1 + 19n}{19})$$

$$+ \left| -1 + \{1 + 2\pi K_1(K - \frac{2 + 19n}{19})\}e^{-2\pi K_1\,(K - \frac{2 + 19n}{19})} \right| \left. U\,(K - \frac{2 + 19n}{19}) \right\} \qquad (135)$$

Equation (135) was computed over nine cycles of the input to ensure that the transient output is identical for adjacent cycles. A plot of the results is shown in Figure 26 for values of K_1 equal to 0.5, 1, 2, 4, and 10. It is obvious from the results obtained that the effect of the interfering multipath signal is quite harmful for a narrowband tracking loop. The loop bandwidth f_n must approach the maximum frequency excursion $9.5f_r$ before the peak transient error is reduced to a reasonable order of magnitude. For $f_n = 10\,f_r$, the peak transient error is 0.238 radians or 13.5°. As the bandwidth becomes narrower, the peak transient output increases rapidly and also lasts for much larger fractions of the total period. Even when the loop bandwidth is as much as four times the difference frequency f_r, the transient error might be classified as intolerable, since it peaks at 0.72 radians or 41.2°. When the loop bandwidth is equal to or less than the input frequency f_r, the transient error
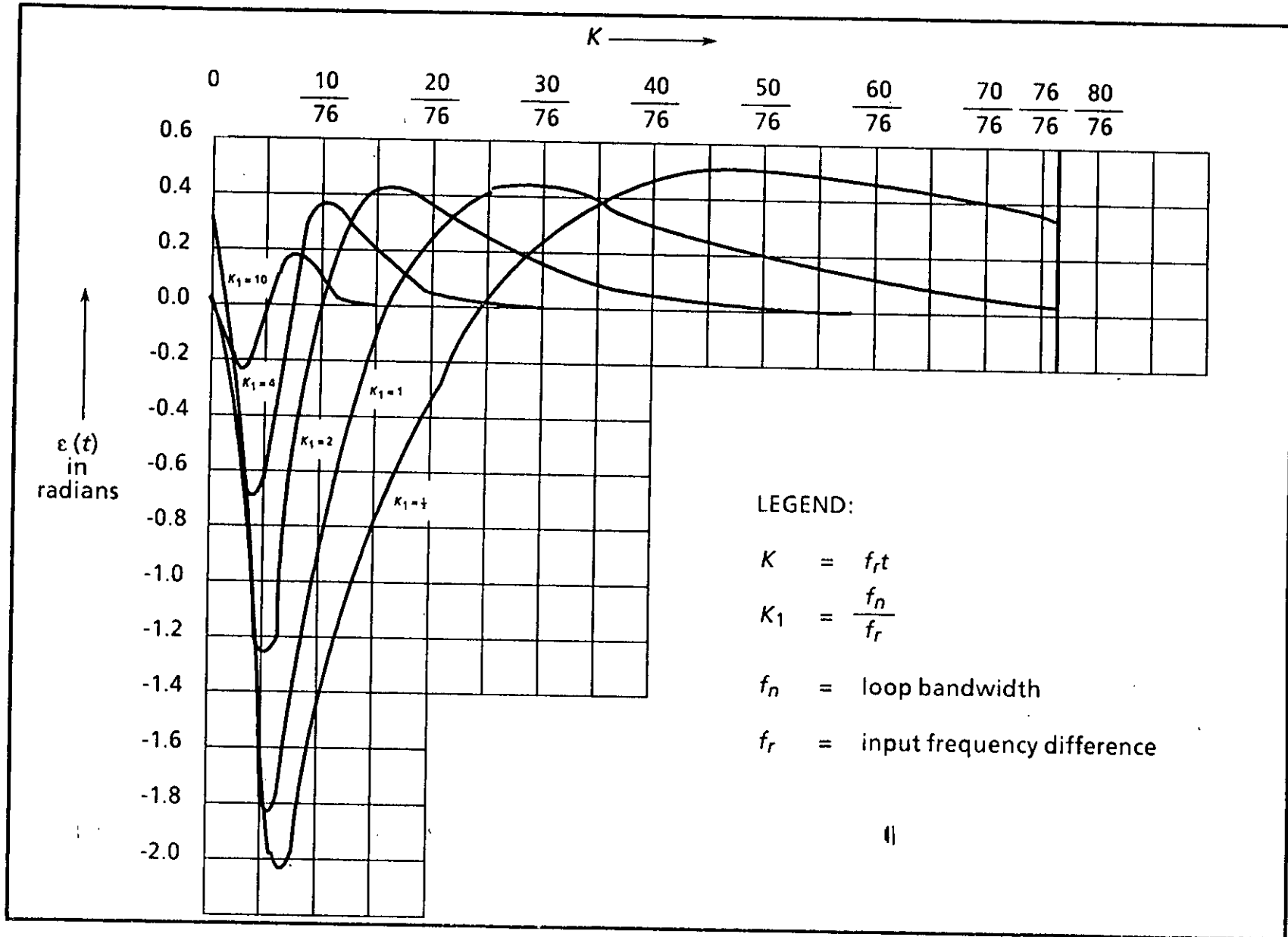
FIGURE 26. <u>The output error plotted over one cycle for various values of K_1.</u>

LEGEND:

$K = f_r t$

$K_1 = \dfrac{f_n}{f_r}$

$f_n =$ loop bandwidth

$f_r =$ input frequency difference

MIL-HDBK-421

69

exceeds the allowable value of 90° for retaining linear lock-on, resulting in loss of synchronization. The precise critical value of f_n, where this occurs, lies somewhere between $f_r < f_n < 2f_r$. Practically it might be considered as occurring at $f_n = f_r$ because the actual input forcing function is not quite as severe as the input postulated. There is a slightly more gradual transition preceding and following the maximum rates of frequency change for the actual input to the loop.

Let us now estimate how these transient errors affect the antenna tracking error for the amplitude monopulse system being investigated. To determine this, consider the difference channel shown in Figure 22. This is redrawn in Figure 27 with the various oscillators and signals identified. Under normal operating conditions, the output of the product detector should be (approximately) linearly related to the input difference amplitude E_1. This occurs when the loop of the sum channel is tracking with a small residual transient error ε. It has been demonstrated, however, that ε may become very large for a narrowband tracking loop.

The effect of this loop error on the antenna tracking operation is to modify the antenna positioning error control voltage, according to the following relation:

$$\varepsilon_\phi = K E_1 \cos \varepsilon \qquad (136)$$

where

$$
\begin{aligned}
KE_1 &= \text{the desired value for } \varepsilon_\phi \\
\varepsilon_\phi &= \text{the antenna-positioning control error.}
\end{aligned}
$$

It is apparent from equation (136) that large loop transients can adversely affect the performance of an antenna servo-tracking system. The instantaneous error variations in the antenna space angle cannot be established only from equation (136) and a knowledge of the variations of ε. To accomplish a complete analysis of the space angular error requires that we postulate a specific servo system (that is, type I, type II, servo loop error-detector characteristics, bandwidth, and damping ratio, if applicable) in addition to identifying its input forcing function (that is, the target dynamics and overall system geometry). One can identify, however, that servo loop error-detector characteristics are seriously altered in a manner equivalent to dynamically changing the antenna loop gain.

Since the analysis is of a general nature, it is of interest to identify how the output frequency of the VCO is following the input excursions. This is readily determined using Laplace transformation notation as follows, since

$$\varepsilon(s) = \theta_i(s) - \theta_o(s) \qquad (137)$$

then

$$\frac{\theta_o(s)}{\theta_i(s)} = 1 - \frac{\varepsilon(s)}{\theta_i(s)} = \frac{\omega_o(s)}{\omega_i(s)} \qquad (138)$$

$$\omega_2 t$$

$$K_2 E_1 \ \sin (\omega_c t - \omega_o t - \omega_1 t + \theta_i{}' - \theta_o - \theta_1)$$

reference
$\cos (\omega_2 t + \theta_2)$

$K_1 E_1 \ \sin (\omega_c t - \omega_o t + \theta_i{}' - \theta_o)$

ϕ shift

$E_1 \ \sin (\omega_c t + \theta_i{}')$

$\sin (\omega_2 t + \theta_2)$

mixer

mixer

product
detector

first LO
$\cos (\omega_o t + \theta_o)$

second LO
$\cos (\omega_1 t + \theta_1)$

$$
\begin{cases}
e_o & = & K_3 E_1 \cos (\theta_i{}' - \theta_o - \theta_1 - \theta_2) \\
e_o & = & K_3 E_1 \cos (\theta_i - \theta_o) \\
e_o & = & K_3 E_1 \cos \varepsilon
\end{cases}
$$
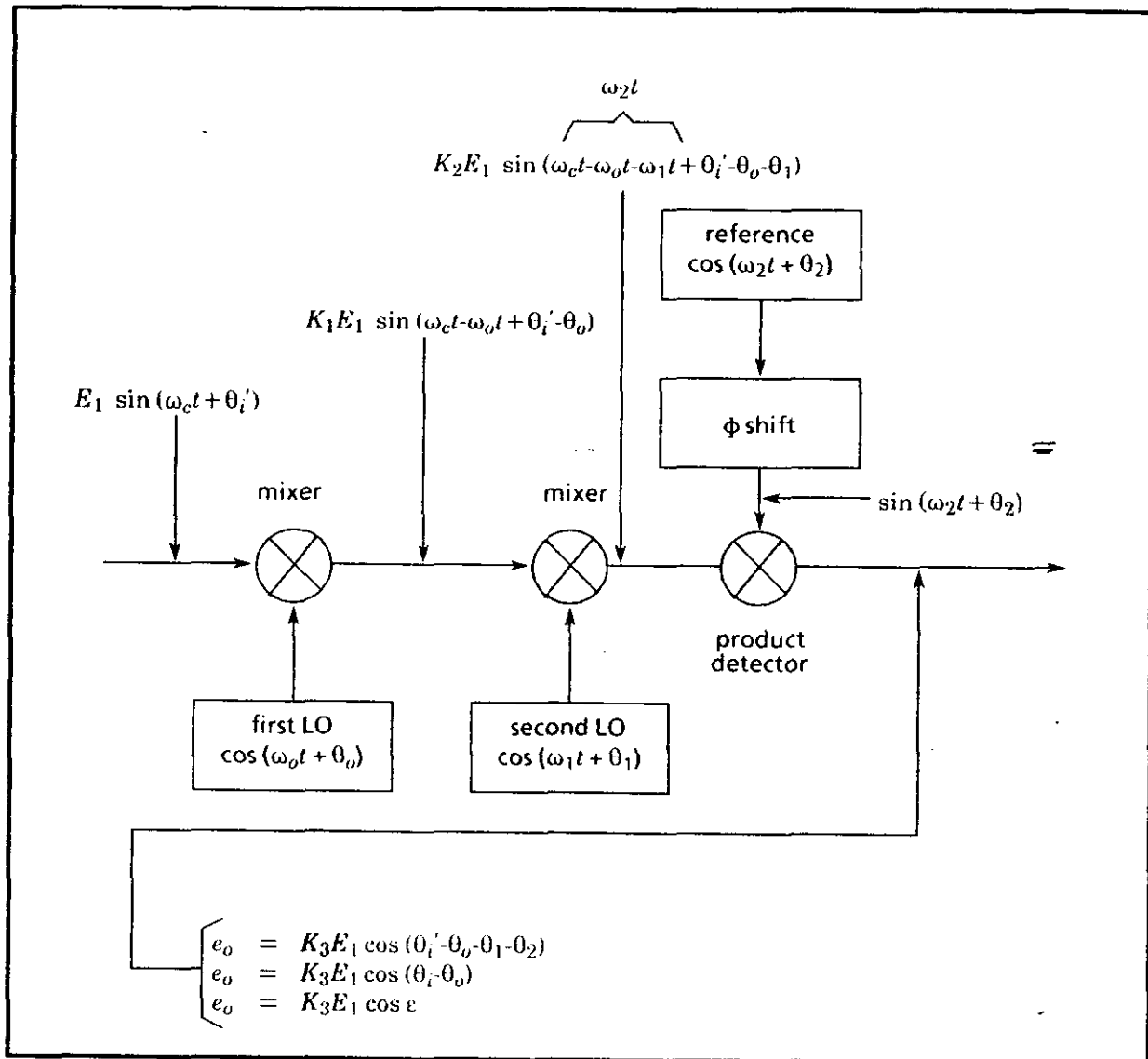
FIGURE 27. <u>Functional block diagram of a difference channel.</u>

Combining equations (125) and (138) yields

$$\omega_o(s) = \frac{2\omega_n s + \omega_n^2}{(s+\omega_n)^2} \times \omega_i(s) \tag{139}$$

Combining equations (139) and (130) and obtaining the inverse Laplace transform results in

$$
\begin{aligned}
\omega_o(t) = 19\,(1.51)\,\omega_r^2 \Bigg\{ &-t\,(1-e^{-\omega_n t})\,U(t-o) \\[2mm]
&+2\,(t-\frac{1}{19f_r})(1-e^{-\omega_n(t-\frac{1}{19f_r})})\,U(t-\frac{1}{19f_r}) \\[2mm]
&-(t-\frac{2}{19f_r})(1-e^{-\omega_n(t-\frac{2}{19f_r})})\,U(t-\frac{2}{19f_r}) \\[2mm]
&-(t-\frac{1}{f_r})(1-e^{-\omega_n(t-\frac{1}{f_r})})\,U(t-\frac{1}{f_r}) \\[2mm]
&+\text{---------------------} \Bigg\} \tag{140}
\end{aligned}
$$

Making the substitutions

$$K_1 = \frac{f_r}{f_n} \tag{141}$$

and

$$K = f_r t \tag{142}$$

and

$$\omega = 2nf \tag{143}$$

and writing the expression in a more compact form, as for the previous derivation, yields

$$f_o(t) = 19(9.5)\, f_r \sum_{n=0}^{\infty} \left\{ -(K-n)(1-e^{-2\pi K_1 (K-n)})\, U(K-n) \right.$$

$$+2\left(K - \frac{1+19n}{19}\right)\left(1 - e^{-2\pi K_1 (K - \frac{1+19n}{19})}\right) U\left(K - \frac{1+19n}{19}\right)$$

$$\left. -\left(K - \frac{2+19n}{19}\right)\left(1 - e^{-2\pi K_1 (K - \frac{2+19n}{19})}\right) U\left(K - \frac{2+19n}{19}\right) \right\} \qquad (144)$$

Equation (144) identifies how the instantaneous frequency of the phase-locked loop is following the input frequency of a limited multipath signal. This equation is plotted in Figure 28 for various values of K_1. Note how closely the VCO follows the input when the loop bandwidth is widened to equal the maximum frequency excursion of the composite input. Although it is not part of this study, it would be very interesting and valuable to determine the average frequency over one cycle for the various values of K_1 to see how much it deviates from $f_r/2$. When it is equal to $f_r/2$, narrowband filtering following the detected loop output recovers the wanted signal. This result is an obvious one for wideband operation (that is, $K_1 = 10$) and is exactly what one would expect. It is equivalent to using a wideband discriminator following a limiter, to reduce the crosstalk effect of a multipath signal with a narrowband output filter in an FM receiver.

5.5 Timing accuracy for a pseudonoise sequence

5.5.1 Basic approach. Figure 29 is a functional block diagram of an optimum system used to obtain a time measurement of an input pseudonoise (PN) sequence. The error detector consists of two correlation detectors. The reference inputs to this detector are one code bit apart in time, and inverted relative to each other. This operation results in the error detector characteristic illustrated in Figure 30. The defining parameters are tabulated below and will be referred to in analyzing the ultimate accuracy capability.
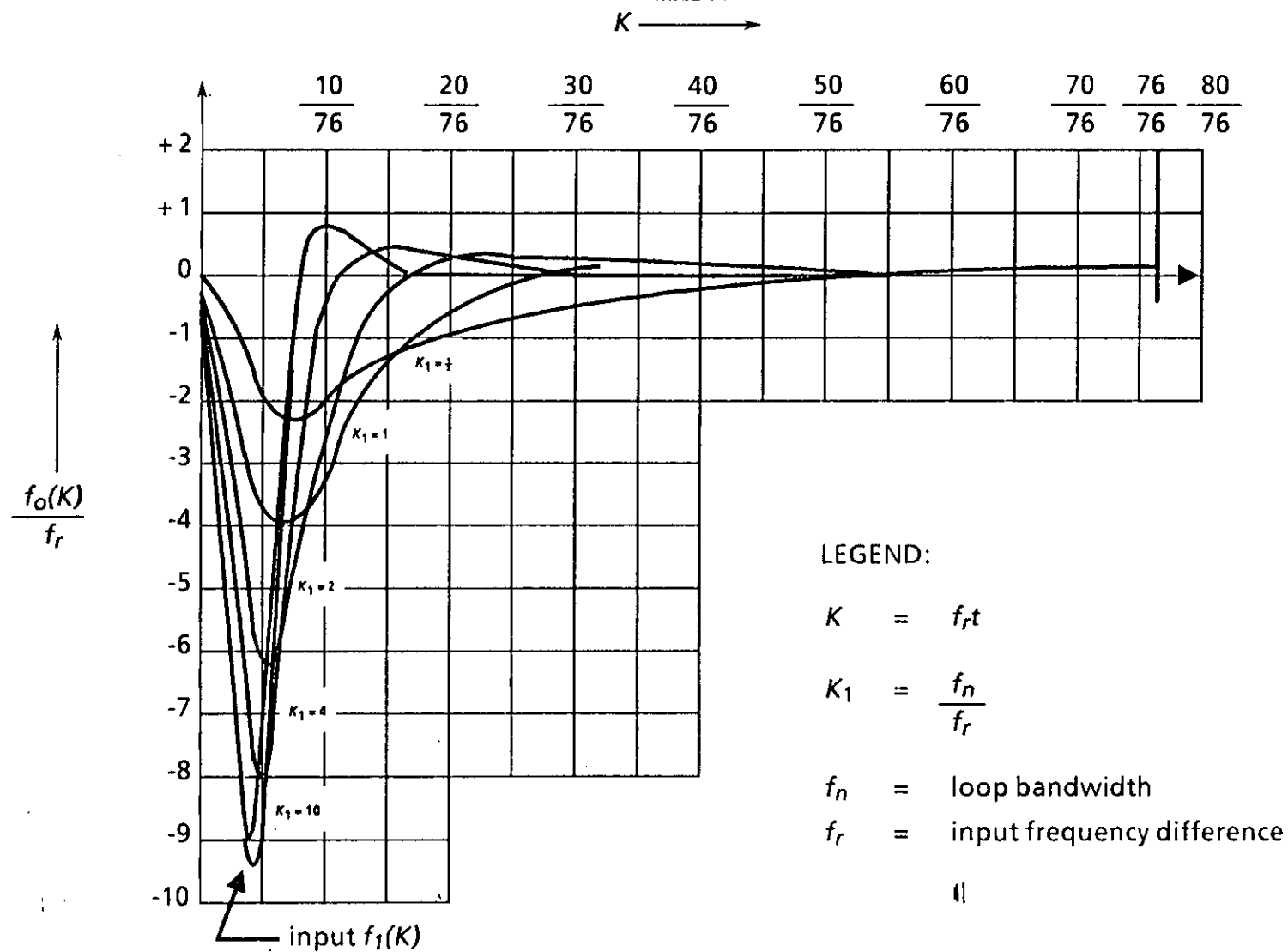
FIGURE 28. The output frequency plotted over one cycle for various values of K_1.

LEGEND:

$$K = f_r t$$

$$K_1 = \frac{f_n}{f_r}$$

$$f_n = \text{loop bandwidth}$$

$$f_r = \text{input frequency difference}$$

74
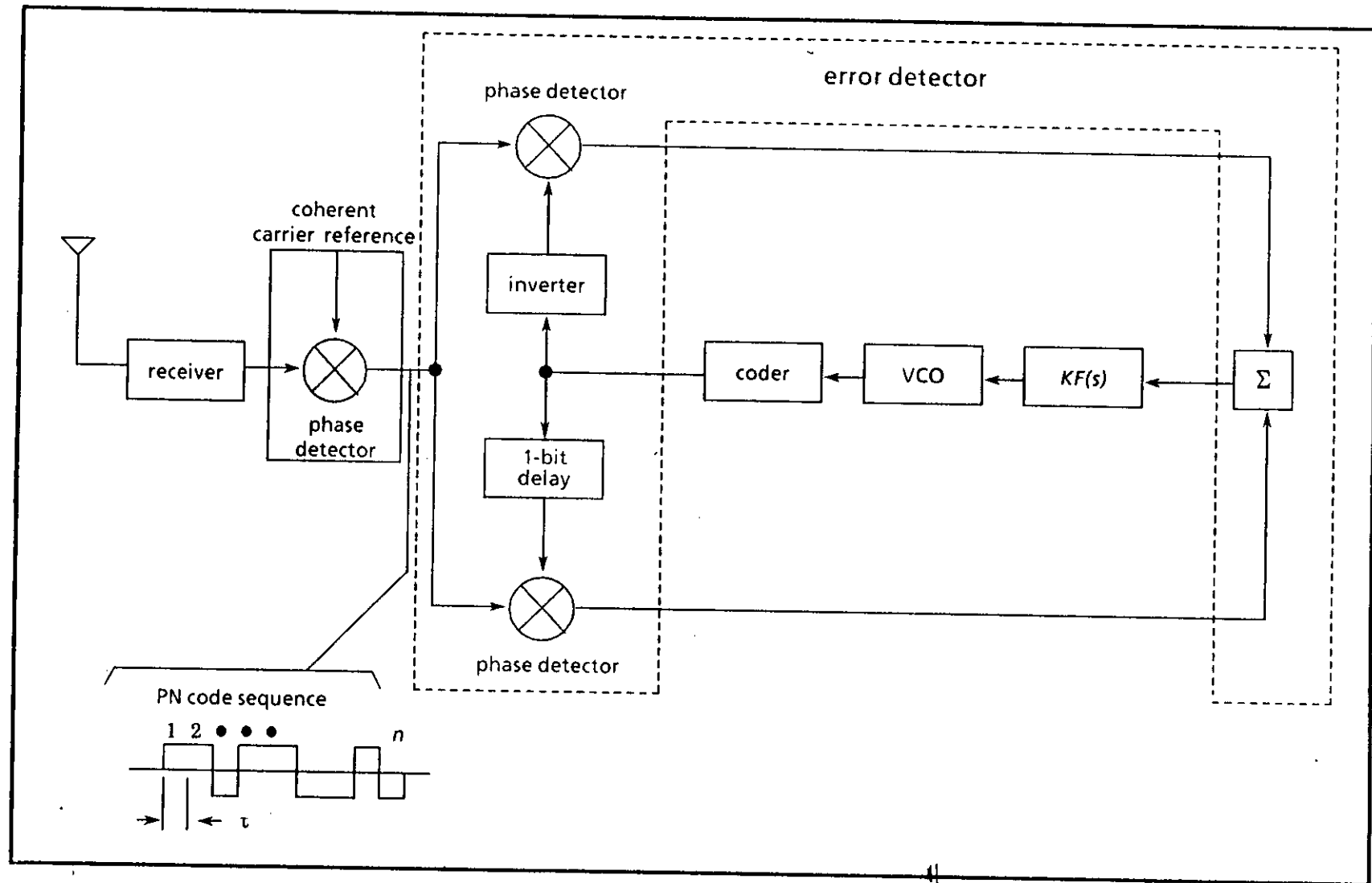
MIL-HDBK-421

FIGURE 29. Basic timing system for synchronizing to a PN code sequence.

MIL-HDBK-421

75
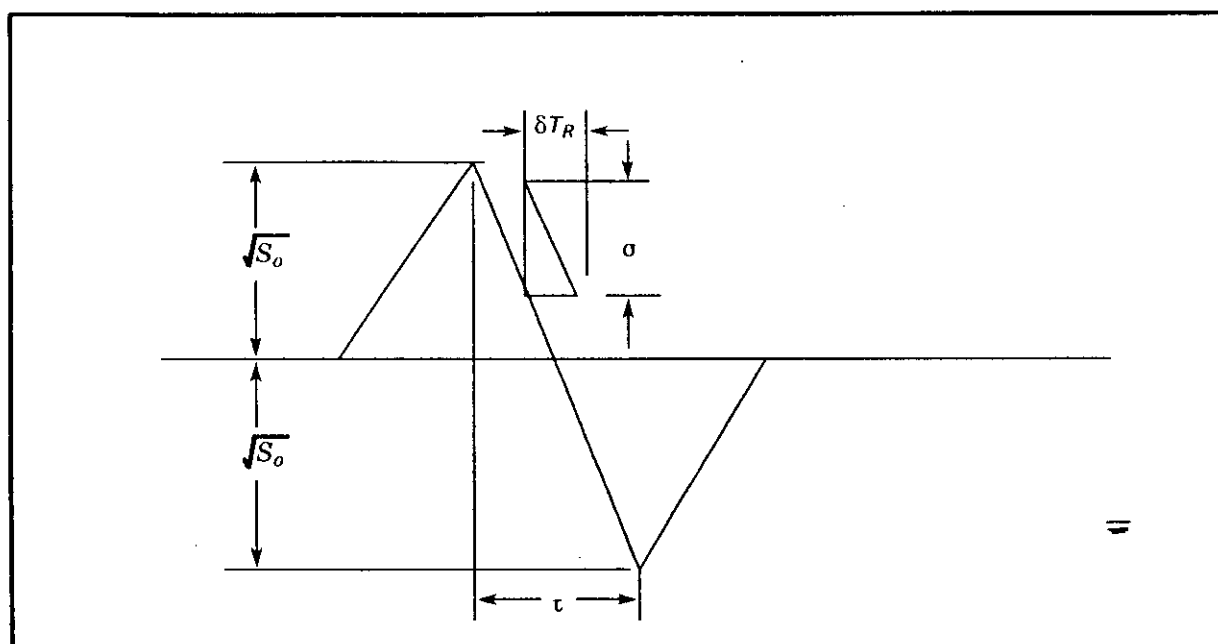
FIGURE 30. Error detector characteristics for a PN code sequence (basic synchronizing system).

Referring to Figure 30

ι = code bit width

σ = output rms noise amplitude $\sigma = \sqrt{2\,N_0}$

where

$\sqrt{2}$ results from the summation of two uncorrelated noise sources in the error detector

N_0 = output noise power

δT_R = output rms noise-time jitter

$\sqrt{S_0}$ = output signal peak voltage

The rms output noise-time jitter may be related to the output rms noise amplitude σ, the code bit pulsewidth τ, and the peak signal voltage $\sqrt{S_0}$ from the geometry of the error detector output characteristics

$$\frac{\delta T_R}{\sigma} = \frac{\tau}{2\sqrt{S_0}} \tag{145}$$

Since

$$\sigma = \sqrt{2\,N_0}$$

then

$$\delta T_R = \frac{\iota}{\sqrt{\dfrac{2 S_o}{N_o}}}$$

(146)

Now each half of the error detector comprises an optimum correlation detector that yields an output $(S/N)_o$ corresponding to that of a matched filter,

that is,

$$\frac{S_o}{N_o} = \frac{2E}{N}$$

(147)

where

E =   signal energy

N =   noise power density

Combining equations (146) and (147) results in:

$$\delta T_R = \frac{\iota}{2 \sqrt{\dfrac{E}{N}}}$$

(148)

It will now be established that coding with the PN code structure achieves a timing accuracy $\sqrt{n}$ times better than for a bandwidth-limited, uncoded, pulsed sine wave.

Skolnick (see Appendix B, 20.2) has derived an expression for the rms timing error for a pulsed sine wave, which is given by

$$\delta T_R = \sqrt{\frac{\iota'}{4BE/N}}$$

(149)

where

ι' =   pulsewidth
B =   bandwidth

Now, for a signal that is bandwidth-limited to the reciprocal of the code bit width and whose pulse length is $n\,\iota$, resulting in the same signal energy as for the coded case, we have

$$B = \frac{1}{\iota}$$

and

$$\iota' = n\iota$$

Hence

$$\delta T_R = \frac{\sqrt{n}\ \iota}{2\sqrt{\dfrac{E}{N}}} \tag{150}$$

A comparison between equations (150) and (148) demonstrates that the code structure improves the rms timing accuracy by $\sqrt{n}$ or the mean-square timing accuracy by n.

It is instructive to emphasize here that the particular error detector characteristics illustrated result from the fact that the code structure is of a PN type. This choice completely eliminates any ambiguity in timing, while at the same time yields the accuracy given by equation (148). Other code structures may provide a slightly better timing accuracy but in general are at the expense of introducing ambiguities. The maximum possible accuracy would be for a sequence of $+1$'s and -1's (or, equivalently, a carrier or subcarrier square wave). In this case the peak-to-peak voltage ratio out of the error detector is $4\sqrt{S_o}$ and results in a timing accuracy given by

$$\delta T_R = \frac{\iota}{4\sqrt{\dfrac{E}{N}}} \tag{151}$$

This is twice as good as for the PN sequence but has $n/2$ ambiguities of equal signal strength.

5.5.2   The Jet Propulsion Laboratory's error detector for locking to a PN sequence. An alternate method of synchronizing to a PN sequence consists of modulating the PN code with a subcarrier whose frequency is half the PN code bit rate. This is the approach used by the Jet Propulsion Laboratory (JPL) for the Mariner System and other similar space projects involving ranging, telemetry, and command functions. This solution does not permit code sequences with a two-level autocorrelation to be used unless the out-of-phase correlation level is 0. A maximal-length sequence code or a quadratic residue sequence (these codes possess an out-of-phase correlation equal to $-1/N$) results in ambiguous timing unless the code structure is modified. In addition, the accuracy achieved in this system is 3 dB poorer than that of the basic approach.

To verify the above claims, consider the following 7-bit maximal-length sequence codes (PN code):

$$1\ 1\ 1\ 0\ 0\ 1\ 0$$

This code may be written as

$$1\ 1\ 1\ 1\ 1\ 1\ 0\ 0\ 0\ 0\ 1\ 1\ 0\ 0$$

to make obtaining correlation functions at half the code chip-width intervals easy. Modulating this PN code with a subcarrier whose frequency is half the code bit frequency results in (PN $\oplus$ f_s), where $\oplus$ indicates modulo 2 addition. This operation yields

$$\overbrace{\overbrace{1\,1\,0\,0\,1\,1\,1\,1\,0\,0\,0\,0\,0\,0}^{A}\,\overbrace{0\,0\,1\,1\,0\,0\,0\,0\,1\,1\,1\,1\,1\,1}^{\overline{A}}}$$

that is,

$$(PN \oplus f_s) = A,\ \overline{A}$$

where

$$\overline{A} = the\ negative\ of\ A$$

$\overline{A}$ occurs since the code bit length is odd, which results in a 180° phase reversal of the subcarrier at the beginning of each 7-bit code length. This phenomena introduces quasi-stable locking positions every other code period. The error detector for synchronizing is now realized by generating (PN $\oplus$ f_s $\angle$ 90°), which is used to cross-correlate with (PN $\oplus$ f_s). A method of implementing the generation and cross-correlation of the identified functions is illustrated in Figure 31.

Let us now perform the cross-correlation indicated. To do this requires that we determine PN $\oplus$ f_s $\angle$ 90°, which is accomplished below:

PN 1 1 1 1 1 1 0 0 0 0 1 1 0 0 1 1 1 1 1 1 0 0 0 0 1 1 0 0

$f_s\angle 90^o$ 1 0 0 1 1 0 0 1 1 0 0 1 1 0 0 1 1 0 0 1 1 0 0 1 1 0 0 1

$PN \oplus f_s\angle 90^o$ $\underbrace{1\,0\,0\,1\,1\,0\,1\,0\,0\,1\,0\,1\,0\,1}_{B}\,\underbrace{0\,1\,1\,0\,0\,1\,0\,1\,1\,0\,1\,0\,1\,0}_{\overline{B}}$

or

$$PN \oplus f_s\angle 90^o\ = B,\ \overline{B}$$

where

$$\overline{B} = the\ negative\ of\ B.$$
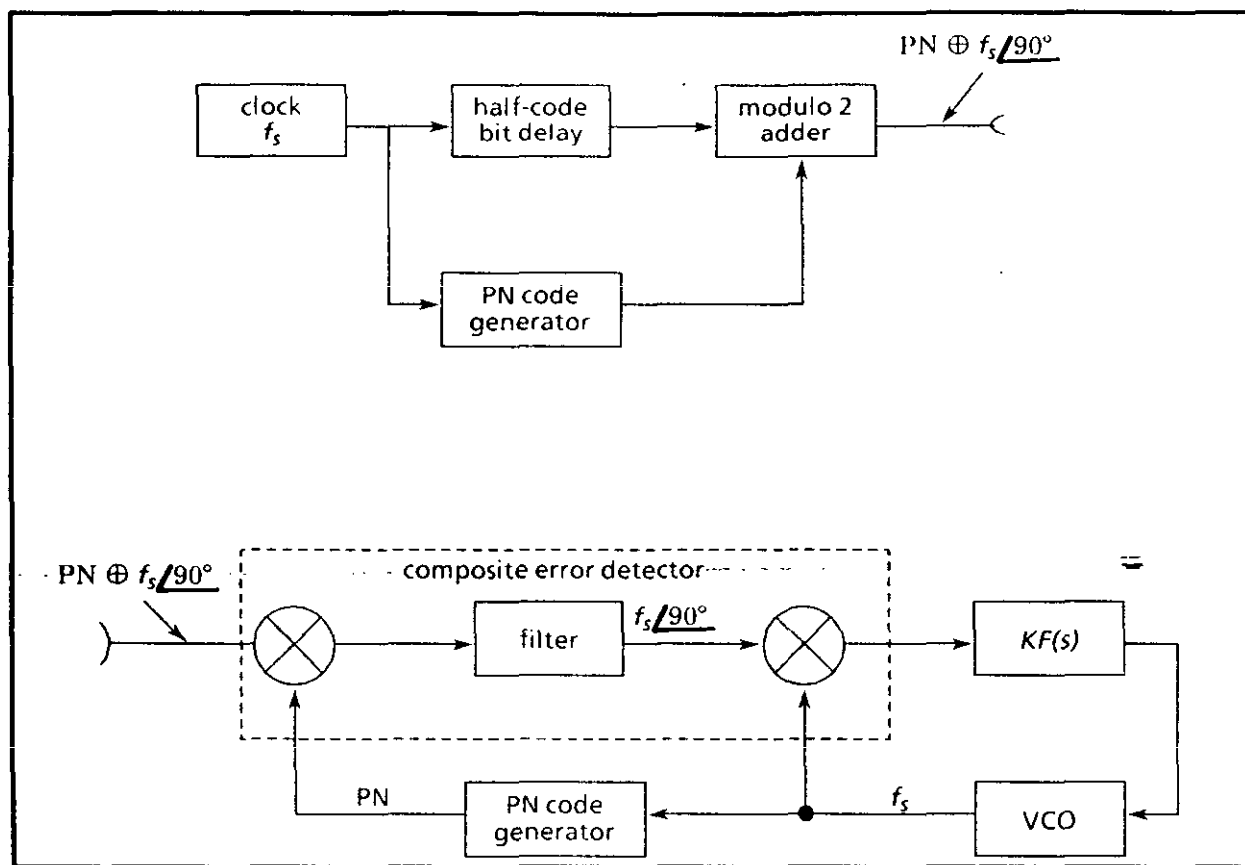
FIGURE 31. Double loop-tracking system for synchronizing to a PN code sequence.

A, $\overline{A}$ cross-correlated with B, $\overline{B}$ results in the correlation function (error curve) illustrated in Figure 32a. Note that in addition to forming quasi-stable conditions, ambiguous stable and quasi-stable locking points also accrue. This was anticipated and is the result of the fact that the autocorrelation function of the code in question is $(-1/N)$ for $\tau \neq 0$. If an even digit code whose out-of-phase autocorrelation function were zero had been used in the system, then neither quasi-stable points nor ambiguous stable points would occur. Of course for a reasonably large number of code bits, the ambiguous locking positions are rather low in signal level compared to the desired locking position.

JPL solves both of the difficulties identified by the simple expedient of following the PN code by its negative, which results in the composite structure PN* (see Figure 32b).

$$\underbrace{1\ 1\ 1\ 1\ 1\ 1\ 0\ 0\ 0\ 0\ 1\ 1\ 0\ 0}_{PN}\underbrace{0\ 0\ 0\ 0\ 0\ 0\ 1\ 1\ 1\ 1\ 0\ 0\ 1\ 1}_{\overline{PN}}$$

or

$$PN^* = PN, \overline{PN}$$

Modulating this code with a subcarrier f_s whose frequency is half the code bit frequency provides PN* $\oplus f_s$.

80

a. PN sequence 1110010

stable

quasi-stable

τ

$\frac{N-1}{2}$

$\frac{N-1}{2}$
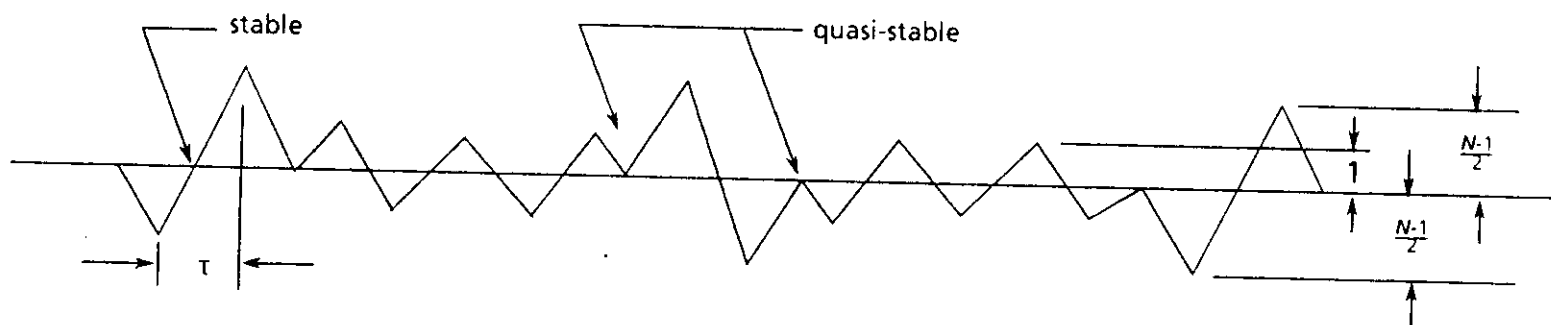
b. PN* = PN, $\overline{PN}$ 1110010 0001101

stable

stable

τ

$\frac{N+1}{2}$

$\frac{N+1}{2}$
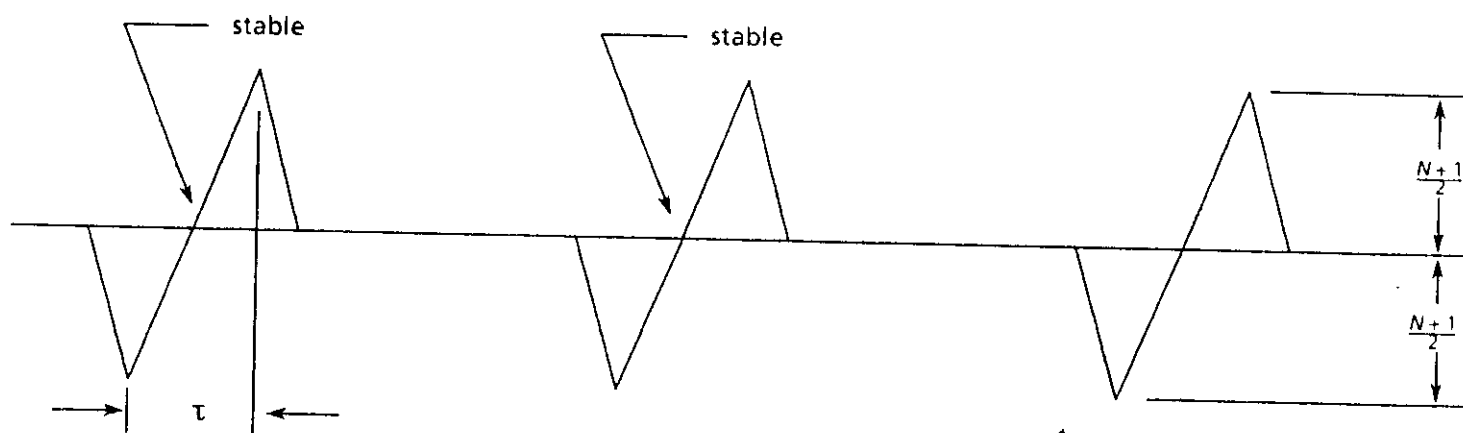
FIGURE 32. <u>Error function for a double loop-tracking system</u>.

MIL-HDBK-421

81

Performing this operation yields

$$\overbrace{\underbrace{1\,1\,0\,0\,1\,1\,1\,1\,0\,0\,0\,0\,0\,0}_{\alpha}\;\underbrace{1\,1\,0\,0\,1\,1\,1\,1\,0\,0\,0\,0\,0\,0}_{\alpha}}$$

Note that the modified PN code modulo 2 added to f_s now results in a repeating structure every 7 code bits.

Equivalently, PN* $\oplus$ f_s $\angle 90°$ becomes,

$$\overbrace{\underbrace{1\,0\,0\,1\,1\,0\,1\,0\,0\,1\,0\,1\,0\,1}_{\beta}\;\underbrace{1\,0\,0\,1\,1\,0\,1\,0\,0\,1\,0\,1\,0\,1}_{\beta}}$$

which also repeats every 7 code bits.

The cross-correlation of α and β now achieves the very desirable property of a single repeating S curve with no quasi-stable points or ambiguous locking positions. This result is illustrated in Figure 32b. It appears that one answer solved two problems.

Let us digress at this point to demonstrate that an even-length, two-level autocorrelation code whose out-of-phase correlation is equal to 0 results in a single stable repeating S curve with no ambiguities. The simplest code with the required properties is the following 4-bit sequence.

$$PN = 1\ 1\ 1\ 0$$

which may be written as

$$PN = 1\ 1\ 1\ 1\ 1\ 1\ 0\ 0$$

or

$$PN \oplus f_s\ \ = 1\ 1\ 0\ 0\ 1\ 1\ 1\ 1$$

also

$$PN \oplus f_s \angle 90^0 = 1\ 0\ 0\ 1\ 1\ 0\ 1\ 0$$

And the cross-correlation of (PN $\oplus$ f_s) with (PN $\oplus$ f_s $\angle 90°$) results in the desired error curve shown in Figure 33.
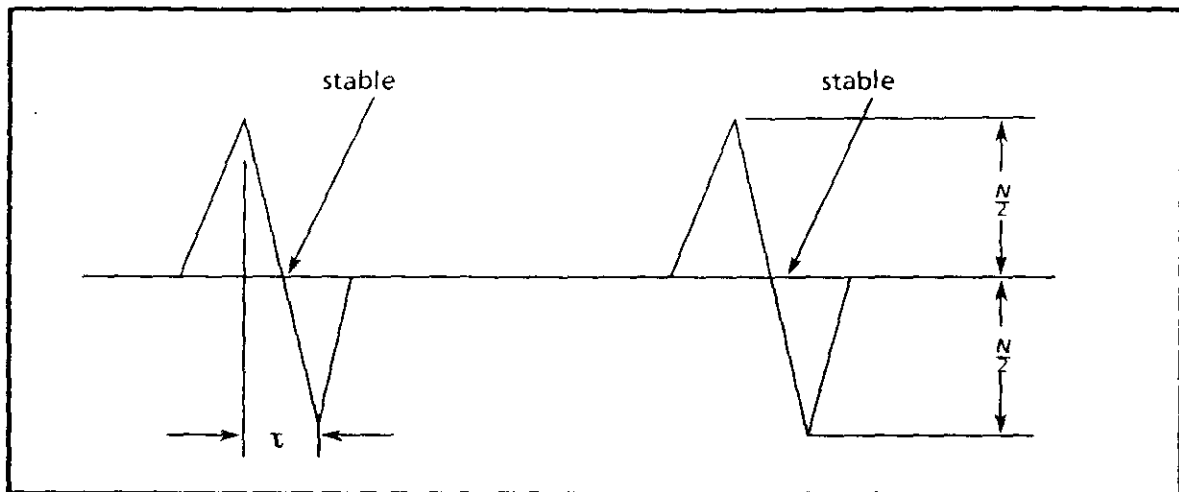
FIGURE 33. Error function for double loop-tracking system with PN = 1⊥10.

Using the identified error curve makes determining the maximum timing accuracy that may be realized in the double loop-tracking system easy. The error function is essentially the same as in the basic approach, with one difference. The peak output amplitude is approximately $N/2$ or half as much. An odd-bit code length of the class examined resulted in

$$\frac{N+1}{2}$$

or

$$\frac{N-1}{2}$$

or when the modified PN^* was used. The even-length sequence illustrated above resulted in exactly $N/2$ for the peak amplitude. In all cases, the peak amplitude may be considered as $N/2$ for a reasonably large N. Hence, the diagram of Figure 30 with $\sqrt{S_0}$ replaced by

$$\frac{\sqrt{S_0}}{2}$$

may be used to determine the output rms time jitter δT_R.

$$\frac{\delta T_R}{\sigma} = \frac{c}{\sqrt{S_0}} \tag{152}$$

In this system the output noise-time jitter σ is given by $\sqrt{N_0}$ since the error detector does not sum two output noise sources.

Hence

$$\delta T_R = \frac{c}{\sqrt{\frac{S_0}{N_0}}} \tag{153}$$

83

since

$$\frac{S_o}{N_o} = \frac{2E}{N}$$ (154)

$$\delta T_R = \frac{\iota}{\sqrt{2}\sqrt{\dfrac{E}{N}}}$$ (155)

Comparing equation (155) with (148) demonstrates that the double-loop timing system accuracy is $\sqrt{2}$ or 3 dB worse than for the basic system. The fundamental reason for the degradation in the alternate system is that the peak output amplitude is obtained when the input and reference are a half code-chip-width apart in time.

5.6 A concept for disseminating precise timing throughout a communications network

5.6.1 Basic concept. The following system concept employs a Doppler-canceling loop for a master satellite ground terminal in conjunction with a multiplexed synchronous loop at each slave satellite ground terminal. The Doppler-canceling loop translates a Doppler-free stable clock to the satellite. Each slave terminal then receives and synchronizes to this reference clock, which now has a Doppler frequency shift that results only from the range variation between the slave ground terminal and the satellite. The retransmission and reception of this signal on a separate multiplexed channel then yields the reference clock shifted by a multiple of the Doppler frequency. The two signals may then be appropriately combined in a mixer to cancel the Doppler frequency variation from the primary standard clock reference at each slave terminal.

The basic ideas involved in accomplishing the desired result are illustrated in Figure 34. A Doppler-canceling loop is employed between the master ground terminal and the satellite, which translates a Doppler-free reference to the satellite by establishing a local oscillator that is synchronized to $(f_o - f_{dm})$

where

f_o = the primary standard reference clock at the master terminal

f_{dm} = the one-way Doppler frequency that exists between the master terminal and the satellite.

f_{ds} = the one-way Doppler frequency that exists between the slave terminal and the satellite

84
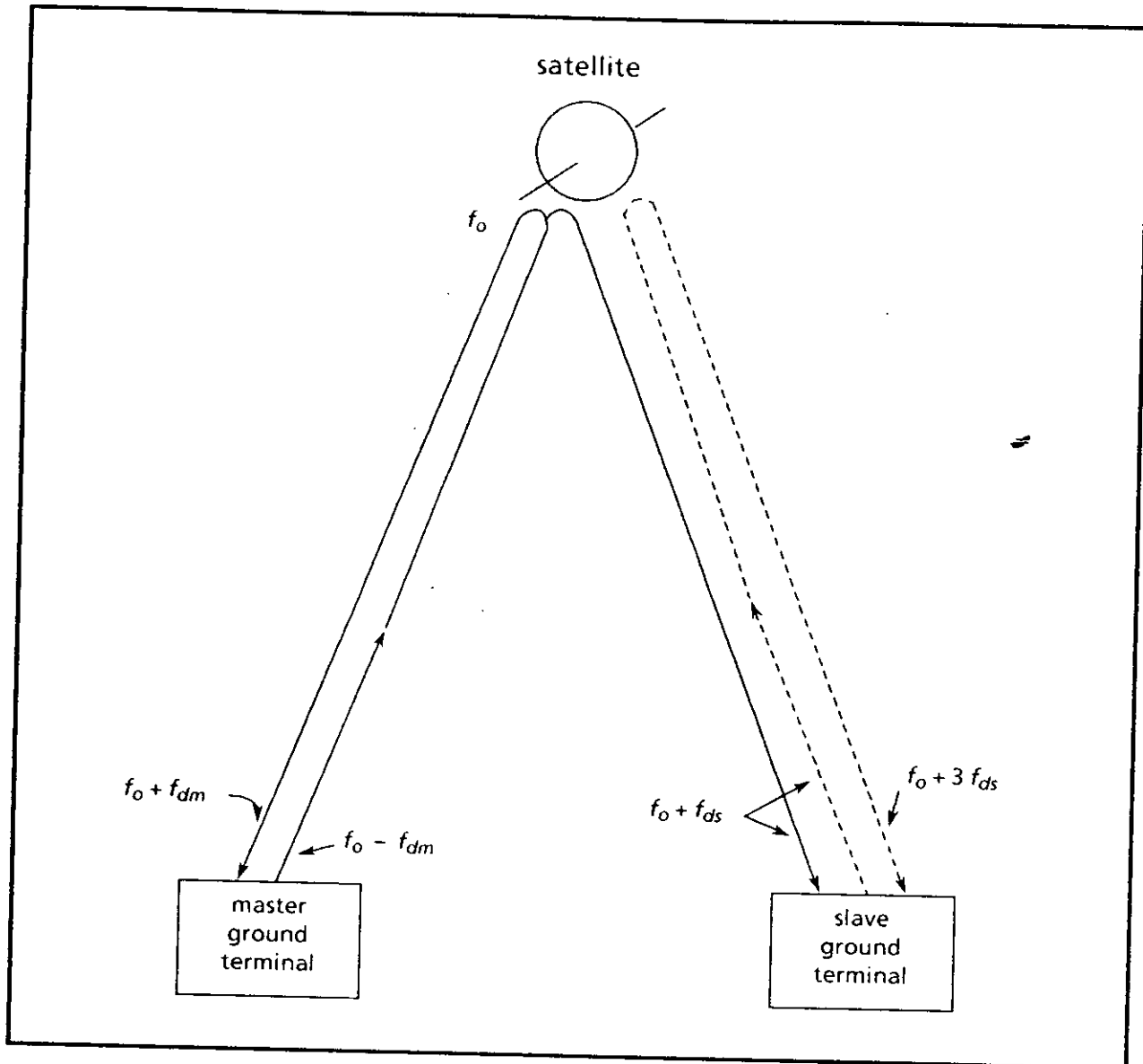
FIGURE 34. System for transferring timing via satellite.

A functional block diagram of the Doppler-canceling loop is shown in Figure 35. The VCO frequency f is transmitted to the satellite and back down to the ground terminal.
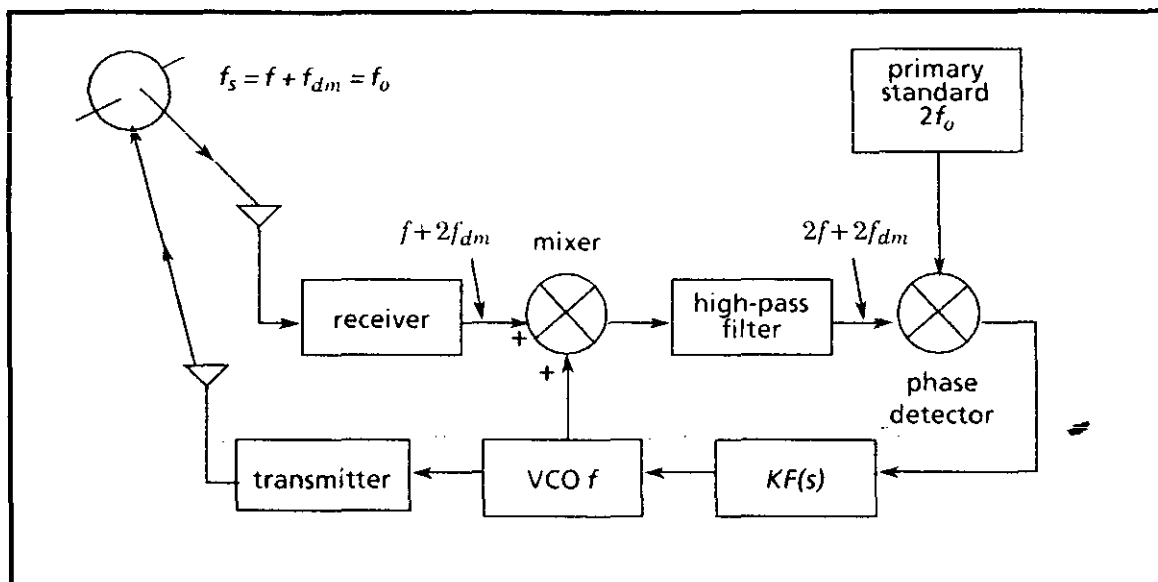
FIGURE 35. Doppler-canceling loop.

This frequency is translated by f_{dm} at the satellite, due to its motion. Back at the ground terminal the Doppler frequency is $2 f_{dm}$. This is mixed with the VCO frequency, and the sum is fed to the phase detector of the phase-locked loop. The phase of the sum frequency ($2f + 2 f_{dm}$) is compared with a frequency $2 f_o$, which is derived from a primary standard clock such as a cesium atomic clock. The phase detector output is then passed through the system loop filter to the VCO. The VCO frequency varies in proportion to the error control voltage until the input to the phase detector is exactly equal to the clock frequency $2 f_o$.

Hence, at lock

$$2f + 2f_{dm} = 2f_o \tag{156}$$

or

$$f = f_o - f_{dm} \tag{157}$$

This condition results in a frequency at the satellite of

$$f_s = f_o - f_{dm} + f_{dm} = f_o \tag{158}$$

An alternate method of providing a Doppler-free reference at the satellite is to physically put a primary clock standard in the satellite. In this case, however, the malfunction of the primary standard loses the highly stable reference. In the proposed concept, any quantity of backup primary standards may be used to achieve any degree of reliability desired.

Each slave ground terminal may now synchronize to the primary standard at the satellite and may extract the Doppler frequency experienced on the satellite-to-slave-terminal link. This is accomplished by retransmitting the received timing signal $(f_o + f_{ds})$ on a separate channel as shown in Figure 36. The returned signal is now $(f_o + 3f_{ds})$. These two signals are then demultiplexed and synchronized in separate phase-locked loops used to accomplish coherent detection. The output frequency of the channel that is synchronized directly to the master terminal $(f_o + f_{ds})$ is then multiplied by 3 and mixed with the frequency of the output from the slave terminal $(f_o + 3f_{ds})$ to obtain the complete extraction of the Doppler frequency. This signal is exactly twice the primary standard, or $2f_o$, and dividing the frequency by 2 provides the primary clock timing signal f_o at the slave terminal.

5.6.2 <u>Alternate solution</u>. An alternate method for separating the Doppler frequency and reference clock at the slave terminal is illustrated in Figure 37. A received transmission loop signal $(f + 2f_d)$ is compared simultaneously in phase with the signal from the master ground terminal $(f_o + f_{do})$ and used to control the loop VCO. This is implemented by employing a separate orthogonal channel for the loop signal frequency f. This is then demultiplexed from the master terminal signal, and both signals are separately and coherently detected using phase-locked loops. The outputs of the individual loops are then compared in a loop phase detector and passed through a system loop filter to the transmission loop VCO. The frequency f of this VCO is changed until the transmission loop is synchronized. This occurs when the loop VCO frequency f is equal to (f_o).

When the transmission loop is locked, the phase detector output is 0, and

$$f + 2f_d = f_o + f_{do} \tag{159}$$

or

$$f + f_d = f_o - f_d + f_{do} \tag{160}$$

where

f_{do} = the one-way Doppler frequency that exists between the slave terminal and the satellite.

Also, at the satellite,

$$f + f_d = f_o \tag{161}$$

Therefore, from equations (160) and (161)

$$f_d = f_{do}$$

and

$$f = f_o - f_{do} \tag{162}$$
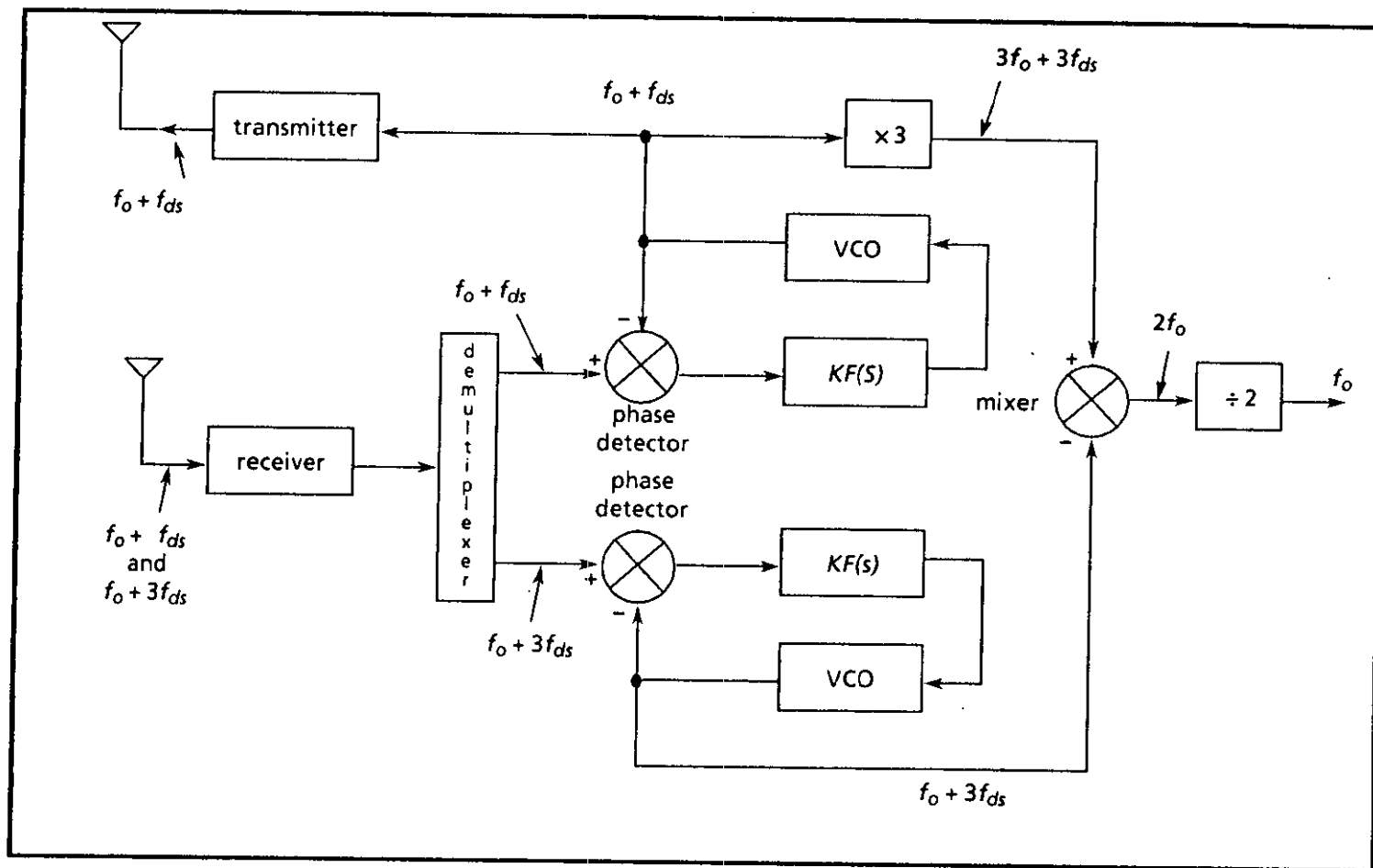
FIGURE 36. Doppler extraction method and slave terminal.
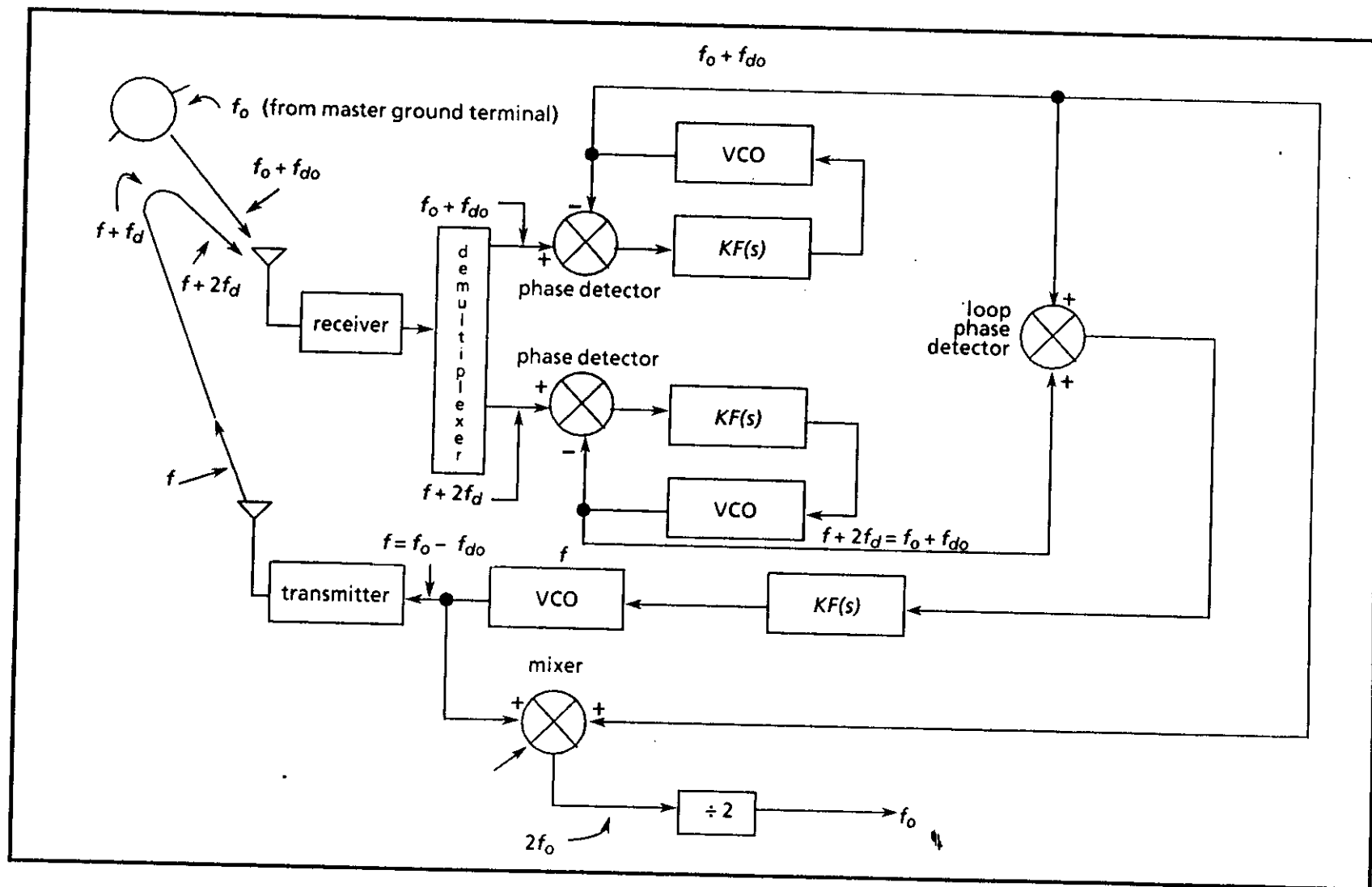
FIGURE 37. <u>Alternate Doppler extraction method for the slave terminal</u>.

MIL-HDBK-421

69

To obtain the frequency f_o now simply requires mixing the loop VCO frequency ($f_o - f_{do}$) with the signal received from the master terminal ($f_o + f_{do}$) and filtering out the sum frequency. The frequency at the output of the mixer is then divided by 2 to provide a Doppler-free stable clock whose frequency is f_o.

5.6.3 <u>Conclusion</u>. The above concepts that have been identified enable precise timing to be translated to any network node location on the globe, using a satellite transmission link. The translated timing signal has all Doppler frequency variations that result from satellite motion completely removed, which provides a synchronous network for both terrestrial and space trunking.

The basic ideas are applicable for a synchronous satellite, a nonsynchronous satellite, or an airborne relay and are relatively inexpensive to implement.

The alternate Doppler extraction method for the slave terminal has an advantage over the basic concept. In the alternate approach, a Doppler-free timing signal is provided automatically from the slave terminal at the satellite, which enables TDMA to be employed directly.

5.7 A synchronous timing system

5.7.1 <u>Background</u>. A concept for disseminating precise timing was presented in 5.6. The method described provides the transfer of a precise primary clock standard to any network node via satellite. The proposed system provides a Doppler-free stable clock at each node. This automatically results in a synchronous network that has negligible time variations for all trunking, resulting from viable propagation delays (this comprises essentially all terrestrial trunking). Additional circuitry is required, however, to extract the Doppler frequency variation from the message traffic channels transmitted over the satellite link. This extraction renders the input synchronous with the terrestrial trunking and may be accomplished by implementing the functional block diagram in Figure 38. As before, an up-down loop is synchronized by comparing the phase of the received transmission loop signal ($f + 2f_d$) with the source signal of a master terminal ($f_o + f_{do}$). This is accomplished in the loop phase detector (No. 1) after demultiplexing the two received signals. The output of this loop phase detector is then passed through the system loop filter [$KF(s)$] and is used to control the frequency f of the VCO. This frequency is varied by the control voltage until synchronization is accomplished. When the loop is locked, the VCO frequency at the ground slave terminal is

$$f = f_o - f_{do}$$

which provides a frequency f_o at the satellite to facilities, accomplishing TDMA through the satellite and, in addition, enabling the Doppler frequency to be eliminated from both the timing channel and the message channels at the ground terminal.

To extract the Doppler frequency from the timing signal simply requires mixing the loop VCO frequency ($f_o - f_{do}$) with the timing signal received from the master terminal ($f_o + f_{do}$) in mixer No. 2 and filtering out the sum frequency. This yields a frequency $2f_o$, which is then divided by 2 to provide a local reference clock timing signal f_o that is free of the timing variation associated with the Doppler effect (see Figure 38.)
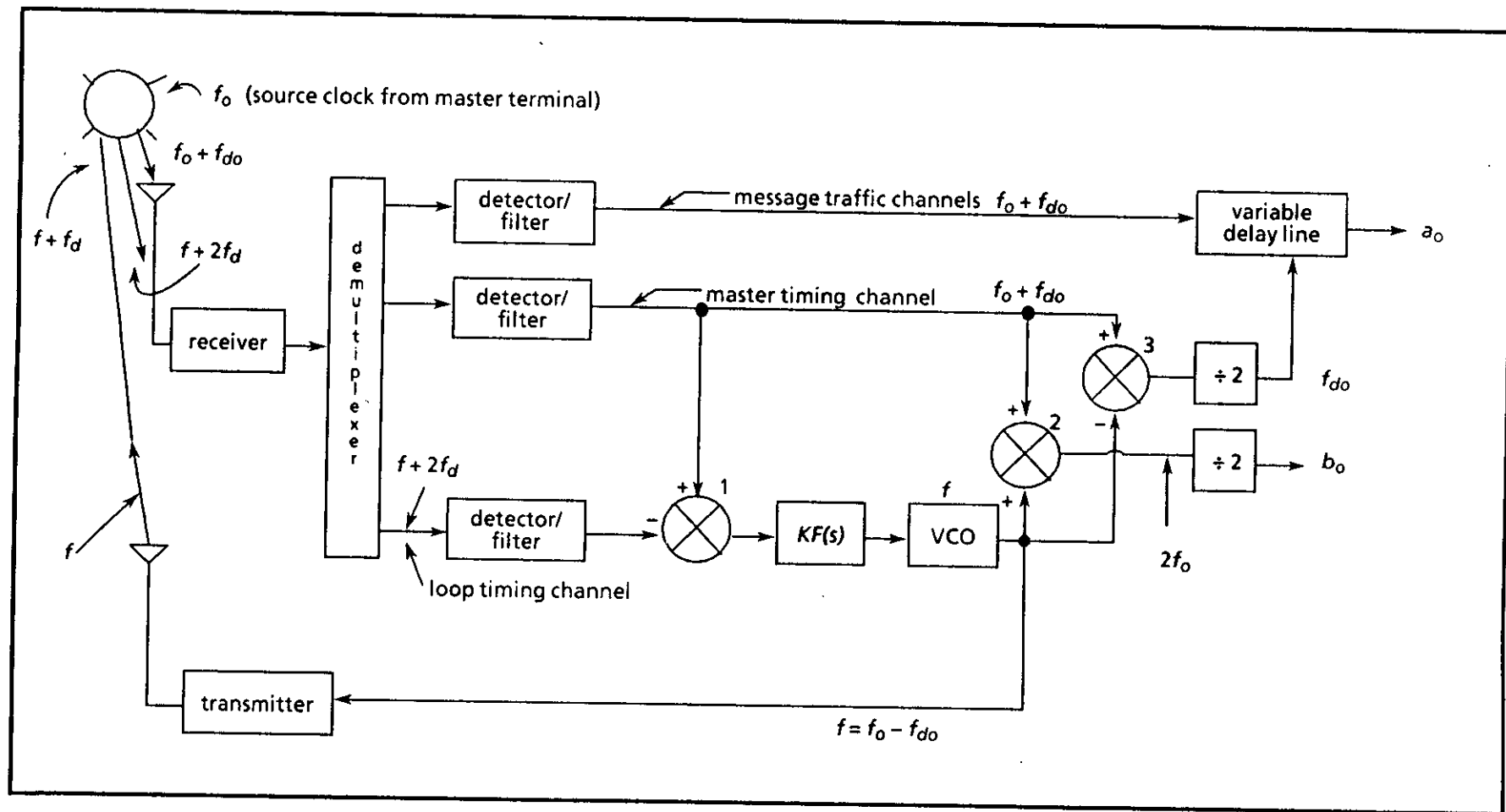
FIGURE 38. Satellite timing system with Doppler frequency extraction.

MIL-HDBK-421

91

The timing variation of the received message channels is now eliminated as follows: First, the clock signal is extracted from the Doppler-varying-timing signal by mixing the VCO frequency ($f_o - f_{do}$) with the timing signal received from the master terminal ($f_o \pm f_{do}$) in mixer No. 3 and filtering out the difference frequency. This yields a frequency 2 f_{do}, which is then divided by 2 to yield the Doppler frequency. This Doppler frequency may then be used to vary the time positions of the message bits in the message traffic channels by adjusting the delay of the variable delay line to provide an output that is free of the timing variation associated with the Doppler effect. The proposal concept is illustrated with a functional block diagram to establish the philosophy involved in accomplishing the desired results. Several alternatives could readily be identified, which yields the same result, and a final preferred equipment design would be influenced by differences in the hardware configuration employed. The fundamental notion involved in the approach is to obtain synchronous frequencies of ($x_1 f_o + y f_{do}$) and ($x_2 f_o - y f_{do}$) on multiplexed timing channels, where f_{do} is the Doppler frequency associated only with the transmission link between the satellite and the slave ground terminal. This results in the same Doppler frequency for all the input message channels, independent of the other ground terminal from which it originated. Tagging a positive and negative Doppler frequency of identical magnitude onto the clock reference enables the use of simple hardware to extract the Doppler frequency component and the clock-reference frequency component.

Although the concept was described for a single satellite relay link, any quantity can be accommodated at each node by using separate orthogonally multiplexed channels for each space (satellite or airborne) relay. Since timing requirements involve very low data rates (limited only by clock stabilities) the frequency spectrum need is nominal, even if a very large anti-jam (AJ) protection that uses spread-spectrum techniques is provided.

5.8 A time-dissemination and Doppler-canceling system for satellite access

5.8.1 Introduction. A concept is presented that provides for the dissemination of a precise primary standard clock via satellite for a frequency-division multiple access (FDMA) satellite system. One unique aspect of the approach is that the Doppler frequency is completely eliminated at all the nodes (slaved satellite ground terminals). This translates a primary ultrastable clock reference to all the ground terminals accessing the satellite, which then provides a synchronous network for all terrestrial and space trunk transmissions.

5.8.2 Concept description. The concept uses a loop-around transmission between a master node ground terminal and each slaved ground terminal, with the phase or timing controlled at the master station. The Doppler-canceling loop translates a Doppler-free primary standard clock to each slave ground terminal. Each slave terminal then uses the received Doppler-free timing clock as its standard in a Doppler-canceling, loop-around timing system to control the frequency of its transmitted signal. The Doppler frequency variation at each ground terminal is thereby eliminated for all the ground terminals accessing the satellite.

The basic ideas of the proposed concept are illustrated in Figure 39. A loop-around Doppler-canceling loop is employed between a master ground terminal and a slave ground terminal, which translates a Doppler-free reference to the slave terminal by having a local VCO synchronize to $(f_o - f_{dm})$

where

f_o = the primary standard reference clock at the master terminal

f_{dm} = the two-way Doppler frequency that exists between the master and slave ground terminals.

The VCO frequency f is transmitted to the satellite and back down to the slave terminal. This received frequency is translated by f_{dm} at the slave terminal, due to the motion of the satellite terminal, and is then transmitted from the slave terminal back to the master ground terminal via the satellite. This signal is then shifted in frequency by $2f_{dm}$ when it is received at the master station and mixed with the VCO frequency f. The sum frequency out of the mixer $(2f + 2f_{dm})$ is then fed to the phase detector and compared in phase with twice the reference clock frequency f_o, which is derived from a primary standard clock such as a cesium atomic clock. The phase detector output is then passed through the system loop filter $[KF(s)]$ to the VCO. The VCO frequency f varies in proportion to the error control voltage until the input to the phase detector is exactly equal to twice the clock frequency, or $2f_o$.

Hence, at lock

$$2f + 2f_{dm} = 2f_o \tag{163}$$

or

$$f = f_o - f_{dm} \tag{164}$$

This results in the frequency f_s received at the slave ground terminal being equal to the Doppler-free stable clock f_o.

$$f_s = f_o - f_{dm} + f_{dm} = f_o \tag{165}$$

Each slave terminal can now use its received clock timing frequency f_o as its reference frequency in a similar loop-around, phase-locked loop to control its transmission of message traffic to other ground terminals. The result is a synchronous network in which a Doppler-free stable clock is provided to all the ground terminals accessing the satellite, without the need of providing expensive primary or secondary atomic clock standards at each ground terminal.

5.9 Quadrature phase-modulated synchronizing system

5.9.1 Introduction. The following proposed system enables a quadrature phase-modulated bit stream to be synchronized directly. The required hardware is relatively simple, and the concept offers the advantage of using all of the bits for the message. No separate circuitry or power is required in the transmitter for synchronization bits.

a. MASTER GROUND TERMINAL TIMING LOOP

satellite (FDMA)

$f + 2f_{dm}$

$f + f_{dm}$

$f + f_{dm}$

slave ground terminal

primary standard $2f_o$

receiver

mixer

high-pass filter

phase detector

$2f + 2f_{dm}$

transmitter ← VCO f ← $KF(s)$ ←

b. SLAVE GROUND TERMINAL TIMING LOOP

received reference clock f_o from master terminal

received slave terminal timing signal

transmitted message traffic and slave timing signal

receiver → × 2 → $2f_o$

receiver

mixer

high-pass filter

phase detector

transmitter ← VCO f ← $KF(s)$ ←

FIGURE 39. Time-dissemination and Doppler-canceling satellite access system.

94

5.9.2 <u>Approach</u>. A functional block diagram of the approach is shown in Figure 40. After mixing down to intermediate frequency (IF), the input is split into two parallel paths. The first path leads to a phase detector, where its phase is compared to that of a VCO. The output of the phase detector is integrated to yield a detected bipolar video pulse train for all the bit pulses whose phase is about equal or opposite to one particular value of the four quadrature phases. The negative pulses are ignored in the threshold detector. This triggers a gate generator (a pulse shaper) to provide a train of gate control pulses that occur for only one of the four input modulating phases. This pulse train then gates out all the input pulsed-carrier pulses that have the same phase. This is then fed to the standard second-order, phase-locked loop for synchronization. As this loop locks, the quadrature phase of the VCO lines up exactly in phase with the input phase that it was closest to when the signal was first received. The VCO may then be phase-shifted to provide a coherent reference for each of the four modulating phases of the input bit stream.

This suggested concept has application in any quadrature phase-modulated system and is inexpensive to implement. It can even be used for a biphase-modulated binary system. In this case it might be necessary to sweep the phase of the VCO. However, this is a requirement only if the input and VCO frequencies are very stable.

5.9.3 <u>Example of an adaptive synchronous coherent detector for a quadrature phase-modulated system</u>.

5.9.3.1 <u>Introduction</u>. The following system identifies an optimum method for detecting quadrature phase modulation. This is accomplished by first obtaining a coherent reference, which is then used to actively match-filter-detect (coherently) the information bits as in an optimum four-level biorthogonal pulse-code modulation (PCM) system.

5.9.3.2 <u>Approach</u>. Figure 41 illustrates a functional block diagram of the implementation means for adaptively obtaining the coherent reference. This is fundamentally the same as the concept described in memorandum for record FSG-94 (see Appendix B, 20.1) except that in the current approach, all of the information bits are used for synchronization.

The bits corresponding to the four phases are separated by adaptively gating them out in four channels. The four different phases are translated to the same phase in this process so that they may be combined (added) linearly and applied to a standard narrowband phase-locked loop to obtain a synchronous carrier reference. The detection process is depicted in Figure 42. The reference is split into the four phases of 0°, 180°, +90°, and −90° using phase splitters and a quadrature phase-shifter. These four outputs are then multiplied by the receiver output and applied to a greatest-of-detector to identify the optimal phase of each incoming bit. The output of this detector comprises two bits of [1,0]; [0,1]; [1,1]; or [0,0] in accordance with the detected phase. If the bit stream comprises two channels, then the first and second bit may be gated out to separate the channels for further processing.

An alternate method of implementing the coherent detector is illustrated in Figure 43. In this system, two phase detectors may be eliminated by applying the inverted detected signals to the greatest-of-detector for the 0° and +90° reference phases.
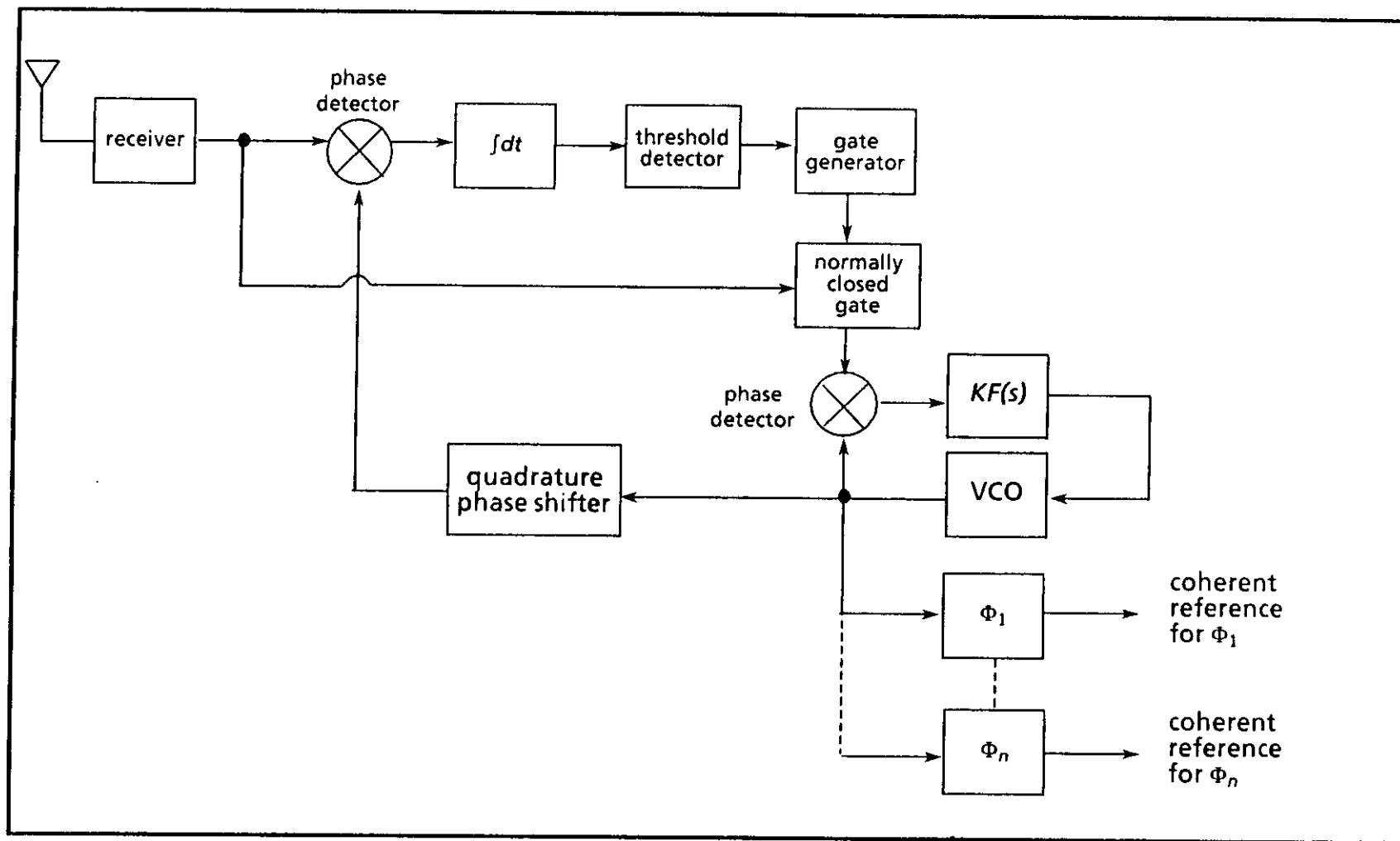
FIGURE 40. Quadrature phase-modulated synchronizing system.

MIL-HDBK-421

96
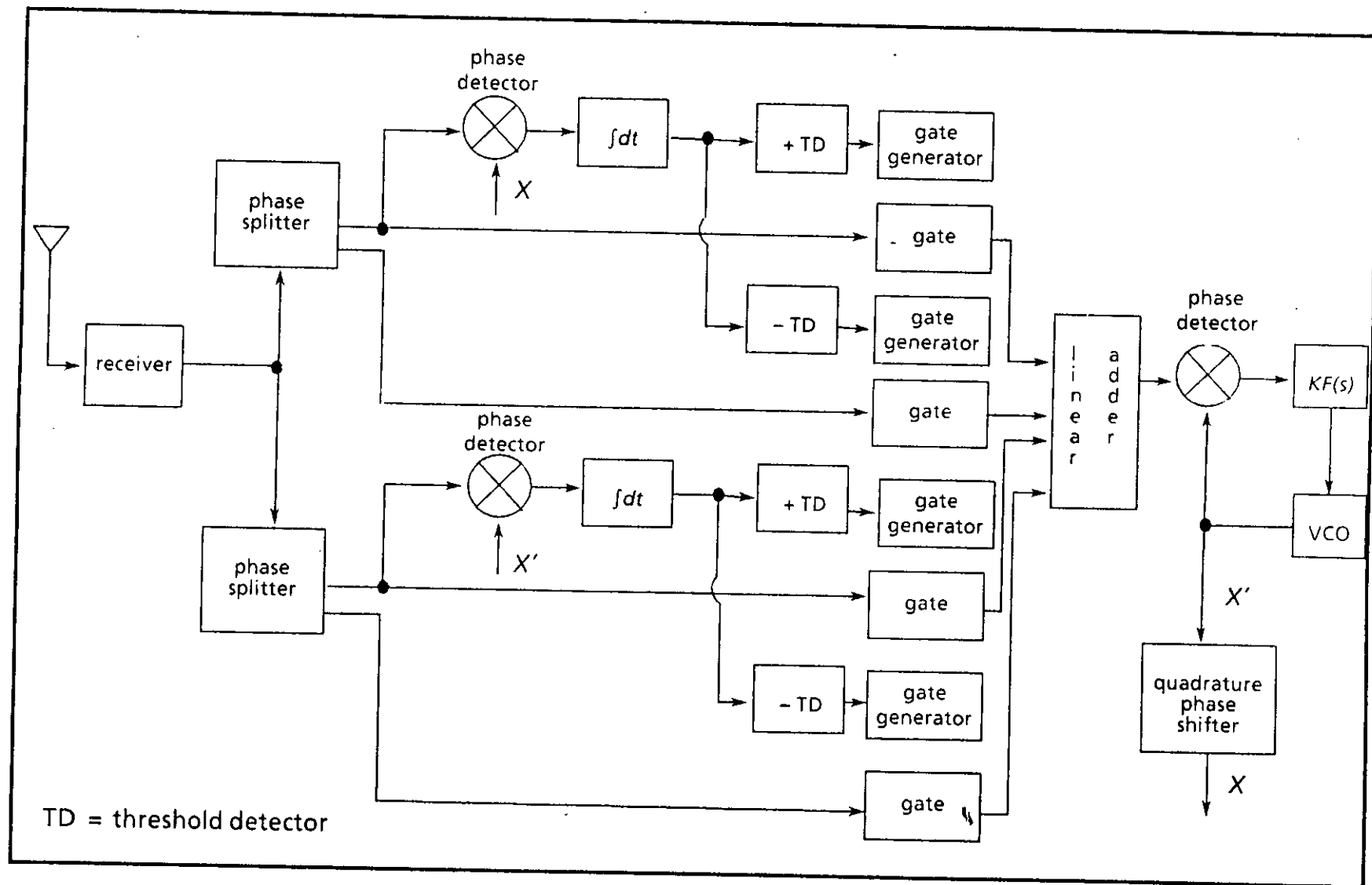
FIGURE 41. An adaptive synchronous coherent detector for a quadrature phase-modulated system (implementation for obtaining a coherent reference).

TD = threshold detector

MIL-HDBK-421

97
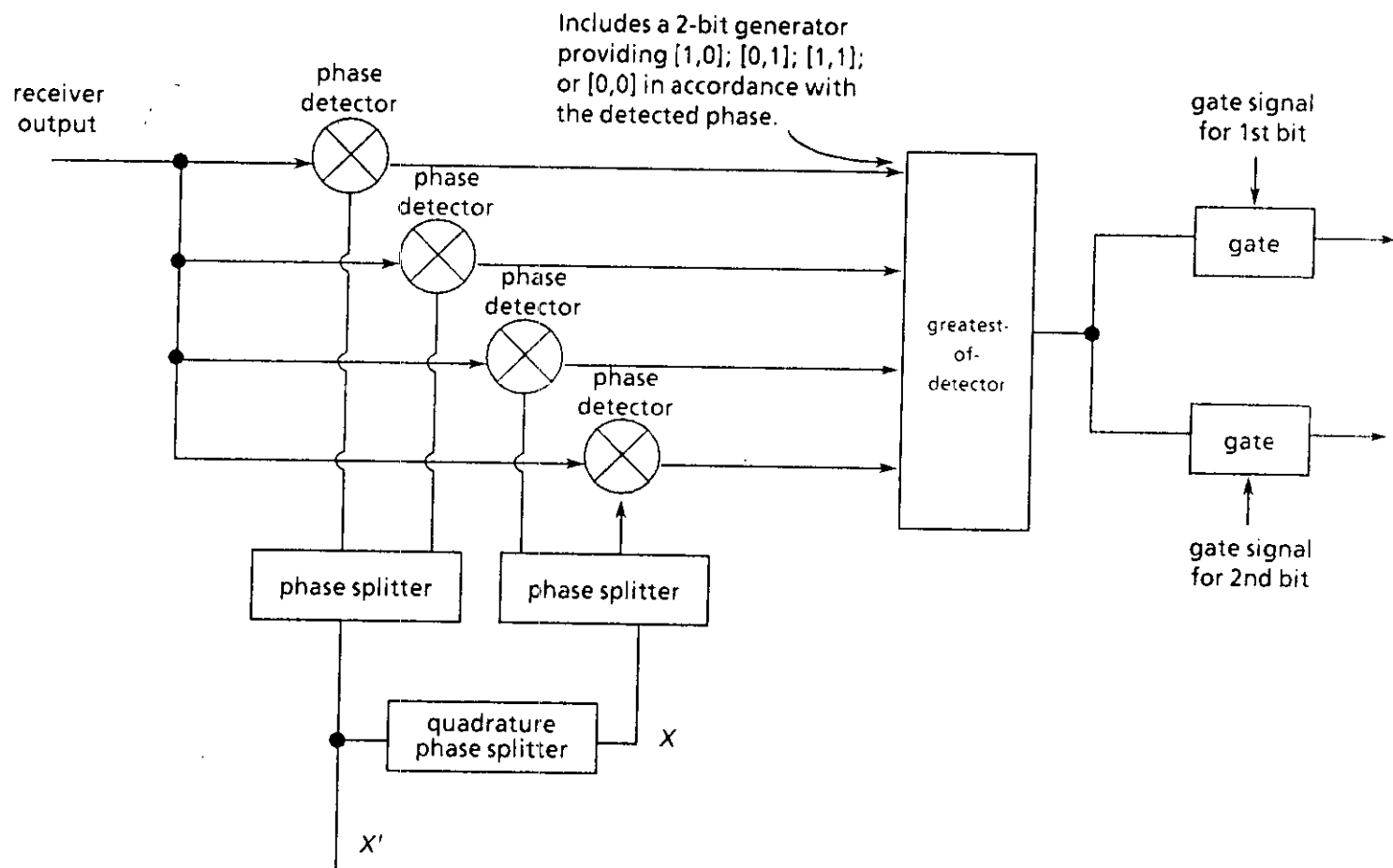
FIGURE 42. An adaptive synchronous coherent detector for a quadrature phase-modulated system (optimum coherent detector).
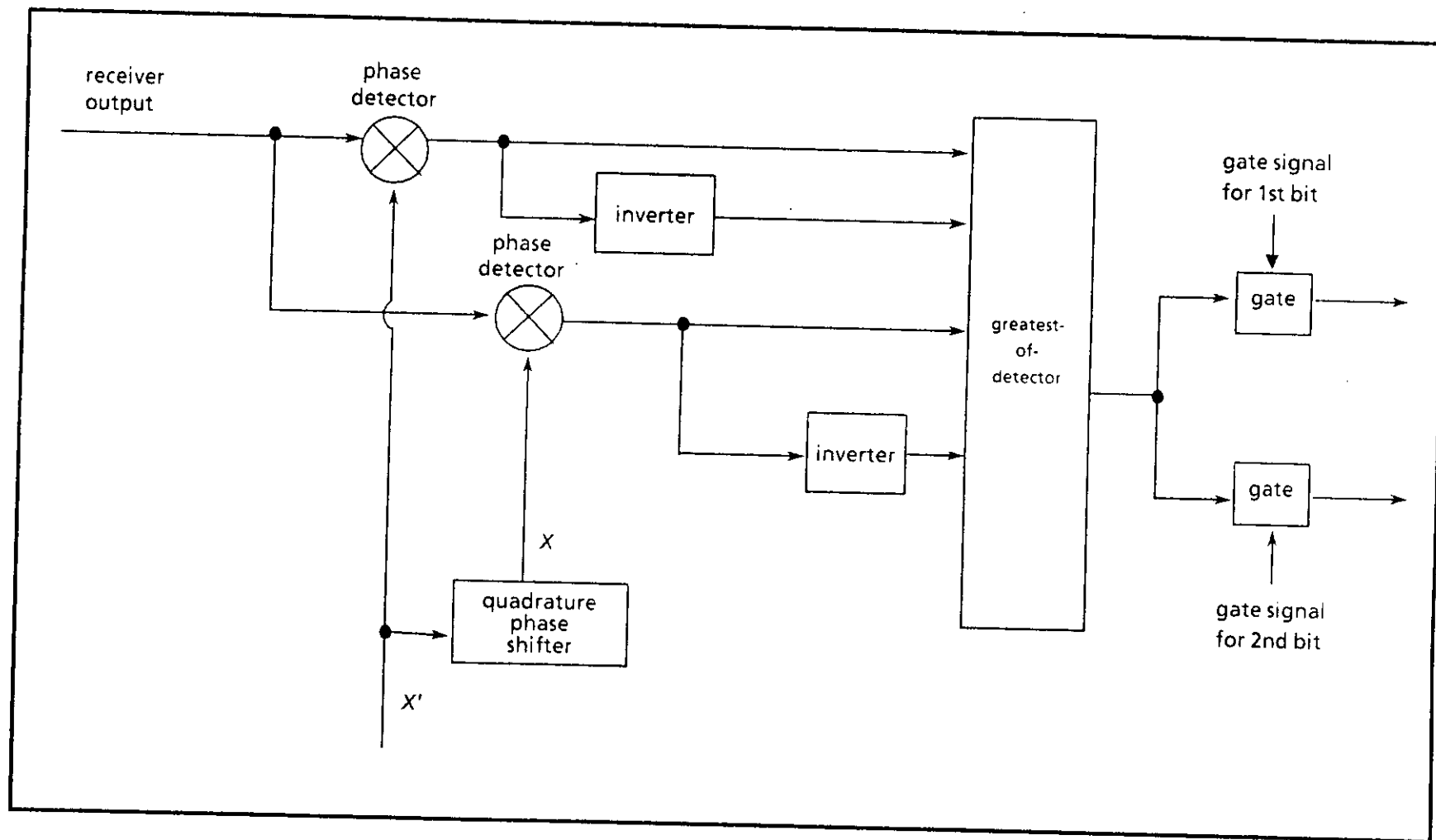
MIL-HDBK-421

FIGURE 43. An adaptive synchronous coherent detector for a quadrature phase-modulated system (alternate approach).

MIL-HDBK-421

66

5.10 <u>Timing errors</u>. Figure 44 shows two independent frequency sources for some stipulated time duration. Each is a step (or constant) frequency difference.
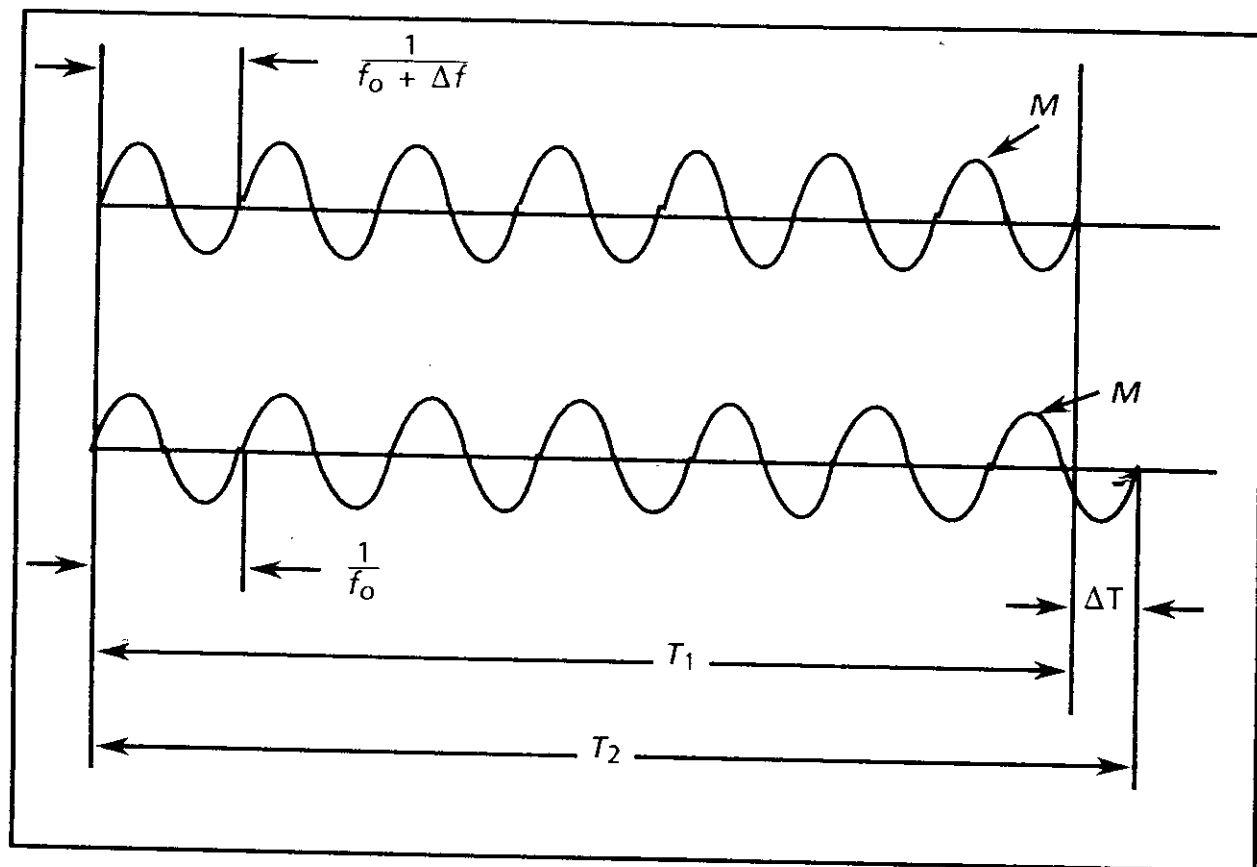
FIGURE 44. <u>Two independent frequency sources.</u>

Over M cycles

$$\Delta T = T_2 - T_1 \tag{166}$$

hence

$$\Delta T = \frac{M}{f_o} - \frac{M}{(f_o + \Delta f)} \tag{167}$$

therefore

$$\Delta T = M \; \frac{\Delta f}{f_o \, (f_o + \Delta f)} \tag{168}$$

If $f_o >> \Delta f$, then from equation (168)

$$\Delta T = M \frac{\Delta f}{f_o^2} = T_2 \frac{\Delta f}{f_o} \tag{169}$$

If stability S is defined as the ratio of the maximum frequency change Δf to the initial frequency f_0 during some given time duration $T_0 = T_2$, then

$$S = \left.\frac{\Delta f}{f_o}\right|_{T_o} \tag{170}$$

and

$$\Delta T = \frac{M}{f_o} S = T_2 S = T_o S \tag{171}$$

Equations (169) and (171) identify the timing error resulting when a step frequency difference exists between two independent sources for a time period T. This represents the worst case and, in general, is not a reasonable assumption. The approach employed above will now be expanded to obtain a general expression that may be applied to any form of oscillator frequency difference. This can be accomplished by considering the frequency's time dependence to form frequency ramp segments, as shown in Figure 45.
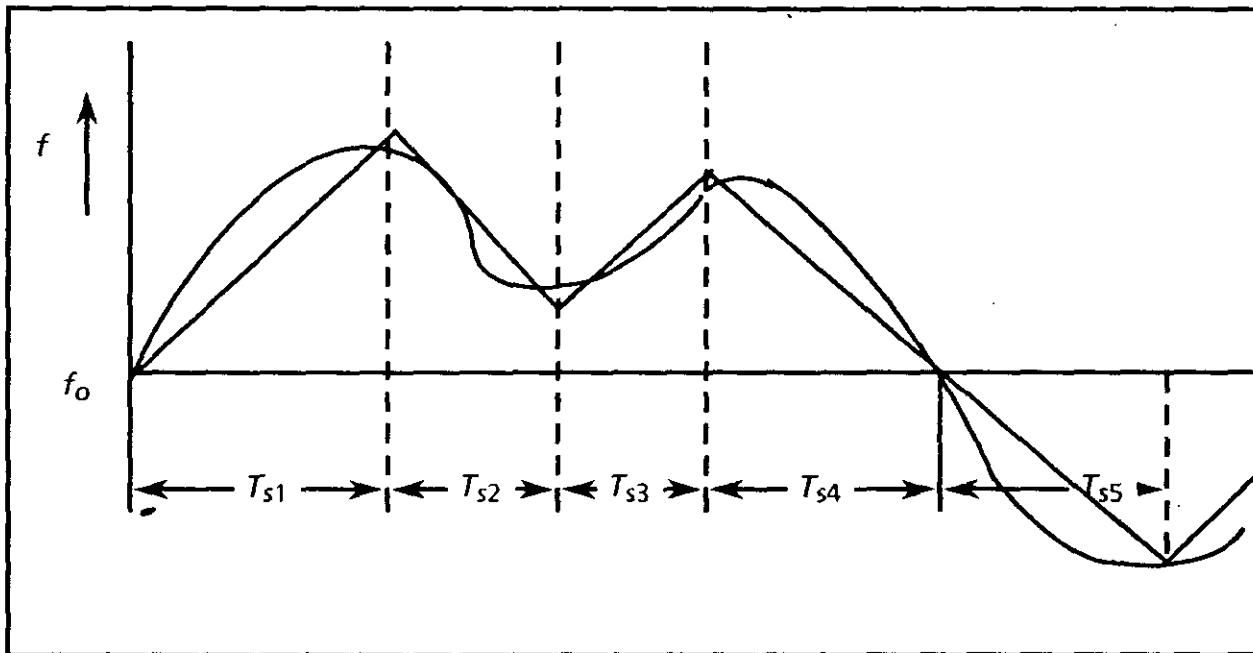
FIGURE 45. Time dependence of the frequency.

The timing error for each segment may then be determined by quantizing each ramp frequency change into small frequency steps, as illustrated in Figure 46.
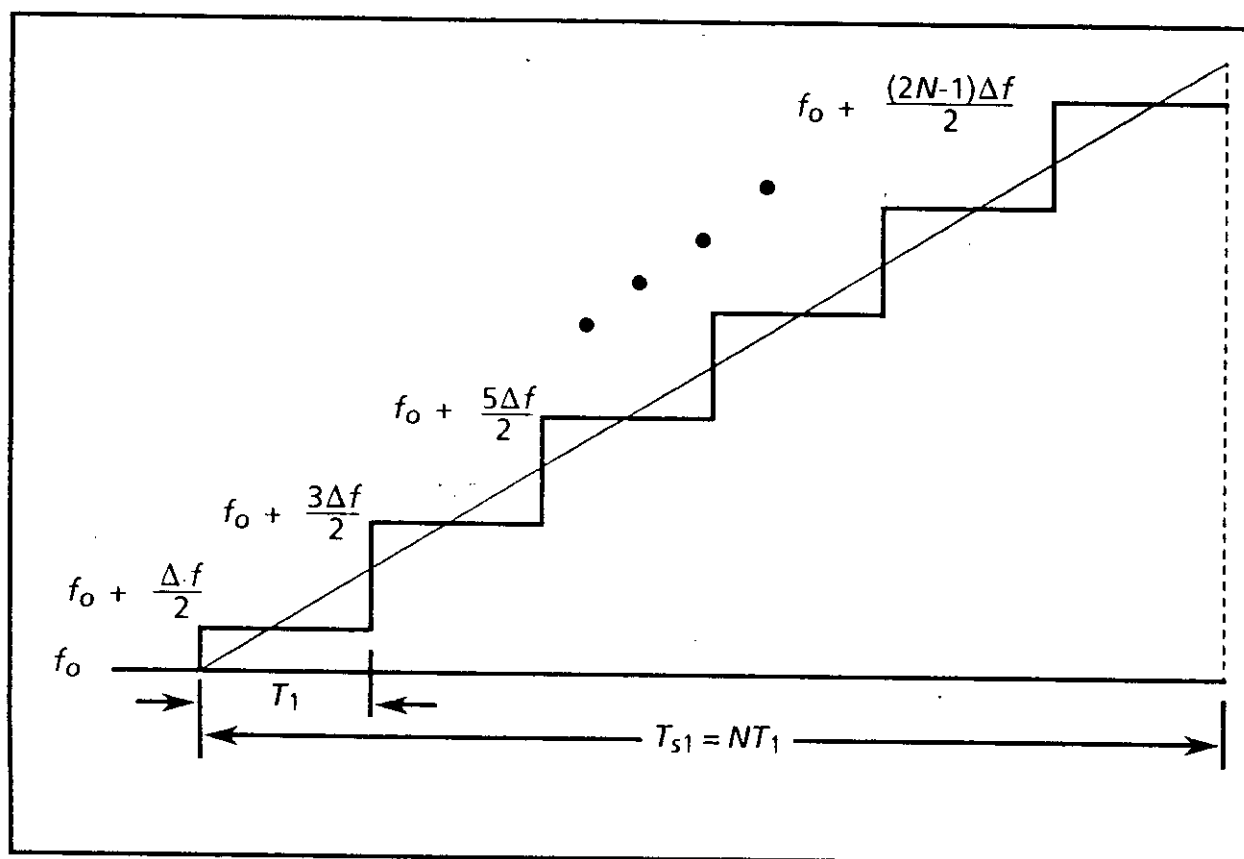
FIGURE 46. Ramp frequency change.

The timing error associated with each subsegment is identified readily by making use of the previous derivation for a step frequency change and considering each frequency ramp segment to constitute a group of constant step frequency changes, as shown in Figure 46. Applying equation (169) to each subsegment then results in

$$\Delta T_1 = \frac{T_1}{2} \left(\frac{\Delta f}{f_o} \right) \tag{172}$$

$$\Delta T_2 = \frac{3T_1}{2} \left(\frac{\Delta f}{f_o} \right) \tag{173}$$

$$\Delta T_3 = \frac{5T_1}{2} \left(\frac{\Delta f}{f_o} \right) \tag{174}$$

$$\bullet$$
$$\bullet$$
$$\bullet$$

$$\Delta T_N = \frac{(2N-1)T_1}{2} \left(\frac{\Delta f}{f_o} \right) \tag{175}$$

and the total timing error ΔT_{s1} occurring in the interval Ts_1 is simply the sum of the error produced in each subsegment.

$$\Delta T_{s1} = \Delta T_1 + \Delta T_2 + ... + \Delta T_N \tag{176}$$

$$\Delta T_{s1} = \frac{T_1}{2}\left(\frac{\Delta f}{f_o}\right)[1 + 3 + 5 + ... + (2N-1)] \tag{177}$$

The bracketed term on the right side of equation (177) is a simple arithmetic progression whose sum may be expressed in closed form as

$$S = \frac{N}{2}[2a + (N-1)d] \tag{178}$$

where

N = the number of terms
a = the first term
d = common difference

Then we have

$$S = N^2 \tag{179}$$

hence

$$\Delta T_{s1} = \frac{T_1 N^2}{2}\left(\frac{\Delta f}{f_o}\right) \tag{180}$$

ΔT_{s1} is positive or negative (that is, the timing error is advanced or retarded) depending on the sign of the instantaneous frequency difference relative to the reference frequency f_o.

A similar analysis applied to the second segment T_{s_2} yields a timing error ΔT_{s_2} of

$$\Delta T_{s2} = \frac{T_2 N^2}{2}\left(\frac{\Delta f}{f_o}\right) \tag{181}$$

or, in general,

$$\Delta T_{si} = \frac{T_i N^2}{2}\left(\frac{\Delta f}{f_o}\right) \tag{182}$$

Equation (182) is a completely general equation that establishes the timing error for each ramp frequency segment in terms of ramp characteristics. The resultant total timing error is obtained readily by summing the individual timing error associated

with each incremental frequency ramp segment. Therefore, the total timing error over m frequency segments is

$$\Delta T_T = \sum_{i=1}^{m} \frac{T_i N^2}{2} \left(\frac{\Delta f}{f_o} \right) \tag{183}$$

Equation (183) can be applied readily to any anticipated or known oscillator frequency change to determine the total timing error introduced.

5.11 <u>Closed-form timing error equation.</u> When the frequency change or difference can be expressed as an integrable function, it is possible to derive a closed-form equation that quantitatively establishes the timing error associated with the frequency variation.

Equation (169) indicates that the timing error for a stipulated time increment ΔT is related to the frequency difference between two clocks, as follows

$$\Delta \varepsilon_T = \frac{\Delta f}{f_o} \Delta T \tag{184}$$

hence

$$\Delta \varepsilon_T = \frac{f - f_o}{f_o} \Delta T \tag{185}$$

This corresponds to the existence of a constant frequency difference during ΔT. The total error is obtained by taking the sum of all incremental errors that occur during ΔT. Taking the limit of this sum as ΔT approaches 0, and n approaches ∞,

$$\varepsilon_T = \lim \sum_{i=1}^{n} \frac{(f - f_o)}{f_o} dt \tag{186}$$

which from the fundamental theorem of integral calculus becomes

$$\varepsilon_T = \int_{o}^{T} \frac{(f - f_o)}{f_o} dt \tag{187}$$

$(f - f_o = f_d)$ is the frequency variation with time that occurs during the interval of time T.

The preceding equation can be used to identify the timing error ε_T associated with any continuously varying and integrable frequency difference f_d.

Consider a step-frequency difference. The timing error is derived by differentiating the closed-form equation over an interval of time T for a step-frequency difference. Figure 47 illustrates a step-frequency difference. The resulting equation is shown in equation (190).
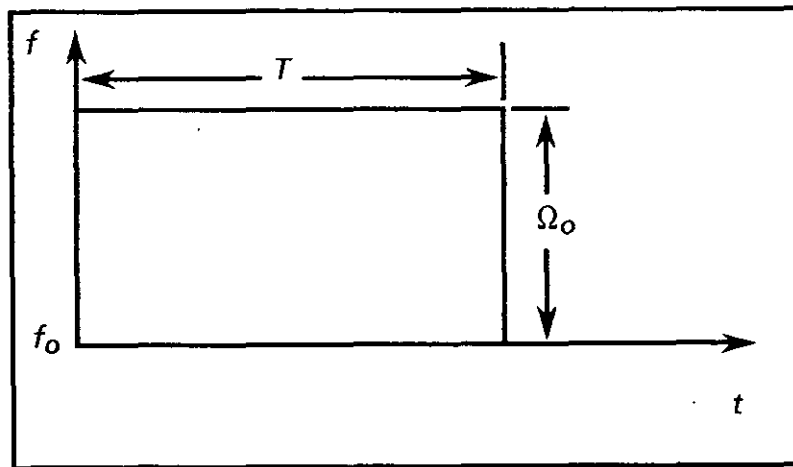
FIGURE 47. Step-frequency difference.

$$f_d = \Omega_o \qquad\qquad (188)$$

From equation (187) we have

$$\varepsilon_T = \int_o^T \frac{\Omega_o}{f_o}\, dt \qquad\qquad (189)$$

which integrates to

$$\varepsilon_T = \frac{\Omega_o}{f_o}\, T \qquad\qquad (190)$$

For a ramp freqency difference, the timing error is derived by differentiating the closed-form equation over an interval of time T for a ramp frequency difference. Figure 48 illustrates a ramp frequency difference. The resulting equation is shown in equation (193).
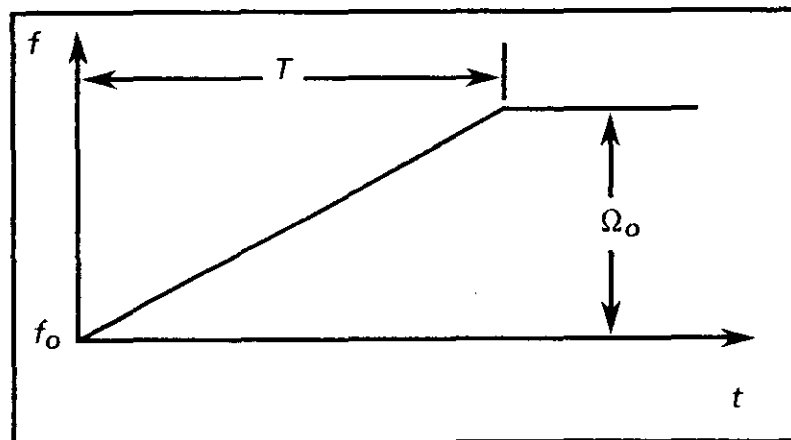
FIGURE 48. Ramp frequency difference.

$$f_d = \frac{\Omega_o}{T} t \tag{191}$$

From equation (187) we have

$$\varepsilon_T = \int_o^T \frac{\Omega_o}{f_o T} t dt \tag{192}$$

which integrates to

$$\varepsilon_T = \frac{\Omega_o}{f_o} \left(\frac{T}{2} \right) \tag{193}$$

For a sinusoidal frequency difference, the timing error is derived by differentiating a closed-form equation over an interval of time T. Figure 49 illustrates a sinusoidal frequency difference. The resulting equation is shown in equation (196).
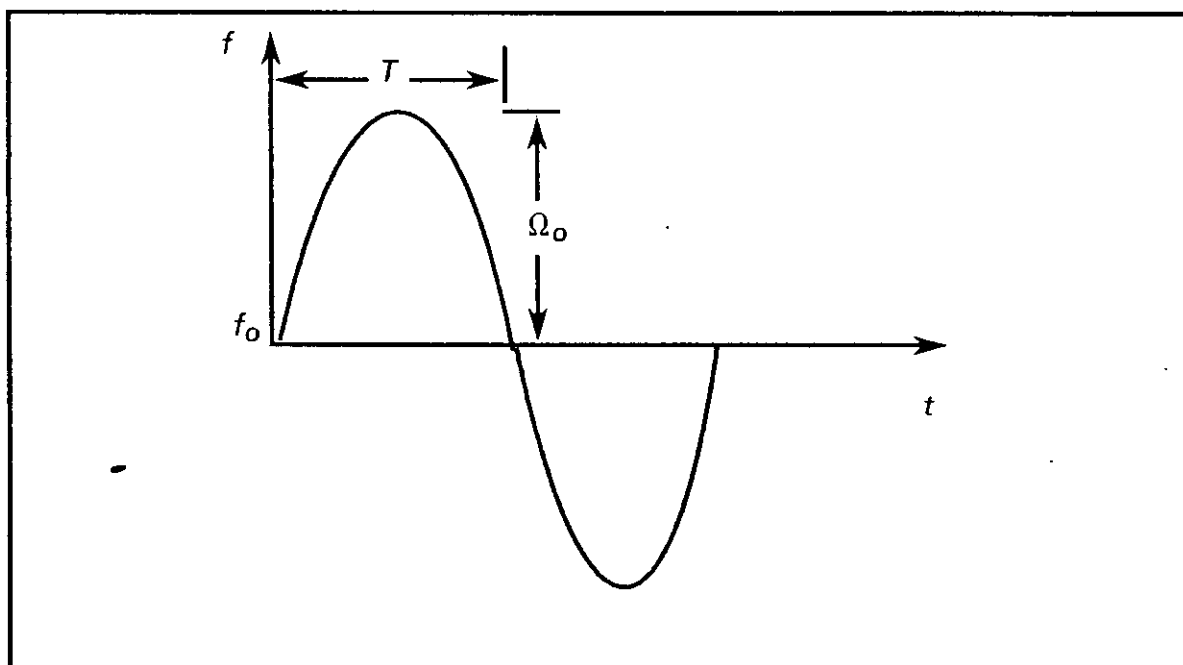
FIGURE 49. Sinusoidal frequency difference.

$$f_d = \Omega_o \sin \left(\frac{\pi t}{T} \right) \tag{194}$$

From equation (187) we have

$$\varepsilon_T = \frac{\Omega_o}{f_o} \int_o^T \sin\left(\frac{\pi t}{T}\right) dt \qquad (195)$$

which integrates to

$$\varepsilon_T = \frac{2\Omega_o T}{\pi f_o} \qquad (196)$$

5.12 Buffer size requirements. The required buffer storage Q is equal to twice the quantity of bits contained in a time duration equal to the timing error, as shown in equation (197). The factor of 2 is required since buffers are reset to their midpoint to allow for both positive and negative time differences, that is,

$$Q = \frac{2\varepsilon_T}{t_r} = 2\varepsilon_T f_r \qquad (197)$$

Equation (197) in conjunction with an appropriate equation for ε_T identifies the buffer storage capacity required to accommodate the frequency variations resulting from clock instabilities and transmission media propagation characteristics.

5.12.1 Buffer requirements resulting from cesium clock instability. The long-term variation for a cesium atomic clock can be maintained to within $\pm 3 \times 10^{-12}$. The total combined frequency difference between two independent cesium clocks is 6×10^{-12}. By using equation (190) and equation (197), we see the required buffer size Q for a buffer reset interval T of 24 hours is given by

$$Q = 1 \times 10^{-6} f_r \; bits \qquad (198)$$

The capacity requirements for the trunk group buffers at nodes equipped with cesium clocks are therefore as given in Table I.

NOTE: If the agreement between clocks is accomplished by calibrating one against the other, calibration errors must be included; in the case of uncalibrated independent clocks, the accuracy specifications govern.

TABLE I. <u>Capacity requirements for trunk-group buffers at nodes equipped with cesium clocks.</u>

Trunk-Group Transmission Rate (in kbps)	Required Buffer Capacity (in bits)
16	1
32	1
64	1
128	1
512	1
1,544	2
2,048	3
20,000	20

5.12.2 <u>Rubidium clock.</u> Although a rubidium clock has excellent stability over a relatively short time period, such as 24 hours, its frequency variation over an extended period is cumulative. There are several sources of error in the use of a rubidium clock. First, there are noise-like variations. Typical values are given in the manufacturer's literature (usually as a plot of stability versus time) and are on the order of 1 part in 10^{12} in a 24-hour period. Second, there is a systematic, long-term drift. A maximum value is also given in the manufacturer's literature and is on the order of 1 to 4 parts in 10^{11} per month. Third, there is a calibration error that depends on the accuracy of the reference used and the calibration system used; this is generally small if the reference is local, but may be large if done via most radio links. If the rubidium standard were calibrated by observation over a period of 1 day with respect to a cesium clock (whose frequency is known to be accurate to 1 part in 10^{11}), the noise-like variations (1×10^{-12}) and the drift during the 1-day period (1.3×10^{-12} or less) are small compared to the reference uncertainty (the rubidium clock is accurate to approximately 1×10^{-11} just after calibration). The stability over 24 hours for a rubidium clock is 1 part in 10^{-11}; therefore, during the first 24 hours after recalibration, the buffer storage required is essentially the same as for the cesium clock, which is typically 1 part in 10^{11} per month. Subsequent 24-hour periods, however, experience larger frequency differences due to the systematic (non-statistical) drift inherent in the rubidium clock. This leads to the need for larger buffers during subsequent 24-hour intervals. If a linear frequency drift is assumed, a frequency drift of 1×10^{-11} per month corresponds to a change of 3.3×10^{-13} per 24 hours. The maximum buffer requirement occurs during the 24-hour period just prior to recalibration. The frequency difference for that interval is

$$f_d = \left| N(2 \times 3.3 \times 10^{-13}) + (2 \times 10^{-11}) \right| f_o \qquad (199)$$

where

N = the number of days between recalibration.

The factor of 2 is to account for the total possible frequency difference between the clocks. A recalibration interval of 6 months (182 days) yields a buffer-size requirement of

$$Q = 2.08 \times 10^{-5} f_r \ bits \qquad (200)$$

The capacity requirements for the trunk-group buffers at nodes equipped with rubidium clocks are therefore as shown in Table II.

TABLE II. Capacity requirements for trunk-group buffers at nodes equipped with rubidium clocks.

Trunk-Group Transmission Rate (In kbps)	Required Buffer Capacity (in bits)
16	1
32	1
64	2
128	3
512	11
1,544	33
2,048	43
20,000	416

5.12.3 Buffer requirements due to propagation time variations for line-of-sight links. Frequency variations due to changes in path length (Doppler) for LOS links are negligible. Buffers should be sized primarily to take care of clock differences.

5.12.3.1 Tropospheric links. Frequency variations associated with tropospheric systems have never been established, but it is known that rapid phase changes are experienced. It is assumed here that under the worst condition the phase can instantaneously change by a time interval corresponding to the maximum range difference that can occur over a tropospheric link. This is approximately 0.4 microseconds (µs) for the parameters associated with a typical tactical tropospheric transmission link. Trunk-group bit rates are to be employed in land-based systems comprised of multiplexed 32-kbps channels, with a maximum capacity of 72 channels. For the maximum size group, this corresponds to a transmitted bit rate of 2.304 Mbps. This reduces to a buffer requirement of only ± 1 bit, as follows

$$Q = 0.4 \times 10^{-6} \times 2.3 \times 10^{6} = 0.92 \qquad (201)$$

5.12.3.2 <u>Satellite links in synchronous orbit.</u> The buffer storage requirement for a satellite link is rather large when the system timing is not made synchronous by eliminating the time variation associated with the Doppler effect. With stationary terminals, the Doppler effect results from the relative motion of the satellite only. For a satellite in synchronous orbit, the radial velocity change is sinusoidal with a period of 24 hours. The largest value of peak range rate occurs when the ground terminal latitude is 72° and the orbital inclination of the satellite is 2.5°. The maximum range rate $\bar{v}$ in this situation is 20 meters per second (mps). The peak Doppler frequency that results from this radial velocity is given by

$$f_d = \frac{2\,\bar{v}\,f_o}{c} = \Omega_o \tag{202}$$

Combining equation (62) and equation (202) identifies the timing error ε_T as

$$\varepsilon_T = \frac{4\,\bar{v}\,T}{nc} \tag{203}$$

and establishes a buffer storage requirement Q of

$$Q = \frac{8\,\bar{v}\,T}{nc}\,f_r \tag{204}$$

where

T = a half period = 12 hours
$\bar{v}$ = 20 mps
c = velocity of light = 3×10^8 mps

Using the known parameter values and accounting for the buffer requirement during the negative Doppler excursion results in

$$Q = 7.32 \times 10^{-3} f_r \; bits \tag{205}$$

The buffer requirements for stationary ground terminals are as shown in Table III.

TABLE III. Buffer requirements for stationary ground terminals.

Trunk-Group Transmission Rate (in kbps)	Required Buffer Capacity (in bits)
16	118
32	235
64	469
128	937
512	3,748
1,544	11,303
2,048	14,992
20,000	146,400

The required storage is identified in terms of trunk-group bit rates. A much larger overall storage requirement occurs if the available satellite bandwidth is shared by many trunk groups that use TDMA. In this case, the storage requirement is dictated by the composite bit rate transmitted through the satellite, and the total buffer storage requirement can be much greater than in Table III.

5.13 A uniformly spaced frequency band generator.

A novel method of generating a uniformly spaced frequency spectrum with the added feature of each term being fully synchronized to a master clock is described below. Here are some of the important advantages of the proposed system:

1.	One master reference clock retains the entire spectrum in synchronism.

2.	Any number of spectral lines can be generated with the use of only two oscillators: one is a reference, the other is synchronized to it.

3.	The only source of drift for the system is from the reference clock; if it does drift, the entire spectrum shifts with it, making the system very desirable for systems using coherent correlation techniques.

4.	Although the system might appear complex in terms of quantity, the building blocks are simple and reliable.

5.	No filters are required for the system, with the exception of one used in the gated phase-locked loop of the second oscillator.

A block diagram of the proposed system is shown in Figure 50.

Figure 50 is a functional block diagram of the proposed system, which will subsequently be explained in detail. The essential elements are the gate generator, the gated phase-locked loop, and the median frequency generators. The gate generator simply counts the basic reference frequency, using standard counter circuitry to provide a gate signal at a PRF frequency of f_r for the synchronous gate of the phase-locked loop

$$f_r = \frac{f_o}{N} \qquad (206)$$

By making the phase-locked loop a gated loop, it can be synchronized easily to any spectral line of the carrier, plus or minus n times the PRF of the gate, that is,

$$f_{VCO} = f_o \pm nf_r \qquad (207)$$

This expedient provides a simple means of obtaining two synchronous frequencies that are close in frequency. For the application in mind,

$$f_o >> nf_r \qquad (208)$$

and $f_o + nf_r$ corresponds to the highest frequency spectral line to be generated. It is now desired to fill in the spectrum from f_o to $f_o + nf_r$ with evenly spaced frequencies and using only these two generated voltages. This is accomplished by first dividing the frequency range in half with the use of a median frequency generator (the detail of this generator will be described later). When two frequencies, f_1 and f_2, are available, a third frequency equal to

$$\frac{f_1 + f_2}{2}$$

can be generated readily. For the two frequencies in question, a third frequency can be obtained equal to

$$\frac{f_o + f_o + nf_r}{2} = f_o + \frac{n}{2} f_r \qquad (209)$$

If this frequency is now combined in a median frequency generator with each of the original two spectral lines, the following two additional frequencies are generated:

$$f_o + \frac{n}{4} f_r \qquad (210)$$

and

$$f_o + \frac{3n}{4} f_r \qquad (211)$$
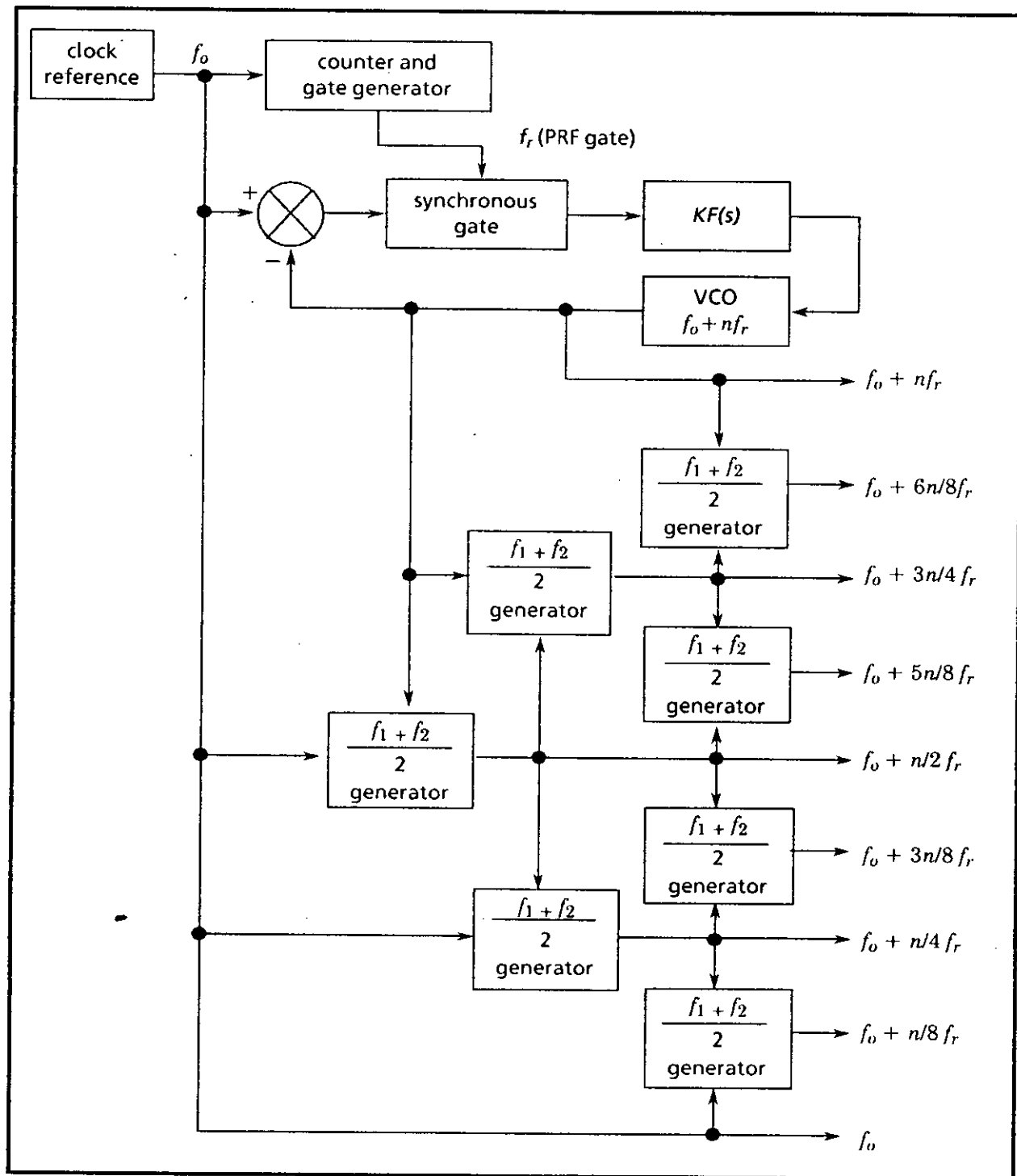
FIGURE 50. Frequency synthesizer.

113

The composite spectrum now contains five frequencies from f_o to $f_o + nf_r$ divided evenly into quarters. Now, if each adjacent pair of spectral lines is combined in a median frequency generator, nine frequencies result, which divide the original spectral width into eighths. If this process continues, the original two frequencies at the two edges of the desired spectrum can be evenly divided into 2^n frequencies. This suggests that the original spacing nf_r be equal to 2^n. This results in the deviation between any two final spectral lines being equal to unity if $2^n - 1$ median frequency generators are used. For example if $nf_r = 4,096$ Hz ($n = 12$), and 4,095 median frequency generators are used in the manner prescribed, then 4,096 frequencies 1 Hz apart from each other are generated. If $2,048 - 1 = 2,047$ median frequency generators are used ($n = 11$), then the final increments are 2 Hz apart or $2^m - 1$ generators result in a frequency separation of 2^{n-m} units or cps. The smallest even-digit separation is for $n = m$.

$$2^{n-m} = 2^0 = 1 \tag{212}$$

The three basic elements of the system will now be reviewed.

5.13.1 <u>Gate generator</u>. The gate generator producing gate pulses at a frequency f_r is obtained by merely counting down from the reference frequency f_o. A counter followed by a standard wave shaping technique is employed to produce a train of pulses whose frequency is

$$\frac{f_o}{N} = f_r$$

and whose duration wants to be as narrow as possible within practical limits. The pulse duration ι is not at all critical, and an appropriate value is a function of the details of any specific application. Preferably it comprises an even number of carrier cycles of f_o, but even this is not essential. In the event that the basic frequency f_o is too high in value to employ standard counters directly, then an intermediate block can be inserted into the system between the reference clock and the counter. One obvious way of dividing a very high frequency is shown in Figure 51.
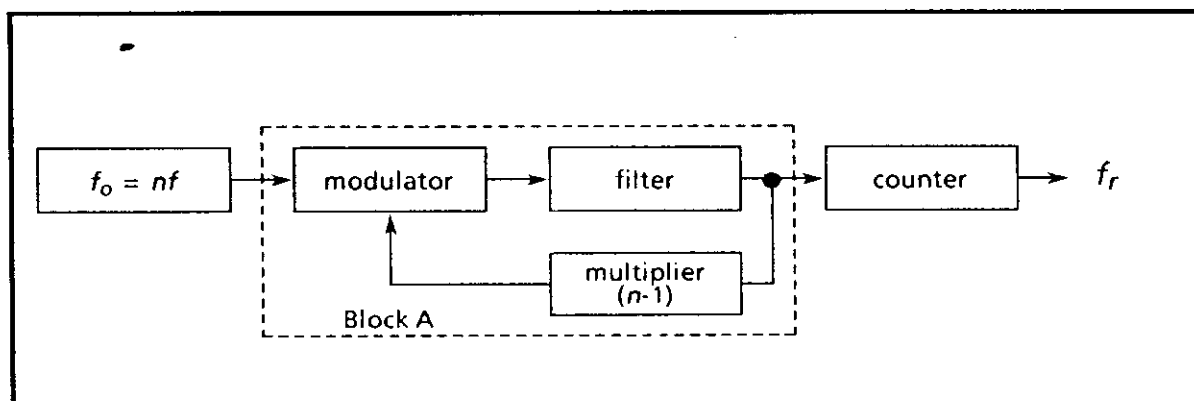
FIGURE 51. <u>Method of dividing a very high frequency</u>.

Actually almost any scheme desired can be used to place the basic frequency in the frequency range, in which counters could be employed.

114

5.13.2 <u>Gated phase-locked loop</u>. The phase-locked loop is a second-order (velocity correction) loop whose basic performance is completely determined by its closed-loop time constant $1/\omega_n$. A unique characteristic of such a gated loop for the application in mind is to frequency-lock the VCO to the carrier frequency plus n times the PRF. The author has demonstrated experimentally that such a condition is readily achievable. Not only can such a loop lock at spectral frequencies that are integral multiples of f_r, but also this condition is stable and all the essential characteristics (such as the locking time, effective closed-loop bandwidth, stability, and transient error) remain the same provided $f_o >> nf_r$. It was demonstrated in a laboratory that stable synchronization can be realized for $nf_r = 7.5°$ percent of f_o.

5.13.3 <u>Median frequency generator</u>. A method of generating a third frequency that lies midway between two existing frequencies without involving the use of a standard modulator or filter is described by L. R. Kahn on page 119 of the January 1960 issue of the *Proceedings of the Institute for Radio Engineers*. The system makes use of the fact that when two equal amplitude sine waves of different frequencies f_1 and f_2 are linearly added, the resultant signal consists of 0 crossings defined by

$$\frac{f_1 + f_2}{2}$$

with a 180° phase reversal occurring at a period equal to the difference between the two frequencies (see Figure 52).
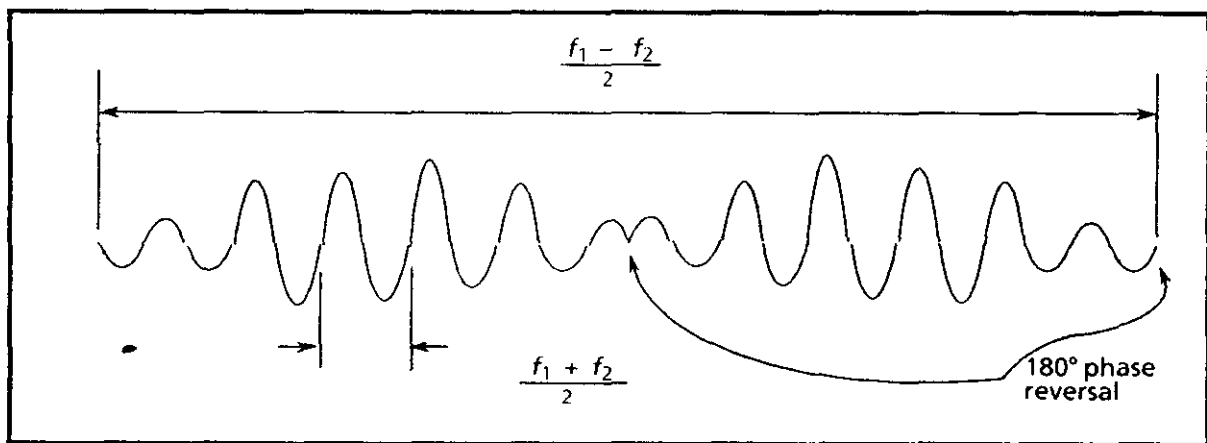
FIGURE 52. <u>Addition of two equal (amplitude sine waves of different frequency)</u>.

Now, if some means can be provided to switch the phase by 180° at each phase reversal point, then the frequency is continuous at a value of

$$\frac{f_1 + f_2}{2}$$

That Figure 52 is a valid interpretation of what is occurring can be verified easily. Consider the linear summation of two frequencies of equal amplitude (unity amplitude is used to simplify the math)

$$e = \sin \omega_1 t + \sin \omega_2 t$$

$$e = \sin \omega_1 t + \sin (\omega_1 + \omega_r) t$$

$$e = \sin \omega_1 t + \sin \omega_1 t \cos \omega_r t + \cos \omega_1 t \sin \omega_r t$$

$$e = \sqrt{2 + 2 \cos \omega_r t} \ \sin (\omega_1 t + \tan^{-1} \frac{\sin \omega_r t}{1 + \cos \omega_r t})$$

At first glance it might appear that the phase portion of this composite signal corresponds to a frequency precisely defined by

$$\frac{\omega_r}{2}$$

since

$$\psi(t) = \tan^{-1} \frac{\sin \omega_r t}{1 + \cos \omega_r t} = \tan^{-1} \ \tan \frac{\omega_r t}{2} = \frac{\omega_r t}{2}$$

However, this equation is valid only for positive values of $(1 + \cos \omega_r t)$.

Also, it is easy to show that when $\omega_r t = n (\pi)$, a discontinuity exists for n equal to any odd integer.

At this point the phase portion $\psi(t)$ is

$$\psi(t) = \tan^{-1} \frac{\sin \pi}{1 + \cos \pi} = \tan^{-1} \frac{0}{0}$$

which is indeterminant.

It can also be shown easily that for an angle slightly less than π (vis. $\pi - \varepsilon$ where $\varepsilon \to 0$) the function $\psi(t)$ is equal to

$$+ \frac{\pi}{2}$$

and for an angle slightly greater than π (vis. $\pi + \varepsilon$ where $\varepsilon \to 0$) the function $\psi(t)$ is equal to

$$- \frac{\pi}{2}$$

The phase portion of the composite wave, therefore, appears as shown in Figure 53.
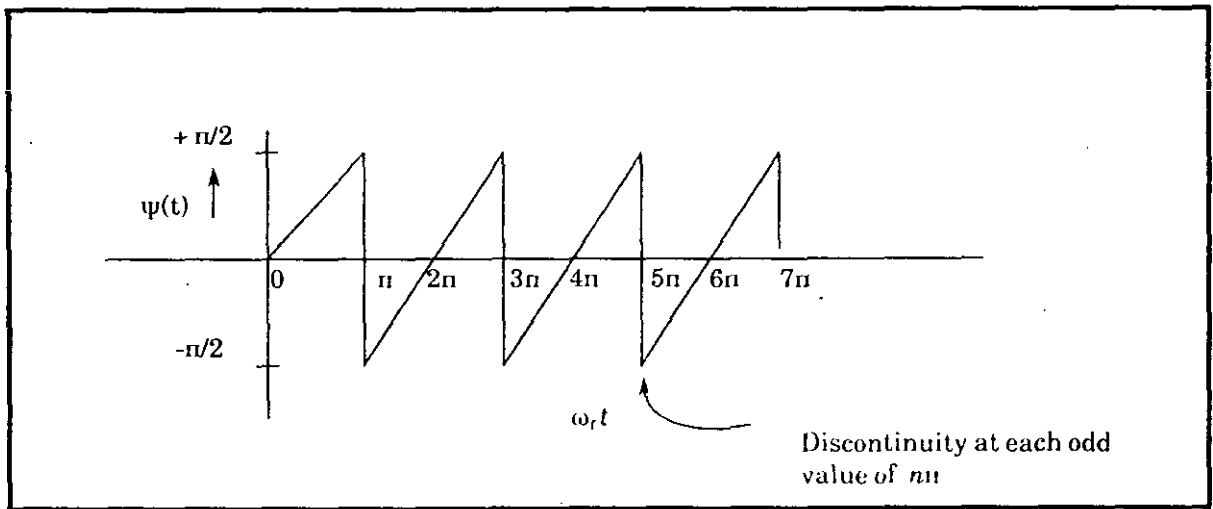
FIGURE 53. The phase portion of the composite wave.

Now if the phase is reversed back at each discontinuity, then the phase changes are equivalent to being continuous and the frequency is given by

$$\omega = \omega_1 + \frac{\omega_r}{2} = \frac{\omega_1 + \omega_2}{2}$$

A method of reversing the phase back at each phase reversal is shown in Figure 54.
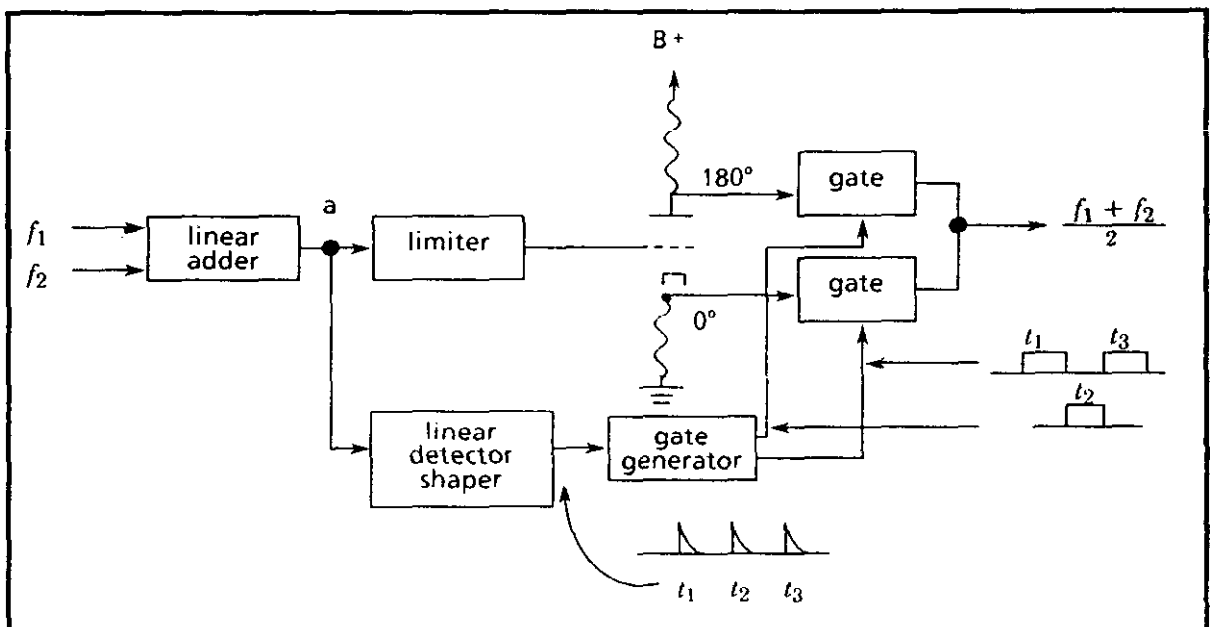
FIGURE 54. Phase reversal system.

The linearly added frequency terms are passed through a limiter to eliminate the amplitude variations and then into a paraphase amplifier to provide two signals 180° out of phase. If these two outputs are now gated-on in synchronism with the phase reversal points occurring at the notches of the composite wave (point a), the result is to continuously vary the phase as though it were a continuous ramp. The required gating signal is achieved by detecting the envelope of the composite signal and operating on this detected envelope to produce a square wave whose switching times occur as shown in Figure 54.

5.13.4 Amplitude requirements for the median frequency generator

The operation of the proposed method of obtaining a median frequency requires that the amplitude of the two sine waves be equal. If there is an amplitude difference, the phase reversal is not as sharply defined and the frequency is altered. The manner in which the frequency is affected may be identified by deriving an expression for the instantaneous frequency when two sine waves of different amplitude are added.

An expression for the summation is given by:

$$e_t = \sqrt{(1 + m\cos\omega_r t)^2 + m^2 \sin^2\omega_r t} \times \sin[\omega_1 t + \psi(t)] \tag{213}$$

$$\psi(t) = \tan^{-1} \times \frac{m\,\sin\omega_r t}{1 + m\cos\omega_r t} \tag{214}$$

where

$$m = \text{the ratio of the amplitude of the two signals } (m < 1)$$
$$\omega_r = \text{the frequency difference between the two signals}$$

Now with the amplitude variation eliminated with a limiter, the instantaneous frequency is given by the derivative of the phase term

$$\omega_i = \frac{d\psi(t)}{dt} = 1 + \frac{m^2 + m\cos\omega_r t}{1 + m^2 + 2m\cos\omega_r t}\,\omega_r \tag{215}$$

We see from equation (215) that for $m = 1$,

$$\omega_i = \omega_1 + \frac{\omega_r}{2}$$

and since

$$\omega_r = \omega_2 - \omega_1$$

then

$$\omega_i = \frac{\omega_1 + \omega_2}{2}$$

118

In general, for values of m close to unity, ω_i appears as shown in Figure 55 with a peak negative value given by

$$\frac{m}{m-1} \times \omega_r$$

The base of the triangle is readily estimated since the average value of ω_i over one cycle is 0.

Hence, from the geometry

$$\frac{m}{1-m} \omega_r \iota = \frac{\omega_r}{2} \times \left(\frac{1}{f_r} - 2\iota \right) \tag{216}$$

from which

$$2\iota = (1 - m) \frac{1}{f_r} \tag{217}$$

Therefore, for $m = 0.99$, the width of the frequency spike is

$$.01 \left(\frac{1}{f_r} \right)$$

or only 1 percent of the period of f_r. Further analysis is necessary to determine if these narrow spikes prevent acceptable performance or if they can be eliminated from the output in a simple way. If accurate phase switchover timing is maintained, then the periodic spikes might simply be gated out. The existence of the spikes in the frequency domain suggests that a discriminator might be used to obtain the synchronized gates for accomplishing phase reversal. This, however, constitutes a somewhat complex method of implementation.

5.14 A simple circuit for implementing a median frequency generator

5.14.1 Introduction. The following concept comprises a simple method for obtaining pulses that coincide with the phase reversals that occur when two signals of different frequencies are added linearly. This enables a frequency that is the median of the two input frequencies to be generated by simply reversing the phase of the summed input at the phase reversal points. A different means of implementing a median frequency generator is described in detail in Appendix A.
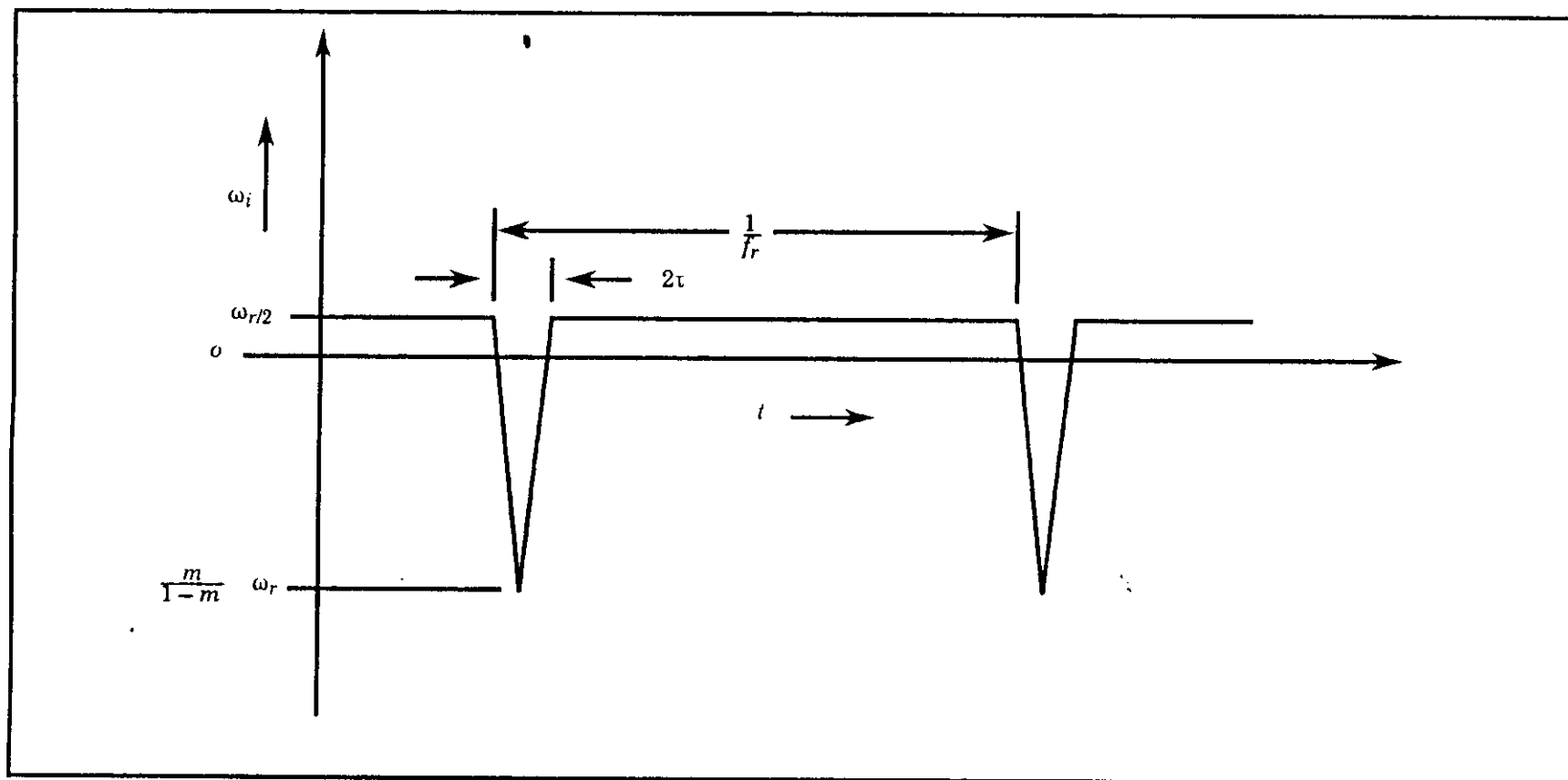
FIGURE 55. Instantaneous frequency ω_i for two limited summed signals.

MIL-HDBK-421

5.14.2 <u>Approach</u>. A functional block diagram of the alternate method proposed here is presented in Figure 56. The waveforms occurring at the various points in the system are shown in Figure 57 to clarify system operation. As before, the system philosophy depends on the fact that when two equal amplitude sine waves of different frequencies f_1 and f_2 are added linearly, the resultant signal consists of zero crossings whose period is

$$\frac{2}{(f_1 + f_2)}$$

with a 180° phase reversal occurring at a period corresponding to the difference between the two frequencies or

$$\frac{1}{(f_1 - f_2)}$$

The linearly added signals are passed through a hard limiter to eliminate the amplitude variations. The limited signal appears as shown in Figure 57a. This signal is then fed directly to one normally closed gate and to a second normally closed gate after being inverted. The gate control signals are obtained in the passive timing system by the simple process of delaying the hard-limited signal by a half-cycle of the period, as shown in Figure 57b, and adding it back to itself. This results in the complete cancellation of the signal everywhere except at the phase-reversed points, as illustrated in Figure 57c. The pulse train at the output of the adder is then used to switch a bistable multivibrator to obtain the required synchronous gates for gating on each appropriate phase condition of the limiter's output. The time sequence of the gates and the output waveform of the median frequency generator are illustrated in Figures 57d and 57e. The frequency of the output f_0 is equal to the median value of the two input frequencies or

$$f_0 = \frac{f_1 + f_2}{2}$$

The proposed alternate system may be improved by adding the circuitry illustrated in Figure 58. This provides all positive pulses of width τ at the phase crossover points to ensure positive triggering of the bistable multivibrator. The effect the change has on system operation is clarified in the waveform diagrams illustrated in Figure 59. For purposes of discussion, the phase reversal point is shown occuring at $7/4\pi$ or 315°.

In this case, the linear addition of the delayed signal with itself appears as shown in Figure 59c. We see that reversals of the carrier phase that do not occur at an integral multiple of π result in unbalanced, split-video pulses. This condition is eliminated easily with the suggested additional circuitry. The positive and negative portions are separated by clipping. Inverting the native pulses and adding them to the positive pulses then yields one-sided pulses whose width is equal to half of the carrier period.

$$\tau = \frac{1}{f_1 + f_2}$$

In addition, the complete pulse train is of the same polarity and is now applied directly to the bistable multivibrator for generating the gates.
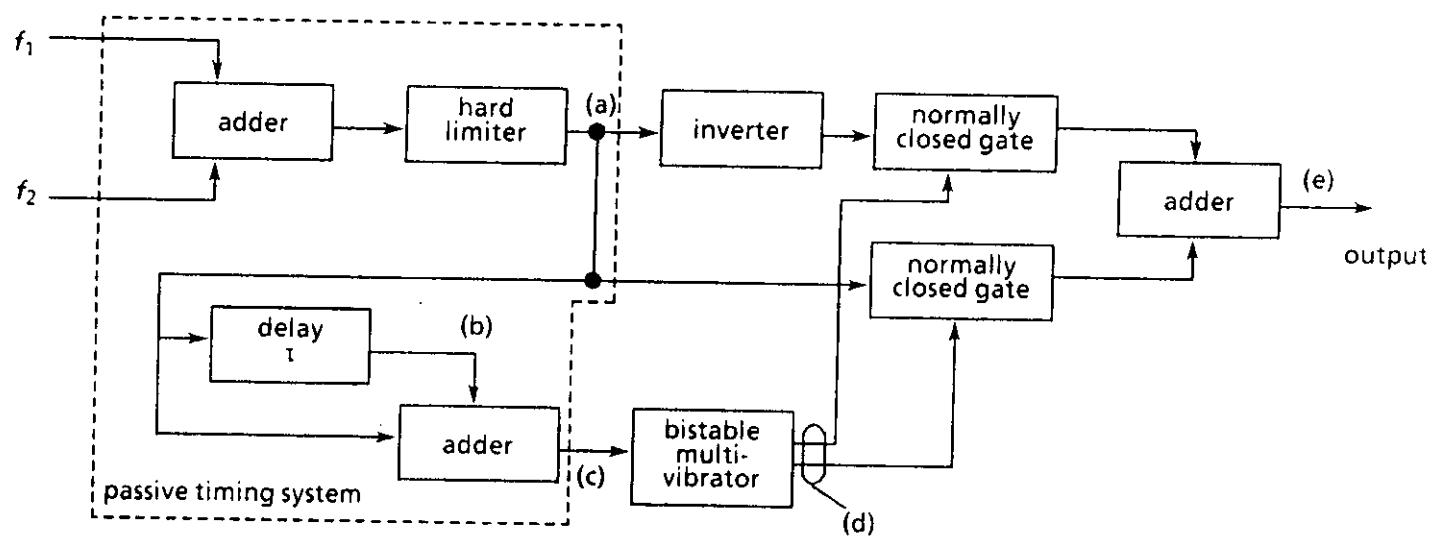
FIGURE 56. Median frequency generator.
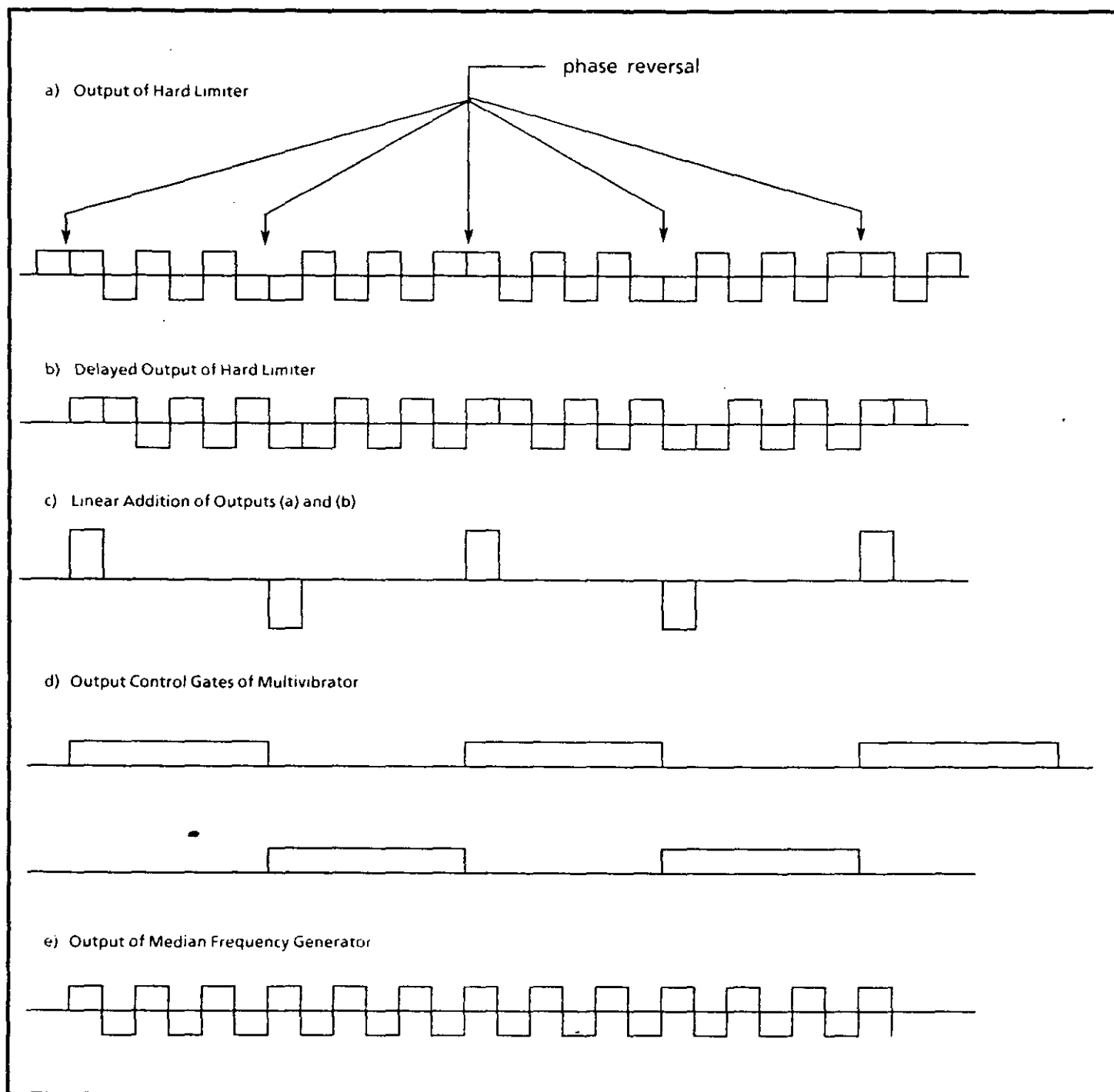
MIL-HDBK-421

FIGURE 57. Median frequency generator waveforms.
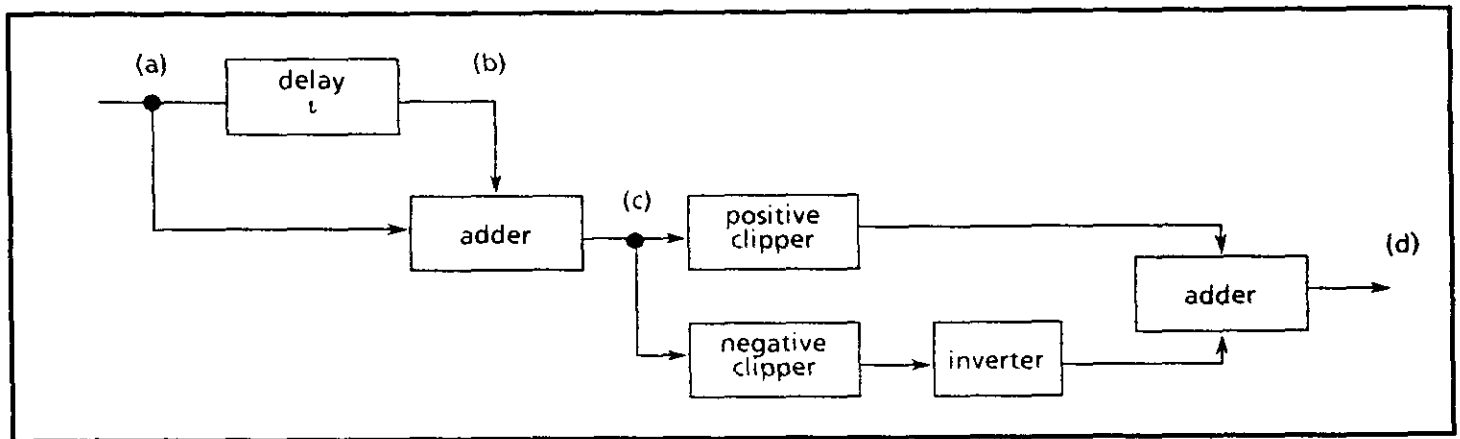
FIGURE 58. Modified passive timing system.

a) Output of Hard Limiter

phase reversal point

b) Delayed Output of Hard Limiter

c) Linear Addition of Outputs (a) and (b)

d) Output Control Gates of Multivibrator
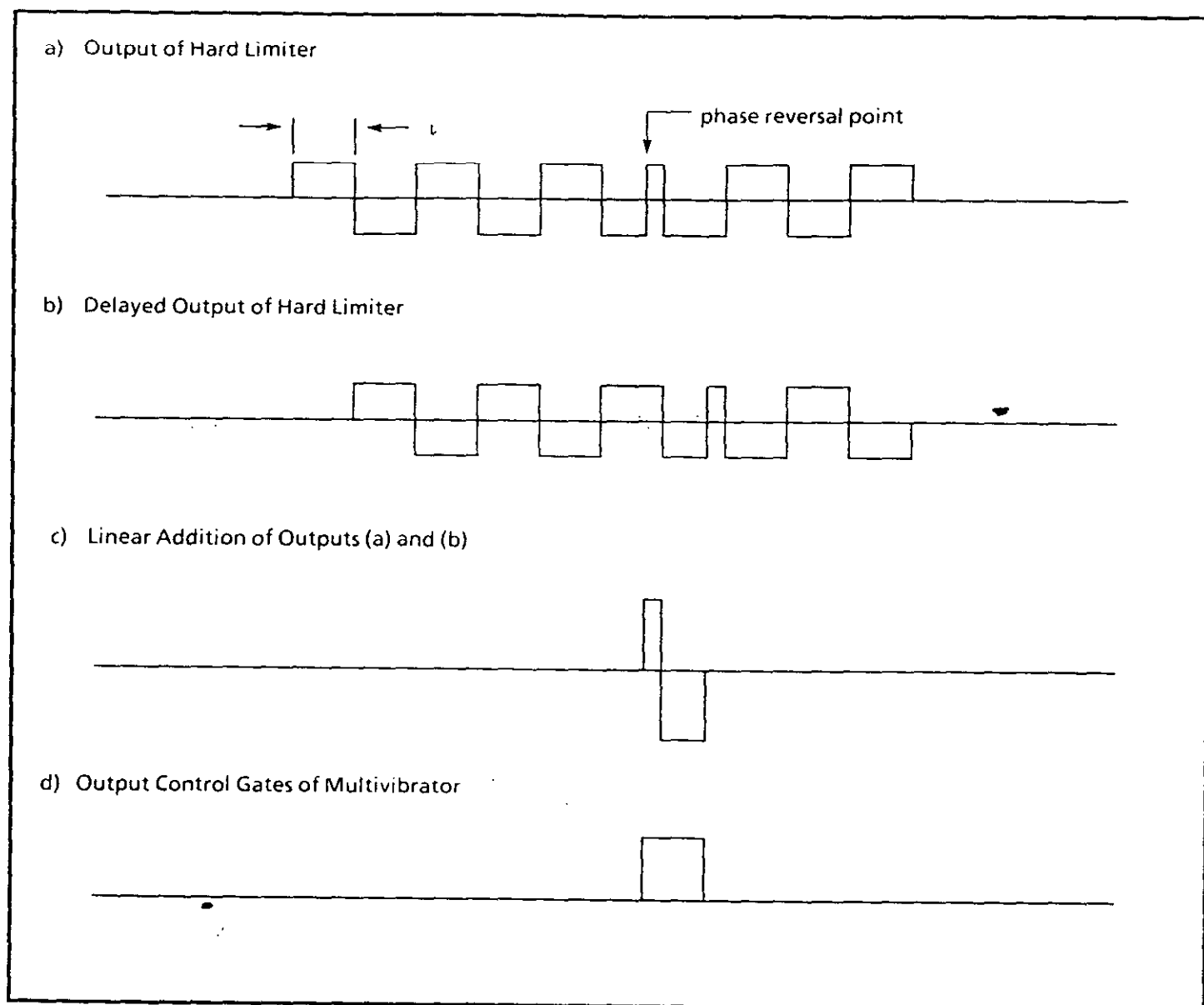
FIGURE 59. <u>Waveforms for the modified system</u>.

MIL-HDBK-421

This page intentionally left blank.

6. TIMING SOURCES

Network timing and synchronization are based on external timing traceable to a Coordinated Universal Time (UTC) source by time-dissemination systems; by long-haul communications systems with a time-transfer capability; and by independent, highly stable nodal clocks for tactical systems. The node's principal clock (or its alternate) supplies a clock signal to all equipment of a synchronous node through a distribution system(s) that is (are) basically hierarchical in nature.

6.1   Common frequency standards. Of the three common frequency standards [cesium beam, rubidium (Rb) vapor, and quartz crystal] the cesium beam is a primary standard. The Rb vapor and quartz crystal are secondary standards. The distinction between a primary standard and a secondary standard is that the former does not require any other reference for calibration and has no inherent frequency drift, whereas the latter requires calibration both during manufacturing and at intervals during use, depending on its accuracy and frequency drift ratio. In general, both primary and secondary standards are very accurate and have excellent frequency stability properties.

6.2   Quartz crystal oscillators. Quartz crystal oscillators are used in nearly every frequency control application, including atomic standards. The quartz crystal has superior mechanical and chemical stability and uses very little energy to maintain oscillation. These properties are most useful in a frequency standard. The piezoelectric properties of quartz make it convenient to use in crystal oscillator circuits. The piezoelectric effect is one in which some materials become electrically polarized when they are mechanically strained. A crystal is not a homogeneous medium but has a certain preferred direction; thus, the piezoelectric effect has a directional dependence with respect to the crystal's orientation.

Physically, piezoelectric resonators consist of carefully oriented and dimensioned pieces of quartz material to which adherent electrodes have been applied. Electrodes are thin, metallic coatings deposited directly on the crystal by an evaporation process. Mechanical support is provided on the crystal at places chosen to avoid inhibiting the desired vibration. If possible, the mounting is such that unwanted vibration modes are suppressed. An alternating voltage applied across the crystal causes it to vibrate with a preference for the mechanical resonance frequency of the crystal.

When the resulting two-terminal resonator is connected into a circuit, it behaves as though it were an electrical network. It is so located in the oscillator circuit that its equivalent electrical network becomes a major part of the resonant circuit that controls the oscillator frequency. To stabilize the frequency and minimize the effects of temperature, crystal oscillators are placed in ovens or are temperature compensated.

Improvements in quartz crystal oscillator technology have been in the following areas:

1.   New, precision resonator cuts (for example, the SC-cut, which is a method of cutting a crystal that results in providing faster oscillator warm-up), improved frequency versus temperature stability, lower drive sensitivity, and increased radiation hardness over the traditional AT-cut. The AT-cut is easier and cheaper to make but does not perform as well.

2.   Improved crystal fabrication techniques, including ultraclean processing, to reduce frequency aging and thermal hysteresis.

3.   Smaller size and lower-power, oven-controlled crystal oscillators (OCXO) that employ microelectronic packaging and high-efficiency thermal insulation.

4.   More accurate, digitally compensated crystal oscillators that use resonator self-temperature-sensing thermometry and microcomputer processing. An inherent characteristic of crystal oscillators is that their resonant frequency changes with time. The *aging rate* (the average rate of change of frequency) may be used, within limits, to predict operation of a well-behaved oscillator after a period of observation against a superior standard, but aging does usually change with time, and other effects (such as room temperature) also change the frequency. The relatively large and variable aging rates of crystal oscillators (compared with atomic standards) make crystal oscillators inferior to atomic clocks as timekeepers. As a frequency reference, a quartz oscillator can also accumulate large errors over a long period of time after calibration. For example, a unit with an aging rate of 5 parts in 10^{10} per day could accumulate a frequency error of several parts in 10^8 in a year; thus, periodic checks and corrections are needed to maintain a quartz-crystal frequency standard.

The quartz oscillator's excellent short-term stability and spectral purity used in atomic standards contribute to high-quality output signals. The advantages of current commercial quartz oscillators are small size, light weight, and low power consumption. Crystal oscillators are suitable for many systems in which size, weight, and power consumption are most important, and in which aging and retrace disadvantages can be tolerated. Crystal oscillators may also change frequency slightly with changes in acceleration (including orientation in the earth's gravitational field); however, some have been made with a sensitivity of approximately 1 part in 10^{10} per g. One area in which this g-sensitivity is important is in mobile applications where the oscillator suffers vibration; although the frequency variation is small, if the frequency is multiplied into the microwave region and employed as a conversion oscillator, the resulting frequency modulation may be disadvantageous for coherent detection or very high bit-rate applications.

Most OCXOs age rapidly in frequency when first turned on and may not reach the ultimate aging rate until, perhaps, a month later; however, recent developments have produced very small, low-power OCXOs that warm-up in a few minutes and have low aging rates. Temperature-compensated crystal oscillators (TCXO) are designed to reduce the change in frequency with temperature and avoid the power drain of a temperature-controlled oven for applications in which very limited power is available.

Development of microcomputer-compensated crystal oscillators (MCXO) have provided new capabilities in precision, low-power timekeeping. The MCXO employs techniques such as pulse deletion and phase-locked loop summing to effect temperature compensation by means external to the crystal oscillator circuit. It circumvents the need to pull the crystal frequency, and thereby allows the use of stiffer SC-cut crystal units that have superior aging and thermal hysteresis characteristics. Also, the trim effect (that is, the degradation in temperature compensation due to pulling the crystal frequency) is eliminated. The MCXO virtually eliminates thermometry-caused errors by permitting resonator self-temperature reusing. Automatic recalibration features can be designed into the

MCXO algorithm. An offset is stored in memory following simple injection of an external, higher-accuracy reference signal. Also, a low-power clock can be designed into the MCXO to maintain accurate time-of-day at extremely low power (a few milliwatts) while in a power-conserving standby mode.

6.3   Rubidium frequency standard. Rb atomic resonance is at 6,834,682,608 hertz. The oscillator is based on the gas-cell method, using optical state selection and optical detection. The Rb vapor standard uses a passive resonator to stabilize a quartz oscillator.

Operation of the Rb standard is based on a hyperfine transition in Rb-87 gas. The Rb vapor and an inert buffer gas are contained in a cell illuminated by a beam of filtered light, as shown in Figure 60.

A photodetector monitors changes, near resonance, in the amount of light absorbed as a function of applied microwave frequencies. The microwave signal is derived by multiplication of the quartz oscillator frequency. A servo-loop connects the detector output and oscillator so that the oscillator is locked to the center of the resonance line.

By an optical pumping technique, an excess population is built-up in one of the Rb-87 ground-state hyperfine levels within the cell. Population of the F-2 level is increased at the expense of the F-1 level. Illuminated Rb-87 atoms are optically excited into upper energy states from which they decay quickly into both the F-2 and F-1 levels. Components linking the F-2 level to the upper energy states are removed by filtering the excitation light. Since the light excites atoms out of the F-1 level only, while they decay into both, an excess population builds-up in the F-2 level. Because fewer atoms are in the state where they can absorb light, the optical absorption coefficient is reduced. Application of microwave energy, corresponding to that which separates the two ground-state hyperfine levels, induces transitions from the F-2 to F-1 level so that more light is absorbed.

The stability performance of Rb oscillators is nevertheless quite spectacular. The Rb standard offers excellent short-term stability. At 1-second sampling times, they display a stability of better than 10^{-11} and perform near the 10^{-13} level for sampling times up to 1 day. For longer averaging times, the frequency stability is afflicted by the frequency aging, which is typically 1 part in 10^{11} per month. This is much less than the aging of crystal oscillators. The Rb standard is not self-calibrating, and during construction it must be calibrated against a reference standard such as the cesium-beam frequency standard. The advantages are small size and light weight (for an atomic oscillator), medium power requirements, and extremely fast warm-up. These advantages, coupled with good performance in hostile environments, make the Rb oscillator attractive for many mobile and tactical systems in which its long-term aging of 1 to 4 parts in 10^{11} per month can be tolerated. Its aging, however, may exclude it as a candidate for some long-term timekeeping jobs.

In the future, this oscillator will probably shrink in size because of further reduction in physics package volume and electronic miniaturization. Performance is not expected to improve significantly, except in aging and short-term stability, where a factor of 5 or 10 improvement may be possible. Performance under vibration, in magnetic fields, and in changing temperature environments may also improve. The larger anticipated demand in the next 20 years, in addition to performance increases
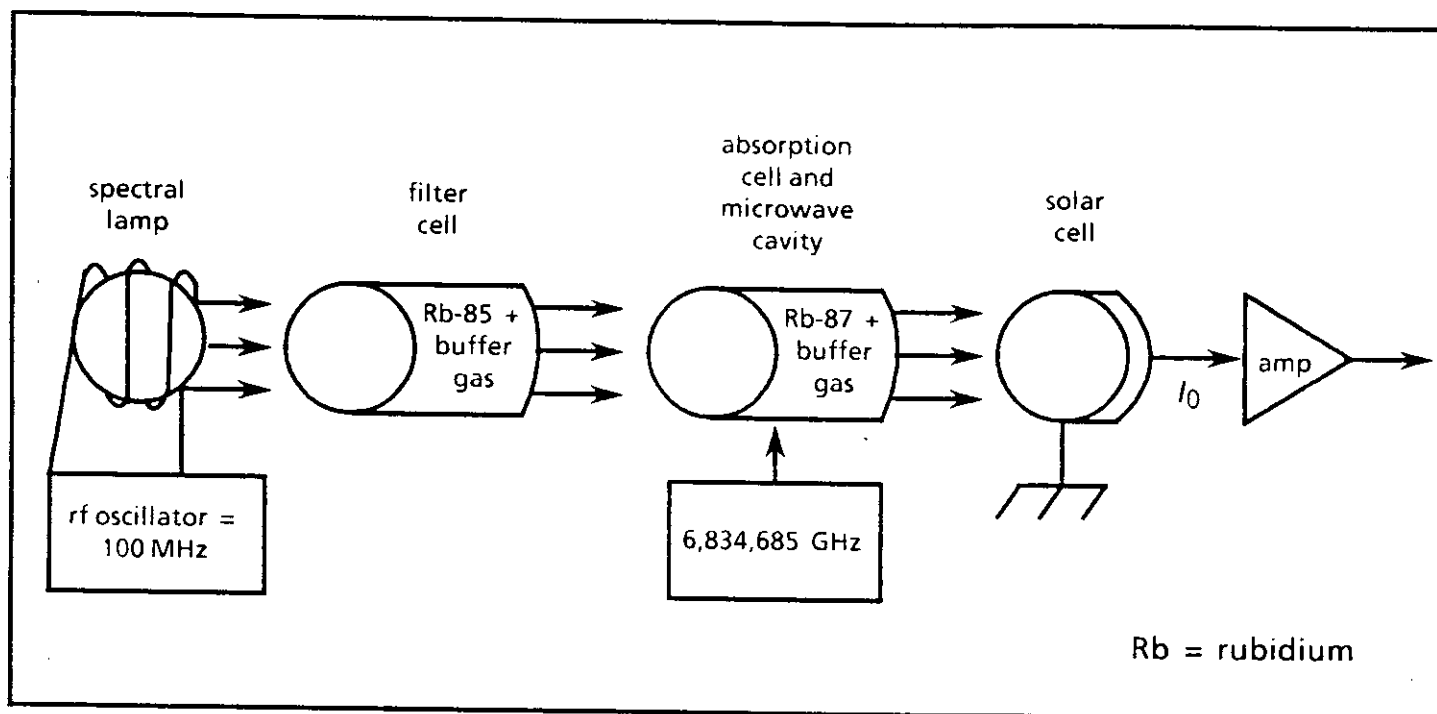
FIGURE 60. Rubidium frequency standard block diagram.

achieved without use of precision manufacturing techniques, should lower the cost per unit.

Precise time can be made available to systems that lack the power required by the Rb frequency standard by employing the Rb crystal oscillator (RbXO). The RbXO, a Rb reference standard combined with a crystal oscillator, can be either an OCXO or MCXO. The crystal oscillator is periodically or intermittently synchronized by the high-stability Rb standard. The Rb standard remains off most of the time. When it is turned on, it stays on for just the few minutes required for it to stabilize and adjust the frequency of the crystal oscillator. The accuracy and long-term stability of the Rb reference is thereby transferred to the crystal oscillator at a total power consumption which is not much more than that of the low-power crystal oscillator alone.

6.4   Cesium-beam frequency standard. For a cesium oscillator, atomic resonance is at 9,192,631,770 Hz. Cesium-beam frequency standards are in use wherever high precision and accuracy in time and frequency standards are needed. Cesium-beam units are the current basis for most national standards.

The cesium-beam standard, an atomic resonance device, provides access to one of nature's invariant frequencies in accordance with the principles of quantum mechanics. The cesium-beam standard is a true primary frequency standard and requires no other reference for calibration to an accuracy of 1 part in 10^{11} or so. Most cesium standards have provisions for minor frequency adjustments and can be made to agree with other references to greater precision.

For the cesium-beam standard, quantum effects arise in the nuclear magnetic hyperfine ground state of the atoms. A particularly appropriate transition occurs between the $F = 4$, $m_f = 0$ and $F = 3$, $m_f = 0$ hyperfine levels in the cesium 133 atom. This transition arises from electron-spin, nuclear-spin interaction and is used for frequency control. The transition is relatively insensitive to external influences such as electric and magnetic fields, but good magnetic shielding is nevertheless required.

A typical cesium-beam device, shown in Figure 61, takes advantage of this invariant transition. It is so arranged that cesium atoms in all sublevels of states $F = 3$ and $F = 4$ leave an oven and are formed into a beam. The beam is deflected in a nonuniform magnetic field (A magnet) by a force component that depends on F_0, m_f, the field, and the field gradient.

The atoms in the $F = 3$ sublevels and the $F = 4$, $m_f = -4$ sublevel are deflected into the microwave cavity, and those in the remaining $F = 4$ sublevels are deflected out of the main beam (getters are used to capture the cesium atoms in the unwanted paths). The atoms in the $F = 3$ sublevels and $F = 4$, $m_f = -4$ sublevel then pass through a low and uniform magnetic field space (C-field) and are subjected to excitation by micro-wave energy.
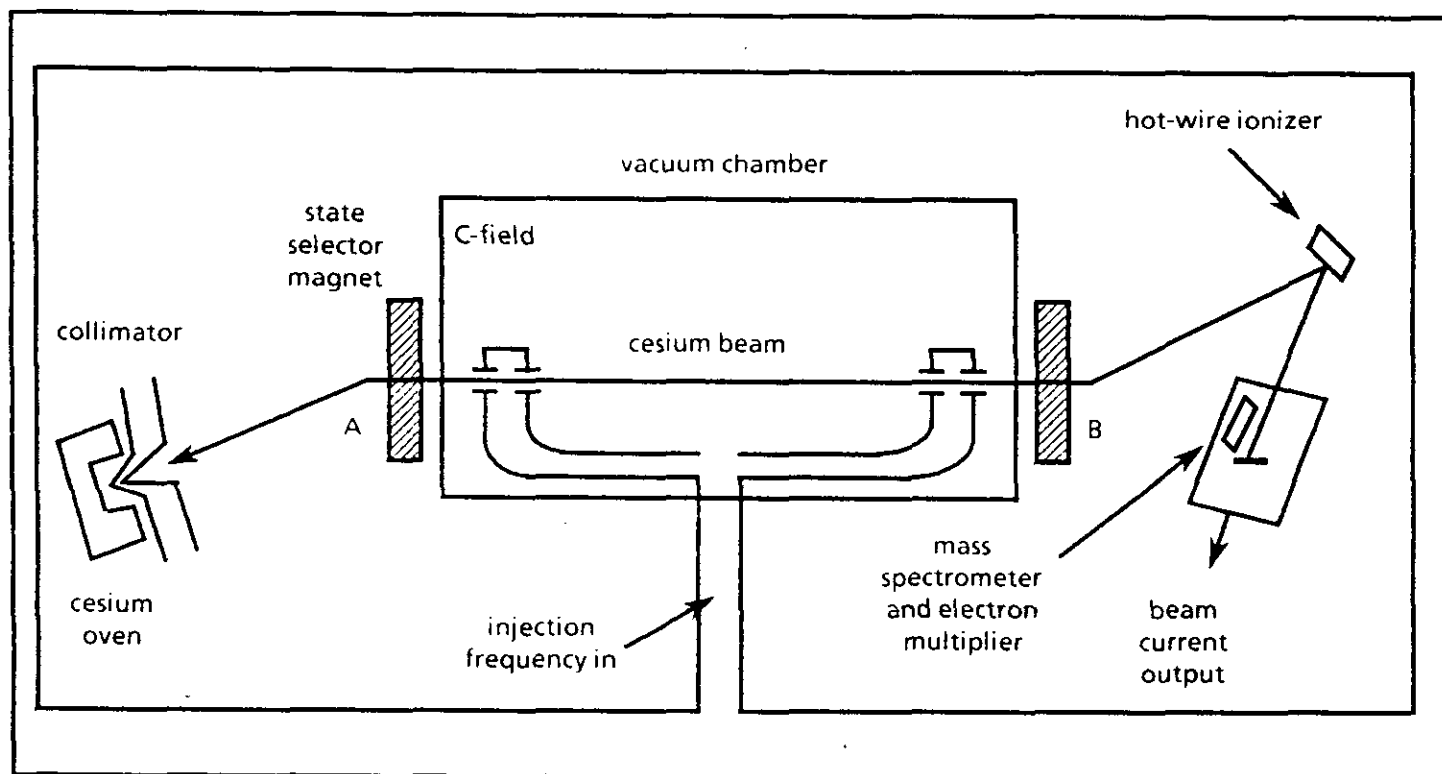
FIGURE 61. Beam tube schematic.

For the control of frequency, the cesium atom is required to perform a resonance absorption of energy from the microwave-exciting signal, corresponding to a transition from the 3.0 state to the 4.0 state. Upon passing through a second magnetic field (B magnet) identical to the first one, those atoms that have undergone the required transition are deflected toward the hot-wire ionizer. Cesium atoms, ionized by the hot wire, then pass through a mass spectrometer and are accelerated toward a multistage electron multiplier. (Common contaminants that may cause noise bursts are removed by the mass spectrometer.) Amplified current then passes through signal processing electronics, which regulate the frequency of a voltage-controlled crystal oscillator. Oscillator output frequency is multiplied and fed back to the cesium beam through the waveguide, thereby closing the loop.

The fractional frequency stability of laboratory and commercial devices can reach parts in 10^{14} at sampling times of less than 1 hour to several days. The short-term frequency stability is limited by fluctuations in the atomic beam intensity, "shot noise," which is basic and unavoidable. These fluctuations affect the frequency stability less, as more intense atomic beams are used. This approach, which is becoming available in both commercial and laboratory devices, improves the stability. In contrast to commercial devices, the laboratory oscillators are designed to allow a more complete and easier evaluation of all effects on the frequency. Cesium oscillators are used extensively where high reproducibility and long-term stability are needed for sampling times of more than 1 day. For most applications, cesium oscillators need not be calibrated. They are the workhorses in most of the accurate frequency and time-distribution services seen today. The advantages are long-term stability, little need for calibration, and medium tolerance to hostile environments. The large size and weight, and the higher power and cost, make the cesium oscillator more useful in stationary and benign environmental applications, such as in providing a reference against which other, less stable oscillators are periodically checked. Where space and power are not at a premium, such as with ships, large aircraft, ground stations, and laboratories, the cesium oscillator is a good choice.

Smaller, lighter, lower-power cesium spacecraft clocks have been developed by the Global Positioning System (GPS) clock program. They weigh 28 pounds, consume 27 watts, and have a 1-day stability of 1 part in 10^{13}.

6.5 Hydrogen maser atomic clock. As a frequency standard, the hydrogen maser provides a frequency that is well defined without reference to any external (reference) standard. An atomic hydrogen beam is directed through a state-selecting hexapole magnet, which selects atoms in states of higher energy and allows them to proceed into a quartz bulb (see Figure 62). The quartz bulb confines the atoms to the uniform magnetic field region in a tuned microwave cavity set to the transition frequency of the hydrogen atom between the $F = 1$, $m_f = 0$, and $F = 0$ energy levels. The quartz bulb has Teflon-coated walls to reduce perturbation of the energy states. However, a small perturbation of the atoms still occurs during collision with the wall and produces a frequency shift. This wallshift can be accurately determined by careful frequency measurements.
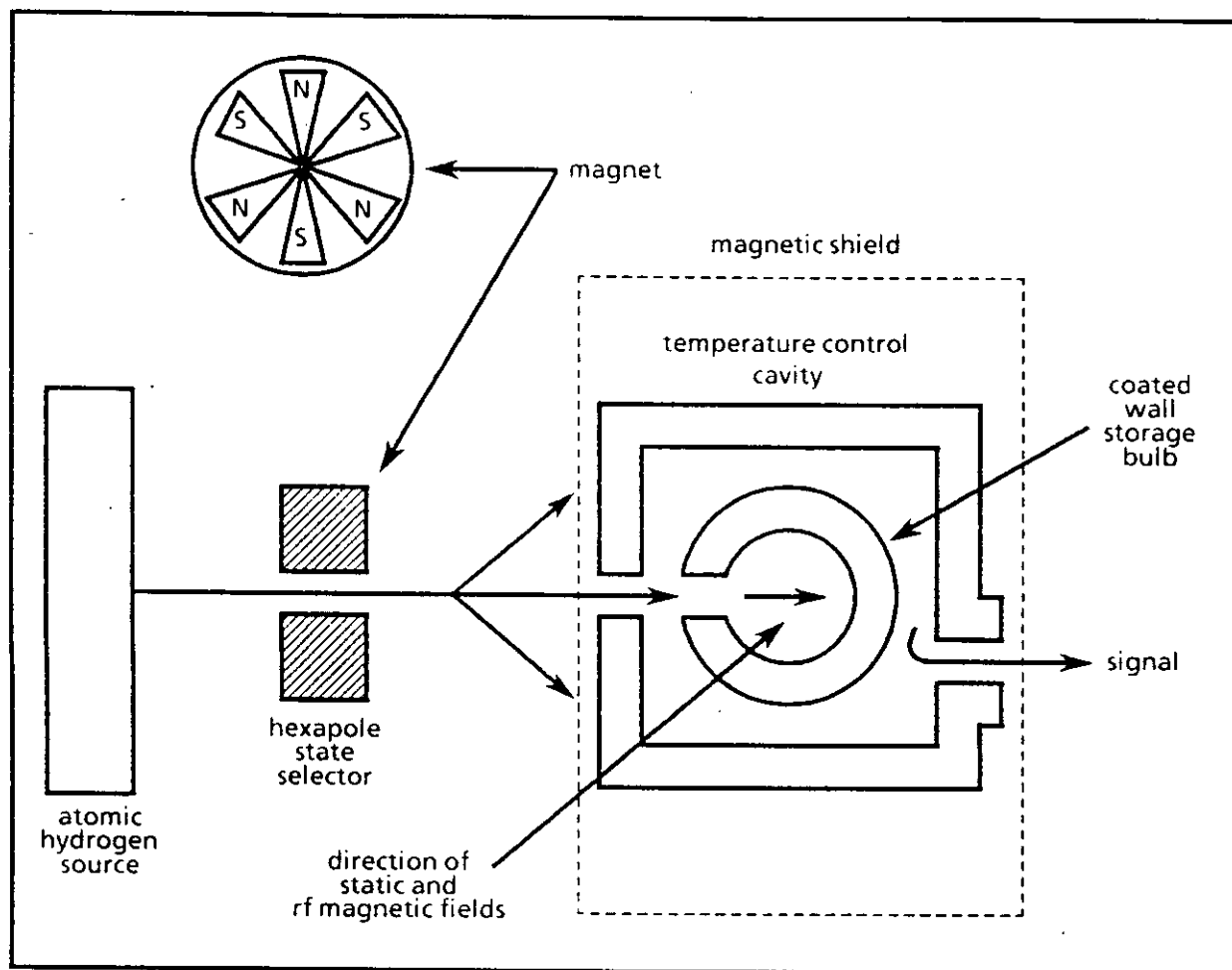
FIGURE 62. Diagram of the hydrogen maser.

Inside the coated quartz storage bulb the hydrogen atoms make random transits and are reflected each time they strike the walls. The atoms undergo many collisions with the walls while in the bulb, and their effective interaction time with the microwave field is lengthened to approximately 1 second. During this interaction process, the atoms tend to relax and give up their energy to the microwave field within the tuned cavity. This field also tends to stimulate more atoms to radiate, thus building in intensity until steady-state maser operation is achieved. The Q values of hydrogen masers are the highest of all traditional frequency standards and are typically 2×10^9, which accounts for the excellent stability of hydrogen masers.

It is also the most stable of all known frequency sources for averaging times of a few seconds to approximately 1 or more. It has proved to be a practical frequency source for a few specialized applications in which these stabilities are critical, and its large size is not a consideration.

Hydrogen masers of conventional (self-oscillating) design are used in ground stations, despite their large size and weight, because of their high stability. Newer designs have employed smaller cavities to reduce size, and they have incorporated automatic cavity tuning to compensate for the long-term drift caused by cavity frequency drift. Other new designs have been developed that employ still smaller cavities whose Qs are not large enough to sustain maser oscillation. These are used either as passive resonators in servos to control crystal oscillators, or with external feedback to enhance the Q of the small cavity and thereby reach the threshold of maser oscillation. These devices approach the size and weight of conventional, commercial cesium-beam standards.

The fundamental limitations in accuracy of the hydrogen maser are the wall collisions and the second-order Doppler effect. The second-order Doppler effect is of the order of 1.4×10^{-11} per degree Kelvin; thus, a control to 1×10^{-14} in the long term requires a temperature stability of slightly better than one-tenth of a degree. Wall collisions cause a phase shift in each collision of a radiating atom with the surface of the storage bulb. The accumulated phase shift during the lifetime of a radiating atom in the storage bulb results in a frequency shift. For typical bulb sizes, the related frequency shift is of the order 2×10^{-11}. The current accuracy of the hydrogen maser is limited by the wall collision effect 1×10^{-12} and is thus considerably worse than that of cesium; however, more thorough use of a few evaluation techniques, such as the variable or flexible storage bulb and use of the temperature dependence of the wallshift, is likely to yield better results. A special incentive toward this goal lies in the documented fact that the wallshift appears to be highly stable in the well-controlled environment inside the vacuum of a hydrogen maser. Masers have run over many years with, at most, 1×10^{-13} drift per year. This estimate is actually the measurement limit of the systems employed.

6.6 <u>Comparison of common timing sources</u>. Table IV provides a comparison of performance, size, and estimated cost (1991 dollars) for the common quartz and atomic oscillators. Figure 63 provides a comparison of accuracy and power. It is intended to facilitate a tradeoff analysis and selection of a source for a given application. The hydrogen maser is intentionally excluded from this group because of its high cost, limited availability, and highly specialized characteristics, which severely limit its tactical applications. Accuracy is stated in terms of an overall accuracy of output frequency that specifies a maximum frequency deviation from an assigned nominal value, due to all combinations of operating and nonoperating parameters within a 122-year period. Except for the temperature range, which is

TABLE IV. Comparison of quartz and atomic oscillators.

	Quartz Oscillators			Atomic Oscillators		
	TCXO	MCXO	OCXO	Rubidium	RbXO	Cesium
Accuracy* (per year)	2×10^{-6}	5×10^{-8}	1×10^{-8}	5×10^{-10}	7×10^{-10}	2×10^{-11}
Aging (per year)	5×10^{-7}	2×10^{-8}	6×10^{-9}	2×10^{-10}	2×10^{-10}	0
Temperature stability (range, °C)	5×10^{-7} (-55 to +85)	2×10^{-8} (-55 to +85)	2×10^{-9} (-55 to +85)	3×10^{-10} (-55 to +68)	5×10^{-10} (-55 to +85)	2×10^{-11} (-28 to +65)
Stability, $y(\tau)$ ($\tau = 1$ s)	1×10^{-9}	1×10^{-10}	1×10^{-12}	3×10^{-11}	5×10^{-12}	5×10^{-11}
Size (cm3)	10	50	20 to 200	800	1,200	6,000
Warm-up time (minutes)	0.1 (to 1×10^{-6})	0.1 (to 2×10^{-8})	4 (to 1×10^{-8})	3 (to 5×10^{-10})	3 (to 5×10^{-10})	20 (to 2×10^{-11})
Power (W) (at lowest temperature)	0.05	<0.04	0.25 to 4	20	0.35	30
Price (~ $)	225	<1,200	2,200	9,000	11,000	44,000

* Including environmental effects [note that the temperature ranges for rubidium (Rb) and cesium oscillators are narrower than for quartz oscillators].

136
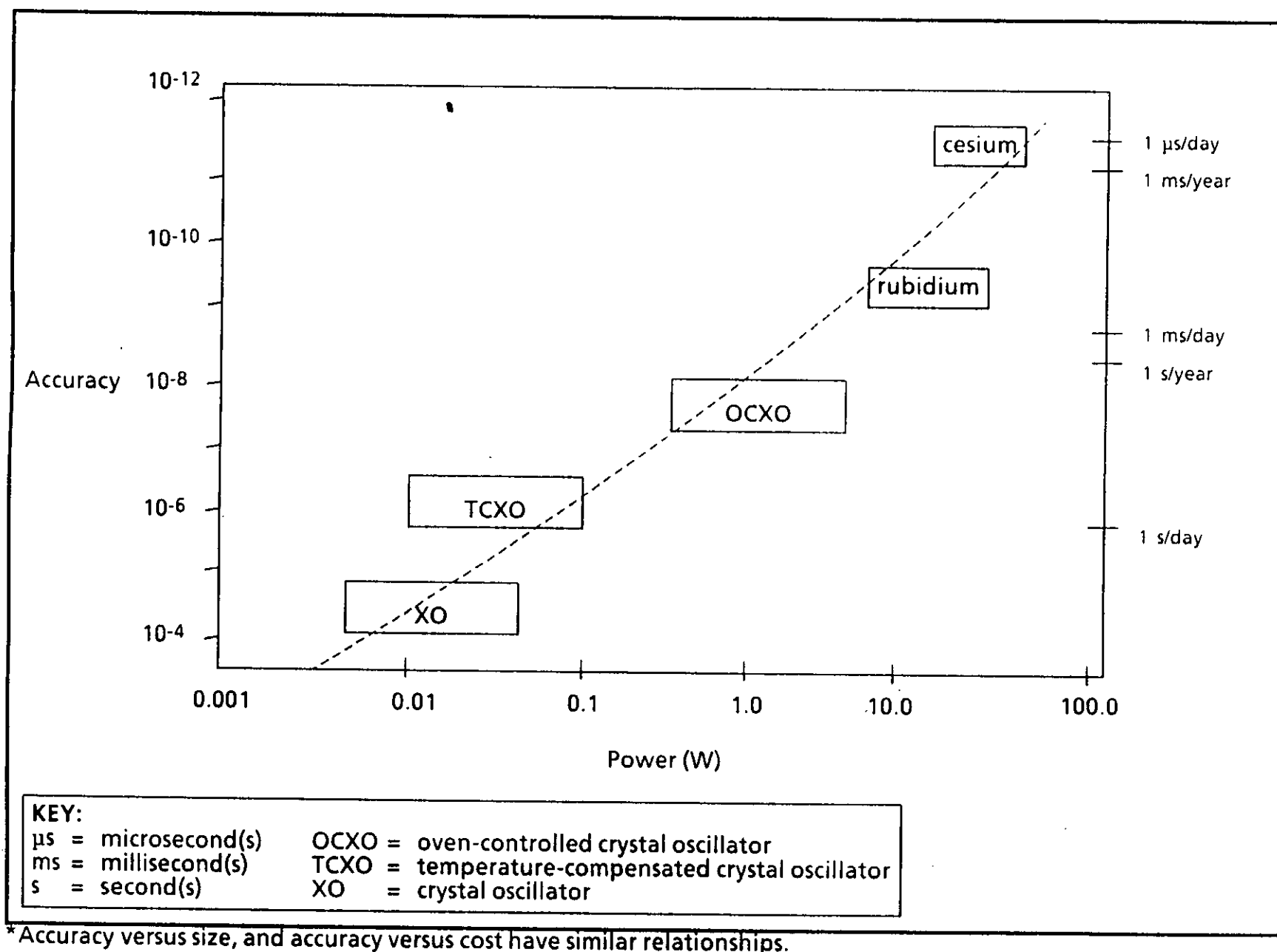
MIL-HDBK-421

FIGURE 63. Accuracy versus power requirement.*

KEY:
μs = microsecond(s)   OCXO = oven-controlled crystal oscillator
ms = millisecond(s)   TCXO = temperature-compensated crystal oscillator
s   = second(s)   XO   = crystal oscillator

*Accuracy versus size, and accuracy versus cost have similar relationships.

MIL-HDBK-421

137

specified, standard tactical military environmental conditions are assumed. Short-term stability is expressed as the square root of the Allan variance, where Ty (T) is the averaging time. For this parameter, steady state (that is, quiescent) conditions are assumed. Warm-up time is expressed as the time, measured from initial power application, required for the oscillator to stabilize its mode of operation within specified limits of final frequency. Final frequency is defined to occur at a given period of time, in minutes or hours, depending on the type of oscillator. Power specifies the maximum average power consumption under the most stringent condition, that is, the lowest operating temperature.

7. EXAMPLES OF TIME-DEPENDENT, TIMING, AND TIME-DISSEMINATION SYSTEMS

7.1   Tactical network timing system. A strong tactical communications system depends on how easily and rapidly that system can be set-up and torn-down. This task becomes even more complex in networks that require highly accurate and precise timing. For example, the network timing subsystem for the tactical switched communications network in Figure 64 is built around a highly accurate cesium-beam standard located in the AN/TSQ-111 Communications Nodal Control Element (CNCE).

Normally each CNCE operates its own timing system from an internal cesium standard that drives a voltage-controlled oscillator (VCO). In these independent clock timing systems, the sending and receiving CNCE cesium clocks are set closely enough that the receiving station's buffer is infrequently filled and emptied. The necessity of interrupting traffic to reset buffers is expected to be once a day (or less) under normal conditions. Additionally, the CNCE has a backup VCO that free-runs if the cesium standard is lost. This enables timing to be derived from either of two incoming transmission groups, and it is used to slave the oscillator (either manually or automatically) to the selected incoming groups.

Below the CNCE-equipped node, at subordinate or access nodes, tactical switches obtain timing from a VCO. In most cases the VCO has a backup unit. These switch-associated VCOs normally derive their timing reference from and are slaved to an incoming conditioned diphase data transmission group that is traceable back to a CNCE cesium standard. However, all switch VCOs have the ability to free-run with reduced stability (a) if the CNCE cesium clock fails, (b) if connection to a CNCE is lost, or (c) if a CNCE is not available.

Tactical radio equipment normally operates in a slaved mode. All such radios derive timing from conditioned diphase data transitions in the traffic data stream. Two potential exceptions to this rule exist: The first exception is the AN/TRC-170 tropospheric scatter (TROPO)/line-of-sight (LOS) digital radio terminal system, which contains a rubidium source to operate as the master timing source, and, in turn, to drive an internal VCO. Without a CNCE or major switch in the system as a timing source, the AN/TRC-170 system has the ability to free-run from the rubidium source, or directly from the VCO, in a stand-alone mode. Subscribers, or small digital switches, can be slaved to the AN/TRC-170's rubidium timing source. Alternatively, the AN/TRC-170 can slave its VCO to incoming data from either over-the-air (radio-side) or subscriber (cable-side) timing sources.

The other exception concerns analog Army radios modified by the addition of digital modems, multiplexers, and orderwire control units (OCU). The OCUs have timing options that permit them to derive timing from a variety of sources. Preferably, these sources are traceable to a CNCE from which they can be manipulated and distributed to satisfy the total timing requirements within the associated assemblage shelter. These OCUs can operate in a free-running mode if the external source is lost. However, this capability is primarily intended to provide timing for the secure digital voice orderwire during circuit set-up or restoral and has no means for distributing the timing signal to other equipment.

In many tactical systems, the clock is kept on when other parts of the system are shut off. As a result, the clock is the major item that determines battery life (and its associated logistics problems). Buffers retime data from other CNCE-equipped nodes, adjust any minor differences between the two CNCEs' cesium-beam

FIGURE 64. Example of a proposed network timing distribution between tactical nodes.

standards, and feed the received data to the local CNCE processor at the local timing rate. The CNCE can also operate its timing system in several other modes that can be selected manually or automatically. If the local cesium beam fails, then the VCO can be set to operate in a free-running mode. The cesium-beam standard can be set to operate within 2×10^{-12} of the desired frequency. The VCO, which normally is slaved to the cesium-beam standard, reverts (in the case of free-running) to a stability of $\pm 10^{-9}$ for a 24-hour period. Although stability is reduced and buffer resets might be more frequent, the system continues to function, but in a degraded mode. Here it must be noted that all subordinate nodes or switches have VCOs and buffers, and they normally operate slaved to the CNCE. When CNCE timing sources are lost, then subordinate elements can also have their VCOs reset to a free-running mode with a loss in stability comparable to that for the CNCE when it switches from cesium to VCO free-run timing. The system continues to function, although in a degraded mode with a more frequent need to interrupt traffic for buffer resets.

7.2 <u>Single Channel Ground and Airborne Radio System.</u> The Single Channel Ground and Airborne Radio System (SINCGARS) has replaced the AN/VRC-12 family of very high frequency (VHF) frequency modulation (FM) radios. It now serves as the principal LOS combat net radio (CNR) for all Army and Marine Corps tactical forces. SINCGARS is designed to provide an anti-jam (AJ) capability because of its frequency-hopping mode within the frequency range of 30 to 87.975 megahertz (MHz). Timing for SINCGARS is significantly different from the timing of Milstar and its various terminals. SINCGARS is probably the largest single use of timing and synchronization subsystems.

7.3 <u>Satellite communications.</u> In Defense Satellite Communications System (DSCS) satellite communications (SATCOM) spread-spectrum systems, local cesium clocks are traceable directly to the Department of Defense (DoD) Master Clock [U.S. Naval Observatory (USNO) Master Clock] and serve as precise time stations (PTS). SATCOM clocks are regularly checked through the inherent worldwide time-dissemination capability of the spread-spectrum links to the USNO, and are occasionally compared with portable USNO cesium clocks and traveling Global Positioning System (GPS) receivers. Dissemination (either portable-clock or satellite-link) is accurate to the order of 100 nanoseconds (ns), and the desired goal is to maintain the clocks within ± 5 microseconds (μs) of the USNO Master Clock. Adjustments that can change the epoch or rate (frequency) of the SATCOM time are done manually, according to a standard operating procedure (SOP), and are performed only by direction of the USNO. PTS network operation is specified in USNO Precise Time and Time Interval (PTTI) SOP-81, to be revised in 1992. A PTS provides a point for local and transient clock checks for both time and frequency, and performs a monitor and reference function for local transmission. In some cases, the accurate time and frequency are made available to other collocated systems, such as channel-packing, the Automatic Digital Network (AUTODIN), crypto-systems, and LOS microwave links. The PTS may also monitor LORAN-C and other time-dissemination facilities. The monitoring function is a part of the system by which the USNO disseminates precise time, since the results are reported to the USNO. At the same time, the monitoring adds to the redundancy of the PTS, because deviations in the local clock can be more effectively evaluated with larger amounts of independently acquired corroborative data. Since SATCOM clocks are regularly rated and updated by the USNO over an extended period of time, their performance histories are well known, and they have the capability to free-run for long periods without accumulating large time or frequency errors. Therefore, the PTS system has a high degree of survivability, and degradation is very gradual and small in the event of a disconnect with the USNO.

7.4   HAVE QUICK. HAVE QUICK, a jam-resistant ultra high frequency (UHF) communications system, uses precise timing data to control frequency hopping. The HAVE QUICK communications system for tactical aircraft communications employs some rubidium clocks to maintain time accuracy. The system can interface with the GPS for time-setting and updating to the required accuracy, which enhances interoperability among and within groups.

7.5   Joint Tactical Information Distribution System. The Joint Tactical Information Distribution System (JTIDS) provides secure digital communications, using a formatted data standard with precise time requirements to support low-capacity, secure, non-nodal, jam-resistant information distribution. The link is capable of operating in severe, adverse electromagnetic environments anticipated in future military operations. Tactical Digital Information Link-J (TADIL-J) incorporates state-of-the-art advances in signal processing and integrated circuit technology to overcome the most severe limitations of previous-generation TADILs, with expected data rates one to two orders of magnitude higher than previous systems. At the same time it incorporates sophisticated spread-spectrum communications and forward-error-correction coding techniques that support very high AJ margins. It also provides a low probability of interception/low probability of exploitation (LPI/LPE) capability.

7.6   VERDIN. The Navy VERDIN very low frequency/low frequency (VLF/LF) communications system (and likely some similar Air Force systems) has a precise time requirement. Submarines and shore stations employ cesium-beam clocks that are required to free-run for extended periods.

7.7   TACAMO. TACAMO aircraft provide a survivable VLF/LF link with Navy units. The system requires precise time, and it provides an alternate means for time-setting and updating.

7.8   Other systems. Other command, control, communications, and intelligence systems of the three services require precise time. Included are a number of systems (such as crypto and sensor) whose details or requirements are classified.

7.9   Time-dissemination systems. Some of the time-dissemination systems in current use are described in 7.9.1 through 7.9.6. These systems are traceable to the USNO and can be used for time-setting and updating within their accuracy and availability limits.

7.9.1   Global Positioning System. The GPS is a passive, worldwide navigation and time-dissemination system that gives position to approximately 30 meters and is time-accurate to 100 ns. (A passive system is one in which the user is not required to emit a signal.) The system, when fully operational, will consist of 21 operational satellites. To ensure system availability, up to three additional satellites will be orbited as active spares, to provide continuous, worldwide service. There are 15 GPS satellites now in orbit, which the USNO monitors and regularly updates.

Cesium and rubidium clocks carried aboard satellites provide for extended survivability in the event of loss-of-contact with the monitor and control stations. The satellites are capable of operating autonomously for extended periods in the unlikely event of a loss of all links with the master control station (MCS) and the monitor stations that act as backups for the MCS.

The MCS clock ensemble is maintained accurately on-time with the USNO Master Clock by simultaneous observation of GPS satellites at the USNO and the MCS. The MCS can keep time autonomously for extended periods.

7.9.2 Navy navigation satellite system (TRANSIT). TRANSIT, a passive, worldwide navigation system, consists of five satellites that are visible at any point intermittently. Nominal time accuracy is in the order of 10 μs, but continuous simultaneous monitoring can give a better time-dissemination accuracy between cooperating field-ground stations operating in a nonpassive mode. The timing is traceable to the USNO. TRANSIT is under the control of the Naval Satellite Operations Center (NAVSOC), whose MCS clocks at Point Mugu, California, are synchronized to the USNO Master Clock by portable clock trips and LORAN-C. The NAVSOC Detachment in Hawaii also maintains accurate time that is compared with the nearby SATCOM station.

7.9.3 LORAN-C. The LF LORAN-C navigation system is a passive system that gives limited ground-wave coverage over much of the Earth's surface, but there are large gaps. Accuracy of time dissemination in the ground-wave areas is normally better than 1 μs. In the larger areas covered by only sky-wave propagation, the accuracy is considerably reduced and is subject to occasional propagation disturbances, including diurnal effects, but is usable for some applications. Since the inherent time ambiguity of LORAN-C is in the order of 5 to 10 milliseconds (ms), time must be known locally to an accuracy of a few ms before precise time can be obtained.

The various chains of the system are monitored by the USNO and by PTSs to give traceability to the USNO. [Public law PL100-223 requires all LORAN-C transmitters to be synchronized within 100 ns of Coordinated Universal Time (UTC).] LORAN-C transmitters employ cesium-beam clocks that can free-run for extended periods without an update. Individual chain transmitters maintain close coordination with the MCS through a monitoring system, but the chain may deviate a few hundred ns from UTC; the USNO publishes corrections daily for each chain. In many areas, inter-ference from LF stations must be rejected with notch-filters. Susceptibility to jamming is a disadvantage.

LORAN-C timing is used in some cases, either for monitoring the long-term performance of local clocks or determining the drift rates of moderate-stability oscillators. Under favorable conditions and using groundwave signals, frequency comparisons can be made to approximately 1 part in 10^{12} over a 1-day observation. Distortions of sky-wave signals degrade frequency measurement capability by a factor of 100 or more. The U.S. Coast Guard manages and operates LORAN-C.

7.9.4 OMEGA navigation system. The VLF OMEGA navigation system has nominal worldwide coverage through a system of eight transmitters. Navigation is accomplished passively by making simultaneous phase comparisons of several transmitters. For timing, the system is useful mainly as a stable frequency source, since time-ambiguity intervals are very small. Although the system employs cesium-beam clocks, diurnal and anomalous variations of the essentially sky-wave propagation make interpretation of frequency comparisons difficult (as with sky-wave LORAN-C), and phase comparisons are normally made over a period of 1 day or more. The OMEGA system is operated by the Coast Guard. Individual transmitters are occasionally taken off the air for maintenance.

7.9.5 High frequency time broadcasts. High frequency (HF) time broadcasts are useful mostly for time-dissemination to an accuracy of approximately 10 ms. Propagation is typically sky-wave, and, unlike navigation-system dissemination and two-way satellite dissemination, there is no inherent provision for determining propagation time. The propagation delay calculated from the best estimate of the radio path involves some uncertainty, especially when the path is long. The unambiguous time is useful, within coverage areas of the HF stations, for moderate-accuracy time-setting and updating, or as a means of resolving the ambiguities of LORAN-C. Coverage is variable and depends on the frequency in use and the existing propagation conditions, as well as the state of interference from other broadcast services or intentional jamming. Broadcasts of the National Institute of Standards and Technology (NIST) HF stations WWV, WWVH, and the National Research Council of Canada (CHU) are traceable to the USNO through the PTSs maintained by NIST in Colorado and Hawaii.

7.9.6 Portable clocks. Portable clocks are used by the USNO as one method of rating and updating PTS clocks and other facilities requiring precise time. The cesium clocks are set to UTC at the USNO Master Clock and are transported (while running continuously) to the facilities that require calibration. (Batteries are used when power mains are not available.) The clocks are rechecked after the trips in a timing "closure," to verify proper, portable clock operation and to pro-rate small deviations through the trip. Accuracy of portable-clock trips is in the order of 100 ns.

Clock trips have also been used to verify other time-dissemination techniques, such as GPS and the SATCOM spread-spectrum method, which have commensurate precision. As the number of valid techniques increases, the number of portable-clock trips is reduced. Portable-clock trips, however, may remain as a backup dissemination method.

7.10 Other dissemination means. Numerous dissemination methods have been developed for both specific and general application. Only a few are mentioned here.

7.10.1 TV line-10. In the television (TV) line-10 method, two or more facilities (a) extract the same synchronization pulse from a cooperative or uncooperative TV broadcast station in common view of the facilities, and (b) compare the broadcast station's timing with their local clocks. The technique requires users to resolve separately the frame ambiguity of about 33 ms. The method also requires data exchange between users. Propagation time-differences must be resolved by distance measurements and portable clocks. Range is limited by the coverage of available TV transmitters in common view. The method is subject to broadcast schedules and other factors that are not under a user's control.

7.10.2 Very long baseline interferometry. Very long baseline interferometry (VLBI) is a dissemination method capable of very high precision. The technique involves simultaneous monitoring of extraterrestrial radiation sources at two or more user sites. The data (time-marked) is then exchanged through a communications medium, such as a shipping of recordings, for subsequent comparison. Operationally, the technique is not generally employed for communications, but it might be used in very precise comparisons of major timing facilities.

Some recent studies of pulsars that have extremely constant rates hold out hope for long-term, passive, precise frequency-acquisition, but the technique has not yet been reduced to an operational status.

7.11   Other dissemination systems. Several other dissemination systems have been developed recently. In the Hawaii PTTI Test Bed, for example, a specially designed spread-spectrum modem and time-transfer unit have been used to make timing comparisons to sub-microsecond accuracy on a microwave LOS communications link. The master-station pilot tone of another microwave LOS network was stabilized by that station's accurate frequency reference, to provide an accurate standard frequency to the other stations of the network. The spread-spectrum modem and time-transfer unit were also used in two-way SATCOM links, to provide accurate time to stations not equipped with spread-spectrum communicatons modems of the types used in SATCOM time-dissemination systems.

Time dissemination, via fiber optics or LOS laser links, has the potential for extremely high precision because of the large available bandwidth, and it has been used experimentally with good results.

These techniques require some means, such as two-way transmission or independent measurements, to determine the propagation time delay. The propagation delay may be measured and considered constant for some fixed links that do not involve variable distances or paths. With satellite links or links that involve mobile platforms, the propagation delay generally must be determined for each time transfer. Automatic methods are usually available to resolve the propagation delay when two-way circuits are involved. The passive navigation systems, such as GPS or LORAN-C, can be used in a (one-way) broadcast mode to provide precise time and accurate frequency dissemination to both mobile and fixed users. The advantage of a passive system is that the user is not required to emit a signal or use any of its communications capacity to exchange data or correct for propagation delay.

MIL-HDBK-421

This page intentionally left blank.

8. NOTES

8.1 Subject term (key word) listing

Acquisition time
Aging
Calibration
Clock
Crystal oscillators
Data buffers
Doppler frequency
Double loop-tracking system
External timing reference
Frequency difference
Frequency hold-in range
Frequency pull-in range
Generator, frequency
Jitter
Phase-locked loop
Pulse stuffing
Quartz oscillators
Spectral purity
Stability
Standard frequency
Timing error
Timing signal
Timing sources

This page intentionally left blank.

APPENDIX A

LORAN-C, OMEGA, and VLF TRANSMITTING STATIONS AND TIME SIGNALS EMITTED
IN UTC SYSTEMS

10. GENERAL

This appendix lists transmitting stations for LORAN-C, OMEGA, and U.S. Navy very
low frequency (VLF) systems. This information is subject to change. Potential users
of these services are advised to obtain up-to-date time service bulletins from the U.S.
Naval Observatory (USNO). This appendix is intended for guidance only.

20. APPLICABLE DOCUMENTS.

This section is not applicable to this appendix.

30. DEFINITIONS.

For purposes of this appendix, the definitions and acronyms in MIL-HDBK-421 and
FED-STD 1037 shall apply.

40. GENERAL REQUIREMENTS

40.1 LORAN-C, OMEGA, and U.S. Navy VLF transmitting stations

40.1.1 LORAN-C transmitting stations (100 kHz)

Central Pacific (4990)
    Johnston Island
    Upolu Point, Hawaii
    Kure, Midway Island

East Coast Canada (5930)
    Caribou, Maine
    Nantucket, Massachusetts
    Cape Race, Newfoundland, Canada
    Fox Harbour, Labrador, Canada

West Coast Canada (5990)
    Williams Lake, British Columbia, Canada
    Shoal Cove, Alaska
    George, Washington
    Port Hardy, British Columbia, Canada

Labrador Sea (7930)
    Fox Harbour, Labrador, Canada
    Cape Race, Newfoundland, Canada
    Angissoq, Greenland

149

Gulf of Alaska (7960)
    Tok, Alaska
    Narrow Cape, Kodiak Island, Alaska
    Shoal Cove, Alaska

Norwegian Sea (7970)
    Ejde Faeroe Islands, Denmark
    Bo, Norway
    Sylt, Germany
    Sandur, Iceland
    Jan Mayen, Norway

Southeast USA (7980)
    Malone, Florida
    Grangeville, Florida
    Raymondville, Texas
    Jupiter, Florida
    Carolina Beach, North Carolina

Mediterranean Sea (7990)
    Sellia Marina, Italy
    Lampedusa, Italy
    Kargabarun, Turkey
    Estartit, Spain

North Central U.S. (8290)
    Havre, Montana
    Baudette, Minnesota
    Gillette, Wyoming
    Williams Lake, British Columbia, Canada

Great Lakes (8970)
    Dana, Indiana
    Malone, Florida
    Seneca, New York
    Baudette, Minnesota

South Central U.S. (9610)
    Boise City, Oklahoma
    Gillette, Wyoming
    Searchlight, Nevada
    Las Cruces, New Mexico
    Raymondville, Texas
    Grangeville, Florida

West Coast USA (9940)
    Fallon, Nevada
    George, Washington
    Middletown, California
    Searchlight, Nevada

Northeast USA (9960)
    Seneca, New York
    Caribou, Maine
    Nantucket, Massachusetts
    Carolina Beach, North Carolina
    Dana, Indiana

Northwest Pacific (9970)
    Iwo Jima, Japan
    Marcus Island, Japan
    Hokkaido, Japan
    Gesashi, Okinawa Island, Japan
    Barrigada, Guam

Icelandic (9980)
    Sandur, Iceland
    Angissoq, Greenland
    Ejde, Faeroe Islands, Denmark

North Pacific (9990)
    St. Paul, Pribilof Islands, Alaska
    Attu, Alaska
    Port Clarence, Alaska
    Kodiak, Kodiak Island, Alaska

40.1.2 OMEGA transmitting stations. (Each station transmits four navigation frequencies -- 10.2, 11.05, 11.33, and 13.6 kHz. A fifth frequency, unique to each station, is also transmitted.

Kaneohe, Hawaii	Unique frequency 11.8 kHz
Monrovia, Liberia	Unique frequency 12.0 kHz
Bratland, Norway	Unique frequency 12.1 kHz
La Reunion Island, Indian Ocean	Unique frequency 12.3 kHz
Golfo Nuevo, Argentina	Unique frequency 12.9 kHz
Melbourne, Australia	Unique frequency 13.0 kHz
La Maure, North Dakota	Unique frequency 13.1 kHz
Tsushima Island, Japan	Unique frequency 12.8 kHz

40.1.3 U.S. Navy VLF communications stations

    17.4 kHz, NDT, Yosami, Japan
    21.4 kHz, NSS, Annapolis, Maryland
    22.3 kHz, NWC, Exmouth, Australia
    23.4 kHz, NPM, Lualualei, Hawaii
    24.0 kHz, NAA, Cutler, Maine
    24.8 kHz, NLK, Jim Creek, Washington
    28.5 kHz, NAU, Aguada, Puerto Rico

MIL-HDBK-421

This page intentionally left blank.

MIL-HDBK-421

APPENDIX B

SUPPLEMENTAL READING

10. SCOPE

This appendix lists references that address the subject of timing and synchronization. These references may be helpful to users of this handbook.

20. APPLICABLE DOCUMENTS

20.1 Government documents

Department of Defense and Department of Transportation, *1988 Federal Radionavigation Plan*, DoD-4650.4/DOT-TSC-RSPA-88-4, Department of Transportation Research and Special Programs Administration, 1988.

Gutleber, F.S., *An Optimum Synchronization Loop Design*, Joint Tactical Command, Control and Communications Agency, FSG-168, 11 July 1984.

Gutleber, F.S., *Architecture for Tactical Switched Communications Systems*, Annex F3, Network Timing, TTO-ENG-031-75-ANF, TRI-TAC Office, Fort Monmouth, NJ, June 1982.

Gutleber, F.S., *A Synchronous Timing System*, FSG-121, JTCO, April 1973.

Gutleber, F.S., *A Concept for Disseminating Precise Timing Throughout a Communications Network*, FSG-120, JTCO, 28 February 1973.

Gutleber, F.S., *Effects of Radio Fades on System Synchronization*, FSG-114, TRI-TAC Office, Fort Monmouth, NJ, October 1971.

Gutleber, F.S., *A Time Dissemination and Doppler Canceling System for Satellite Access*, TRI-TAC Office, Fort Monmouth, NJ, July 1971.

Gutleber, F.S., *Inherent Fly-Wheeling Capabilities of Synchronizing Systems*, FSG-112, TRI-TAC Office, Fort Monmouth, NJ, July 1971.

Gutleber, F.S., *General Derivation Relating Frequency Stability Requirements to Fade Duration for Synchronization Systems*, FSG-111, TRI-TAC Office, Fort Monmouth, July 1971.

Gutleber, F.S., *An Adaptive Synchronous Coherent Detector for a Quadriphase Modulation System*, FSG-105, U.S. Army ECOM, Fort Monmouth, NJ, 25 August 1970.

Gutleber, F.S., *Threshold Extension Revisited*, Research and Development Technical Report, ECOM-3215, Tactical Communications Systems Office, U.S. Army ECOM, Fort Monmouth, NJ, January 1970.

Gutleber, F.S., *A Simple Circuit for Implementing a Median Frequency Generator*, FSG-98, U.S. Army ECOM, Fort Monmouth, NJ, 10 October 1969.

Gutleber, F.S., *Transient Analysis of a Frequency Following Phase Lock Loop*, FSG-100, U.S. Army ECOM, Fort Monmouth, NJ, October 1969.

Gutleber, F.S., *Threshold Extension Revisited for Tactical Net Radio Systems*, FSG-99, U.S. Army ECOM, Fort Monmouth, NJ, October 1969.

Gutleber, F.S., *A Quadrature Phase Modulated Synchronization System*, FSG-94, U.S. Army ECOM, Fort Monmouth, NJ, October 1969.

Hellwig, H. *Frequency Standards and Clocks: A Tutorial Introduction*, NIST Technical Note 616, 1977, Time and Frequency Division, NIST, Boulder, Colorado, 80303.

Stein, S.R., and Vig, J.R., *Frequency Standards for Communications*, U.S. Army Laboratory Command Research and Development Technical Report SLCET-TR-91-2, January 1991 (copies available from NTIS, ADA231990).

20.2 Non-Government documents

Beser, J., and Parkinson, B.W., "The Application of NAVSTAR Differential GPS in the Civilian Community." *Navigation*, Vol. 29, No. 2, Summer 1982.

Bottom, V.E., *Introduction to Quartz Crystal Unit Design*, Van Nostrand Reinhold Co., 1982.

CCITT Recommendation G.811, *Performance of Clocks Suitable for Plesiochronous Operation of International Digital Links*, CCITT Yellow Book, Fascicle III.3, Geneva, 1981.

CCITT Recommendation G.822, *Controlled Slip Rate Objectives on an International Digital Connection*, CCITT Yellow Book, Fascicle III.3, Geneva, 1981.

Daly, P., and I.D. Kitching, *Characterization of NAVSTAR GPS and GLONASS On-board Clocks*, IEEE Plans '90 Position Location and Navigation Symposium, pp. 1-8, 1990.

Franks, L.E., "Carrier and bit synchronization in data communication--a tutorial review," *IEEE Trans. on Communications*, COM-28, No. 8, part 1, pp. 1107-21, August 1980.

Frank, Robert L., "History of Loran C," *Navigation*, Vol. 29, No. 1, Spring 1982.

Gutleber, F.S., *Timing Accuracy for PN Sequences*, FSG-41, ITT, April 1966.

Gutleber, F.S., *Phase Lock Loop Performance in a Multipath Environment*, FSG-33, ITT, May 1965.

Gutleber, F.S., *A Precision Digital Frequency Ramp Generator*, FSG-10, ITT, May 1960.

Gutleber, F.S., *A Uniformly Spaced Frequency Band Generator*, FSG-9, ITT, May 1960.

Klepczynski, William J., *Time Transfer Techniques: Historical Overview, Current Practices and Future Capabilities*, Proceedings of the Seventh Annual Precise Time and Time Interval (PTTI) Applications and Planning Meeting, pp. 385-402, December 1985.

Lindsey, W.C., *Synchronization Systems in Communication and Control.* Englewood Cliffs, NJ: Prentice-Hall, 1972.

Parzen, B., *Design of Crystal and Other Harmonic Oscillators*, John Wiley and Sons, 1983.

Proceedings of the Annual Symposium on Frequency Control. Information on obtaining the early volumes of these Proceedings is available from NTIS, 5285 Port Royal Road, Sills Building, Springfield, VA 22161; for obtaining the latest volumes, contact IEEE, 445 Hoes Lane, Piscataway, NJ 08854.

Proceedings of the Annual Precise Time and Time Interval (PTTI) Applications and Planning Meeting. Information on obtaining copies of these Proceedings is available from the U.S. Naval Observatory, Time Services Department, 34th and Massachusetts Avenues, N.W. Washington, D.C. 20392-5100.

Proceedings of the European Frequency and Time Forum. Copies available from the Swiss Foundation for Research in Microtechnology (FSRM), Rue de l'Orangerie 8, CH-2000 Neuchatel, Switzerland.

Skolnick, Merrill I., *Introduction to Radar Systems*, McGraw-Hill, second edition, 1980.

Synchronization Interface Standards for Digital Networks, ANSI TI.101-1987.

This page intentionally left blank.

Custodians:

Air Force	--	90
Army	--	SC
DCA	--	DC
Navy	--	EC
NSA	--	NS

Preparing Activity:

DC

Director, JTC3A
ATTN: C3A-STT
Fort Monmouth, NJ
07703-5513

Review Activities:

Air Force	--	RADC
Army	--	SC, CR, SATCOMA
DCA	--	DC
Navy	--	EC, MCDEC, USNO, NRL
NCS	--	TS
NSA	--	T25

User Activities:

Air Force
Army
DCA
Marine Corps
Navy
NSA

Project No.: SLHC-4210

MIL-HDBK-421

This page intentionally left blank.

MIL-HDBK-421

INSTRUCTIONS: In a continuing effort to make our standardization documents better, the DoD provides this form for use in submitting comments and suggestions for improvements. All users of military standardization documents are invited to provide suggestions. This form may be detached, folded along the lines indicated, taped along the loose edge (DO NOT STAPLE), and mailed. In block 5, be as specific as possible about particular problem areas such as wording which required interpretation, was too rigid, restrictive, loose, ambiguous, or was incompatible, and give proposed wording changes which would alleviate the problems. Enter in block 6 any remarks not related to a specific paragraph of the document. If block 7 is filled out, an acknowledgement will be mailed to you within 30 days to let you know that your comments were received and are being considered.

NOTE: This form may not be used to request copies of documents, nor to request waivers, deviations, or clarification of specification requirements on current contracts. Comments submitted on this form do not constitute or imply authorization to waive any portion of the referenced document(s) or to amend contractual requirements.

(Fold along this line)

(Fold along this line)

OFFICIAL BUSINESS
PENALTY FOR PRIVATE USE $300

NO POSTAGE
NECESSARY
IF MAILED
IN THE
UNITED STATES

BUSINESS REPLY MAIL
FIRST CLASS   PERMIT NO. 4966 Alexandria, VA

POSTAGE WILL BE PAID BY

Director
Joint Tactical Command, Control and
  Communications Agency
ATTN: C3A-STT
Fort Monmouth, NJ 07703-5513

STANDARDIZATION DOCUMENT IMPROVEMENT PROPOSAL
(See Instructions — Reverse Side)

1. DOCUMENT NUMBER	2. DOCUMENT TITLE
MIL-HDBK-421	Military Handbook, Communications Timing and Synchronization Subsystems

3a. NAME OF SUBMITTING ORGANIZATION

4. TYPE OF ORGANIZATION *(Mark one)*

☐ VENDOR

☐ USER

☐ MANUFACTURER

☐ OTHER *(Specify):* _____

b. ADDRESS *(Street, City, State, ZIP Code)*

5. PROBLEM AREAS

a. Paragraph Number and Wording:

b. Recommended Wording:

c. Reason/Rationale for Recommendation:

6. REMARKS

7a. NAME OF SUBMITTER *(Last, First, MI)* — Optional	b. WORK TELEPHONE NUMBER *(Include Area Code)* — Optional
c. MAILING ADDRESS *(Street, City, State, ZIP Code)* — Optional	8. DATE OF SUBMISSION *(YYMMDD)*